

U.S. DEPARTMENT OF COMMERCE
National Technical Information Service

AD-A031 146

Electromechanical Actuation Feasibility Study

AiResearch Mfg Co of California Torrance

May 76

302083

AD A031146

AFFDL-TR-76-42

ELECTROMECHANICAL ACTUATION FEASIBILITY STUDY

AIRSEARCH MANUFACTURING COMPANY OF CALIFORNIA

MAY 1976

TECHNICAL REPORT AFFDL-TR-76-42

Approved for public release; distribution unlimited

DDC
RECEIVED
OCT 26 1978
REGISTRY

A

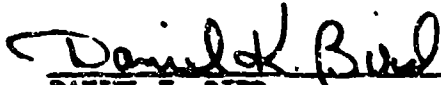
REPRODUCED BY
NATIONAL TECHNICAL
INFORMATION SERVICE
U. S. DEPARTMENT OF COMMERCE
SPRINGFIELD, VA. 22161

AIR FORCE FLIGHT DYNAMICS LABORATORY
AIR FORCE SYSTEMS COMMAND
WRIGHT-PATTERSON AIR FORCE BASE, OHIO 45433

NOTICE

When Government drawings, specifications, or other data are used for any purpose other than in connection with a definitely related Government procurement operation, the United States Government thereby incurs no responsibility nor any obligation whatsoever; and the fact that the government may have formulated, furnished, or in any way supplied the said drawings, specifications, or other data, is not to be regarded by implication or otherwise as in any manner licensing the holder or any other person or corporation, or conveying any rights or permission to manufacture, use or sell any patented invention that may in any way be related thereto.

This technical report has been reviewed and is approved for publication.



DANIEL K. BIRD
Project Engineer/Technical Monitor

FOR THE COMMANDER



JAMES M. RAINEY, Lt Col., USAF
Chief, Flight Control Division
AF Flight Dynamics Laboratory

Copies of this report should not be returned unless return is required by security considerations, contractual obligations, or notice on a specific document.

This report has been reviewed by the Information Office (OI) and is releasable to the National Technical Information Service (NTIS). At NTIS it will be available to the general public, including foreign nations.

UNCLASSIFIED

SECURITY CLASSIFICATION OF THIS PAGE (When Data Entered)

REPORT DOCUMENTATION PAGE		READ INSTRUCTIONS BEFORE COMPLETING FORM
1 REPORT NUMBER AFFDL-TR-76-42	2 GOVT ACCESSION NO.	3 RECIPIENT'S CATALOG NUMBER
4 TITLE (and Subtitle) Electromechanical Actuation Feasibility Study		5 TYPE OF REPORT & PERIOD COVERED FINAL REPORT 1-75 to 12-75
		6 PERFORMING ORG. REPORT NUMBER
7 AUTHOR(s) Neal E. Wood, E.F. Echols, John H. Ashmore		8 CONTRACT OR GRANT NUMBER(s) F33615-75-C-3055
9 PERFORMING ORGANIZATION NAME AND ADDRESS AirResearch Manufacturing Company A Division of the Garrett Corporation 2525 West 190th Street Torrance, CA 90509		10 PROGRAM ELEMENT PROJECT, TASK AREA & WORK UNIT NUMBERS Project 1987 Task 198701
11 CONTROLLING OFFICE NAME AND ADDRESS Air Force Flight Dynamics Laboratory AFSC/AFWAL, United States Air Force Wright-Patterson AFB, Ohio 45433		12 REPORT DATE May 1976
		13 NUMBER OF PAGES 192
14 MONITORING AGENCY NAME & ADDRESS (if different from Controlling Office)		15 SECURITY CLASS. (of this report) UNCLASSIFIED
		15a DECLASSIFICATION DOWNGRADING SCHEDULE
16 DISTRIBUTION STATEMENT (of this Report) Approved for Public Release, Distribution Unlimited		
17 DISTRIBUTION STATEMENT (of the abstract entered in Block 20, if different from Report)		
18 SUPPLEMENTARY NOTES		
19 KEY WORDS (Continue on reverse side if necessary and identify by block number) Power-by-Wire Fly-by-Wire "Pure Earth" Samarium-Cobalt Magnets Brushless D.C. Motor Permanent Magnet Rotor		
20 ABSTRACT (Continue on reverse side if necessary and identify by block number) An alternate to hydraulic actuation of primary flight control surfaces is desirable. Electromechanical actuation of primary flight controls is feasible and practical using the most recent advances in the state-of-the-art in magnetic materials for high-performance servomotors, high-current-capacity transistor switches for motor power control, and digital microprocessors for servo and redundancy management logic. Electromechanical actuation is consistent with current, proven, fly-by-wire technology and with the developing power-by-wire techniques. The control surface performance requirements and methods of analysis		

DD FORM 1 JAN 73 1473 EDITION OF 1 NOV 68 IS OBSOLETE

UNCLASSIFIED

SECURITY CLASSIFICATION OF THIS PAGE (When Data Entered)

PRICES SUBJECT TO CHANGE

UNCLASSIFIED

SECURITY CLASSIFICATION OF THIS PAGE(When Data Entered)

BLOCK 20:
are presented for direct drive electromechanical power servos. Trade studies were conducted to evaluate the aircraft power source and distribution options; actuator motor and controller options; and geared rotary hinge actuator configuration options. A weight comparison is given between the hydraulic actuation system for the F-100 and the electromechanical system studied. Reliability assessments and redundancy management considerations also are included. A preliminary design of the electromechanical actuation system and test plan are presented. These data were developed using a selected baseline problem statement which was derived from existing hydraulic actuator specifications.

SECURITY CLASSIFICATION OF THIS PAGE(When Data Entered)

FOREWORD

This document is the final report of a study conducted for the United States Air Force under Contract F33615-75-C-3055, Electromechanical Actuation Feasibility Study. The contract was administered by the Air Force Flight Dynamics Laboratory, Wright-Patterson Air Force Base, Ohio, Mr. Daniel K. Bird (FGL), Project Engineer. The technical effort, performed from January 15, 1975 to November 30, 1975, was undertaken by AIRsearch Manufacturing Company of California. Mr. Neal Wood was principal investigator.

Rockwell International, Los Angeles Aircraft Division, contributed to this study as a subcontractor. Mr. John E. Schibler, Project Engineer, provided detailed analyses, air frame data, and actuation system consultation for the flight control requirements and interfaces based upon the F-100 aircraft.

This document has been reviewed and approved.

RECEIVED	
PIE	NOV 1975
DOC	NOV 1975
APPROVED	
DATE	
BY	
U.S. AIR FORCE - WRIGHT-PATTERSON AIR FORCE BASE	
TITLE	
NO. 100	

TABLE OF CONTENT

<u>Section</u>	<u>Page</u>
1. INTRODUCTION	1
1.1 Background	1
1.2 Program Objectives and Scope	2
2. SUMMARY	4
3. BASELINE SYSTEM REQUIREMENTS	6
4. ACTUATION SYSTEM REQUIREMENTS ANALYSIS	9
4.1 Requirements Review	9
4.2 Baseline Actuation System Problem Statement	9
4.3 Analysis of Actuation System Requirements	10
5. ACTUATION SYSTEM STUDIES	19
5.1 Power Source Options	19
5.2 Actuator Drive Options	25
5.3 Actuator Element Options	51
5.4 Reliability Considerations	65
5.5 Aircraft Actuation System Integration	71
6. PRELIMINARY DESIGN	79
6.1 Design	79
6.2 Preliminary Performance Specification	93
6.3 Analog Analysis	104
6.4 Mockup	104
7. PROGRAM PLANS	108
7.1 Program Plan	108
7.2 Preliminary Test Plan for Actuation System Demonstration	111
8. REFERENCES	121
<u>Appendix</u>	
A F-100 AIRCRAFT CHARACTERISTICS	123
B B-52 RUDDER AND ELEVATOR CONTROL SYSTEM	138
C F-15 RUDDER CONTROL SURFACE ACTUATOR PERFORMANCE	141
D F-8 RUDDER CONTROL SURFACE ACTUATOR PERFORMANCE	142
E TOROIDAL DRIVE ANALYSIS	143

ILLUSTRATIONS

<u>Figure</u>		<u>Page</u>
1	Versatility of Electromechanical Actuation can be Fully Realized Through Recent Technological Advances	2
2	The 10-Month Program Comprised Six Tasks	3
3	Generalized Electromechanical Actuation System	6
4	Amplitude Ratio	8
5	Phase Lag	8
6	Characterization of Control Surface Velocity and Torque	11
7	Load Acceleration Capability	13
8	Initial Screening of Power Options	20
9	Control Approach Similarity	21
10	Power Source Characteristics	21
11	Alternator Characteristics	22
12	Rectifier	23
13	Power Transmission, Continuous Duty	24
14	Candidate Drive Options	26
15	Power Capability of Stopper Designs	27
16	Typical Motor Performance	29
17	Comparison of Magnet Materials	30
18	Rotor Critical Speed	31
19	Motor Power Characteristics	33
20	Variable-Frequency Motor Drive	34
21	Ac Inverter Voltage Schedule	34
22	Motor Thermal Analysis for MIL Power Dash	36
23	Thermal Analysis Results for Parked Aircraft on USAF Standard Hot Day	37

ILLUSTRATIONS (Continued)

<u>Figure</u>		<u>Page</u>
24	Thermal Analysis Results for 50,000-ft Cruise	37
25	SCR Commutation Circuit	41
26	Transistor Commutation Circuit	41
27	Dc Drive Functions' Block Diagram	43
28	Ac Drive Block Diagram	45
29	Harmonic Contents of 5% Notching 3-Phase Inverter	47
30	Ac and Dc Motor Thermal Management Comparison	49
31	Selected Drive System	52
32	Initial Screening of Actuator Elements	53
33	Harmonic Drive	54
34	Hinge-Line Actuator	56
35	Parametric Rotary Actuator Data	56
36	Harmonic Drive	57
37	Mechanical No-Back Characteristics	58
38	Mechanical No-Backs	60
39	Ball Ramp Type of No-Back	60
40	Energy Absorbing No-Back: Input Driving and Opposing Load	61
41	Energy Absorbing No-Back: Input Driving and Aiding Load	61
42	Output Torque Limiting of F-100 Aileron	63
43	Power Regeneration	63
44	Thermal Capability of Energy Absorbing No-Back	64
45	Control Surface Drive Redundancy Arrangement	68
46	Reliability System Model	69
47	Study Concept	70

ILLUSTRATIONS (Continued)

<u>Figure</u>		<u>Page</u>
48	F-100 Electromechanical Actuator Block Diagram	74
49	F-100 Electromechanical Actuator Installation at Allerton Station 199.250	75
50	Microprocessor Motor Control	81
51	Motor Thermal Analysis Results	87
52	Functions implemented by a Microprocessor	89
53	Microprocessor Program Flow Chart for Dc Motor Controller	90
54	Nonrecursive Digital Filter Mechanization Diagram	94
55	PWM Generator Functional Block Diagram	94
56	Shaft Position Sensor	95
57	Analog Input Encoder Mechanization Diagram	96
58	System Model	97
59	Motor Performance	99
60	Actuator Servo-Loop Functional Block Diagram	105
61	Amplitude Ratio vs Frequency	106
62	Phase Lag vs Frequency	106
63	EM Actuator Mockup	107
64	Program Schedule for Design, Fabrication, and Evaluation Testing of Electromechanical Rotary Hinge-Line Actuator	109
65	Test Logic Diagram	113
66	Performance Test and Test Setup	114
67	Frequency Response	115
68	Stiffness Test	116
69	Power Efficiency Test	117
70	Acceleration Test	118

ILLUSTRATIONS (Continued)

<u>Figure</u>		<u>Page</u>
71	Position Resolution Test	119
72	Velocity Test	120
A-1	F-100 Hydraulic Power Distribution System	124
A-2	Candidate Electrical Power Distribution System	124
A-3	F-100 Aileron System	125
A-4	Aileron Operating Requirements, Hinge Moment vs Deflection Rate	127
A-5	Aileron Operating Requirements, Hinge Moment vs Aileron Deflection	127
A-6	Rudder Operating Requirements	128
A-7	Rudder Operating Requirements	128
A-8	Rudder Duty Cycle	130
A-9	Rudder Deflection During Emergency Descent	130
A-10	Aileron Duty cycle	131
A-11	Estimated Aileron Deflection Required for Emergency Descent From 42,000 ft to Sea Level, Engine Inoperative	131
A-12	Rudder Temperature Zones	134
A-13	Aileron Coordinates, View Looking Down LH Wing	135
A-14	Rudder Coordinate System	135
E-1	Generalized VRD Arrangement	144
E-2	Variations of Function A with Roller Tilt	147
E-3	Variations of Function B with Roller Tilt	148
E-4	Variations of Function B with Roller Tilt	149
E-5	Variations of Function B with Roller Tilt	150
E-6	Example to Check Equations	151

ILLUSTRATIONS (Continued)

<u>Figure</u>		<u>Page</u>
E-7	Variation of Gear Ratio with Control Roller Tilting Angle	E-4
E-8	Variations in Gear Ratio with Changes in Roller Tilt	E-5
E-9	Conformity Between Toroid and Roller	E-6
E-10	Radius of Curvatures	E-7
E-11	Envelope Restrictions	E-7
E-12	Variation of Toroid Radius of Curvature with Tilting Angle	E-8
E-13	Methodology in Calculating Roller Contact Areas	E-9
E-14	Hertz Stress for Unit Normal Load	E-10
E-15	Force and Torque Balance	E-11
E-16	Kinematics of Variable Roller Drive	E-12
E-17	Schematic of Selected Design	E-13
E-18	Allowable Contact (Hertz) Stresses	E-14
E-19	Roller Drive Performance Summary	E-15

TABLES

<u>Table</u>		<u>Page</u>
1	Baseline Actuation System Performance Requirements	7
2	Baseline Control Surface Performance Requirements	10
3	B-52 Elevator Performance	17
4	F-100 Control Surface Performance	18
5	Power Source Tradeoffs	24
6	Ac Induction Motor Performance During Startup	35
7	Ac Induction Motor Losses	35
8	Motor Comparison	48
9	Comparison of Controller Types	49
10	Comparison of Drive System	50
11	Similarities in Motor Control Concept Application	50
12	Drive System for Preliminary Design	51
13	Actuator Comparison	57
14	Typical Control Surfaces and Backup Required	66
15	Aircraft Reliability Data	69
16	Reliability Estimates	70
17	Redundancy Management Tradeoff	72
18	Electromechanical Components Sized for F-100 Application	72
19	F-100F Electromechanical System Weights	75
20	F-100F Hydraulic Flight Control System Weight Reductions	77
21	Weight Comparison of EM and Hydraulic System for B-52 Elevator Problem Statement	78
22	Baseline Problem Statement	79
23	Brushless Dc Motor Electrical Losses	87

TABLES (Continued)

<u>Table</u>		<u>Page</u>
24	Sequencer Controller Truth Table	96
25	Controller Characteristics	98
26	Motor Characteristics	98
27	Actuator Characteristics	101
A-1	Summary of Surface Deflection Rates and Hinge Moments as a Function of Flight Conditions	126
A-2	Control Surface Mass Properties	133
A-3	F-100F Revised Flight Control System Deletions	137
B-1	Actuator Performance Characteristics	138
B-2	Actuator Performance Requirements	139
B-3	HPS Component Characteristics	140
E-1	Example Results	152
E-2	Evaluation of Force Balance Equations	163
E-3	Verification of Design Parameters	167
E-4	Frequency Response for Selected System	170
E-5	Summary of Design Parameters	171

DEFINITION OF TERMS AND SYMBOLS

The following listing is a summary of the most pertinent terms and symbols used in this report. An explanation of each symbol is also included in the text of the report where the symbol is used.

<u>Term</u>	<u>Definition</u>
Back Iron	The magnetic conducting path located at the outer periphery of the stator used to transmit magnetic flux between poles.
Commutation	A means by which switches are turned on and off to control current in an electric circuit.
Efficiency	A ratio of power input to power output, P_1/P_0 .
Electrical time constant	The stator winding inductance divided by the stator winding resistance. Expressed as τ , sec, it is numerically equal to 63.2 percent of the time required for the current to increase to the final value based on a step input change in applied voltage, and the rotor locked.
Mechanical time constant	The no-load velocity divided by the stall torque. Expressed as τ , sec, it is numerically equal to time required for the speed to increase to 63.2 percent of the final value based upon a given step input voltage change.
No-load	A condition at the (motor or actuator) output wherein there are no aiding or opposing static or acceleration forces.
Rotor	The mechanically rotating part of the motor, which can be either a permanent magnet or electromagnet design
Stall torque	Maximum output torque, lbf-in.
Stator	The stationary, outer part of the motor, which can be either electromagnetic or permanent magnet design
Toothless stator	A stator consisting of the back iron magnetic flux path but without the teeth.
PM	Permanent magnet
PMG	Permanent magnet generator
A	Amplitude, radians

B	Flux density, gauss
f	Frequency, Hz
G	Gear ratio (input speed/output speed)
I	Inertia, lbf-in.-sec ²
L	Reactance, henries
MMF	Magnetomotive force
P	Power, watts
Q	Electrical power dissipated as heat in the motor, watts
S	Slope of torque, speed relationship, rad/sec/lbf-in.
T	Torque, lbf-in.
δ	Angle between interacting magnetic fields
$\dot{\theta}$	Velocity, radians per sec
$\ddot{\theta}$	Acceleration, radians per sec ²
τ	Time constant, sec
ω	Angular velocity, radians

1. INTRODUCTION

1.1 BACKGROUND

The development of aircraft primary flight control actuation systems over the last 20 to 25 years has been primarily based upon state-of-the-art hydraulic techniques. To keep pace with developing high-performance aircraft, alternate techniques for actuation of aircraft primary flight control surfaces must be considered. The need to explore alternate actuation techniques derives from recent advances in aircraft control technology now available for application to design problems such as:

- Optimization of the control surface hinge-line location
- Simplification of modifying actuation system characteristics to aircraft operating mode (programmed rate, torque, and compensation networks)
- Improved reliability through new concepts of redundancy
- Decreased vulnerability (for military aircraft)

To evaluate these areas for providing improved aircraft flight control, the flight dynamics laboratory of Wright Patterson Air Force Base granted a contract to AiResearch Manufacturing Company of California, a division of The Garrett Corporation, to study the most recent electromechanical hardware approaches to primary flight control surface actuation. Electromechanical actuation designs are compatible with the most advanced fly-by-wire and control-by-wire actuation systems. Electromechanical actuation also is described as power-by-wire, since airborne alternators are the power source. This document presents the results of this study program.

Electromechanical actuation systems are of particular interest because of recent advances and the availability of production quantities of high-performance magnetic materials; high-current-capacity, solid-state switching devices; and micro-miniature, solid-state, digital computer/logic networks. Combining these components in a flight control actuation system provides a fast-acting, adaptive flight control servo with the following features:

- (a) Rare-earth-cobalt magnet material provides improved motor torque and acceleration capabilities (compared to earlier alnico magnets) and therefore results in weight and volume savings.

- (b) Dual power transistors with the capacity to handle high-current (50 to 75 amp) use simple circuitry to control actuator output torque and velocity.
- (c) High-speed digital microprocessors can be programmed to function primarily as a servo control, but also have the capability to monitor failures and isolate malfunctions, provide self-test, and most importantly, to be programmed to modify critical servo performance characteristics (gain, bandwidth, filter bandpass) based upon aircraft operating data peculiar to each aircraft maneuver and operating mode (altitude, attitude, and speed).

The evolution of electromechanical actuation is shown in Figure 1, which indicates application of new technology to provide a direct-drive servo system approach. This offers advantages of high performance, predictable operation, simple hardware, and proportional control.

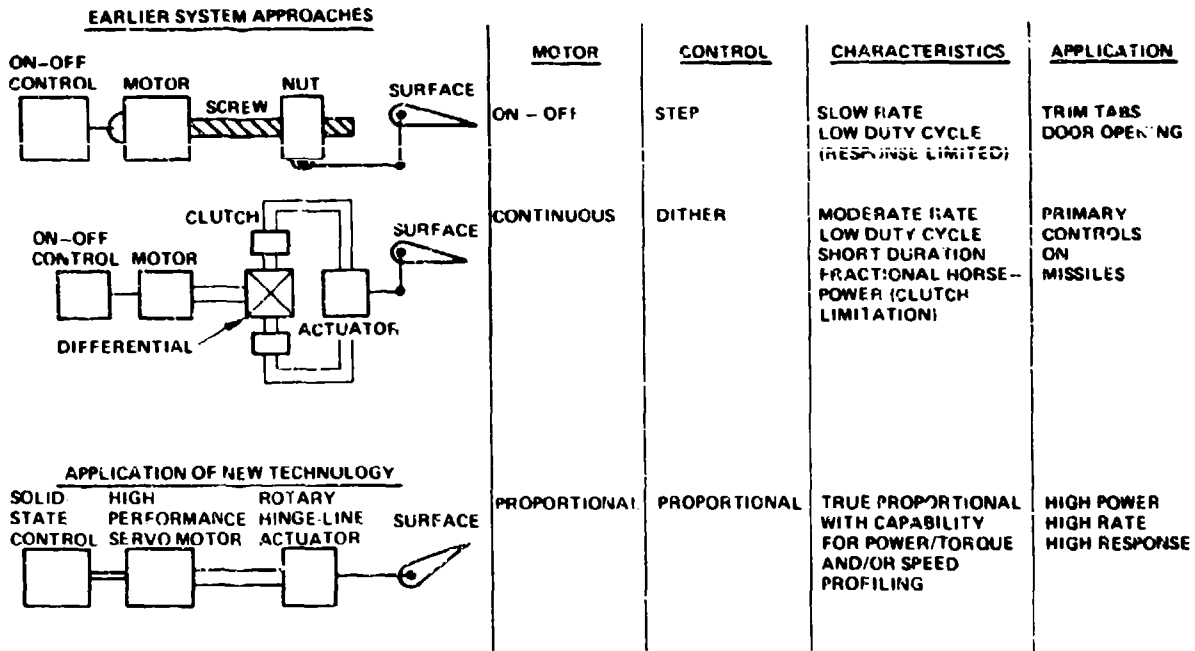


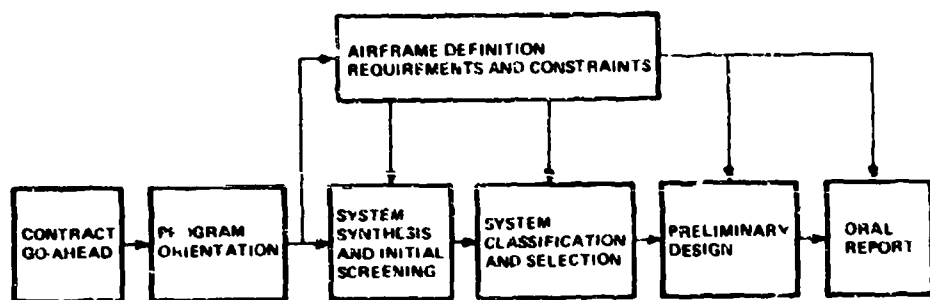
Figure 1. The Versatility of Electromechanical Actuation can be fully Realized Through Recent Technological Advances

1.2 PROGRAM OBJECTIVES AND SCOPE

This program was conducted by AiResearch Manufacturing Company of California under USAF contract to study electromechanical (EM) servoactuation systems as applied to aircraft primary flight control. The major program objectives were to:

- (a) Establish feasibility and advantages for EM primary flight control
- (b) Perform trade studies of EM actuation systems
- (c) Define optimum preliminary design
- (d) Fabricate an EM actuation system mockup

To accomplish these objectives, the study was organized into six discrete work tasks as shown in Figure 2, which depicts the relationships of these tasks. To obtain aircraft installation, performance, and operations data for use in the actuation system studies and evaluation, a subcontract was awarded to a major airframe manufacturer. Completion of these tasks has led to planning for development of an electromechanical actuation system for laboratory demonstration.



5-76650

Figure 2. The 10-Month Program Comprised Six Tasks

2. SUMMARY

The feasibility of using electromechanical actuation for primary flight controls was determined by:

Analysis of aircraft control surface requirements

Definition of candidate actuation components

Tradeoffs and selection of preferred approaches

Design of a preliminary representative actuation system

A baseline actuation system problem statement was developed from the actuation system performance requirements for the B-52 rudder and elevator; the F-100 aileron, rudder, and elevator; the F-15 rudder; and the F-8 rudder. The characteristics of the F-100 and B-52 aircraft were used to (1) evaluate the electromechanical (EM) system concept in terms of ease of installation and performance capability, and (2) compare the EM system to existing actuation systems in terms of weight, reliability, and compatibility with interfacing subsystems.

Application of the EM system approach to control surface actuation was determined optimum from tradeoffs conducted in the following areas:

- Power Source Options--Includes aircraft power source, power distribution, and conditioning for an all-electrical aircraft using EM flight control actuation.
- Actuator Drive Options--Includes ac and dc electric motors and analog and digital controllers.
- Actuator Options--Includes various gear actuator configurations, characteristics of devices for redundancy management, and mechanization of load-limit and/or gust relief for a control surface.

Component selection and optimization resulted in the preliminary design of an EM system with the following features:

- A permanent magnet generator, solid-state rectifier, and 270-vdc aluminum-conductor electric power bus results in a weight savings compared to conventional electrical power sources and distribution systems. Applying these concepts emphasizing the new approach and flexibility to power generation and distribution which is a fracture of the all-electrical aircraft.

- A digital microprocessor for servocentral logic. The programmable controller logic is flexible and adaptable to operation with either ac or dc motors. Matching the controller characteristics to the total aircraft is accomplished by software rather than hardware modifications. Flexibility is a major advantage of the microprocessor over conventional analog servo circuits.
- A controller that provides a programmed current and voltage to the servomotor, resulting in the optimum torque and rate at the control surface and the minimum power demand from the electrical power source and distribution system. The programmable controller may also be used to vary the servo compensation and filter networks as functions of aircraft operating modes.
- A brushless dc, permanent-magnet servomotor using high-performance, rare-earth-cobalt magnets in the rotor with a fast-response, power servo configuration that results in high operating efficiency and minimum power loss as heat. The improved thermal characteristics of this inside-out design allows the motor to operate at the required 3-hp output level continuously. Brushless commutation provides long life and flexibility in commutation logic. The 4-in.-dia dc servomotor has twice the duty cycle capability, is capable of 17 percent higher acceleration, and results in a 10 percent weight saving compared to the equivalent 4-in.-dia ac induction servomotor design.
- A planetary geared actuator operating as the control surface hinge results in weight savings and provides superior life and structural stiffness compared to harmonic drives or toroidal transmissions. A high-efficiency output stage is used to limit required power input.
- Dual-redundancy in performance-critical areas provides reliability equivalent to existing redundant hydraulic actuation systems while remaining weight competitive.
- Reduced weight using the geared rotary actuator as the hinge of the control surface to distribute structural loads more uniformly than the single-point loading used in the conventional linear hydraulic actuation system.
- Provision for built-in-test, continuous fault monitoring, and fault isolation circuits accomplished by the versatility of the controller.

Electromechanical actuation of aircraft control surfaces is feasible, practical, and can be implemented using the most recent advances in the state-of-the-art in magnetic materials for high-performance servomotors, high-current-capacity transistor switches for motor control, and digital microprocessors for servo and redundancy management logic.

3. BASELINE SYSTEM REQUIREMENTS

To maximize technical benefit in the areas expected to be most favorable to application of electromechanical actuation system concepts, certain study constraints were applied as follows:

- Primary flight control surface actuation
- Structurally integrated, rotary hinge-line actuator
- 3-hp required at surface (maximum)

To present parametric data useful in system analysis and to examine a range of applications, a detailed baseline actuation system was derived (See Figure 3). This baseline serves as a common point of reference throughout the report, including the preliminary design, and is used to support comparisons and evaluate technical options. When analysis shows variations in system configuration are required to meet extremes of the application range, these special areas of application are discussed in detail. Baseline system requirements are presented in Table 1.

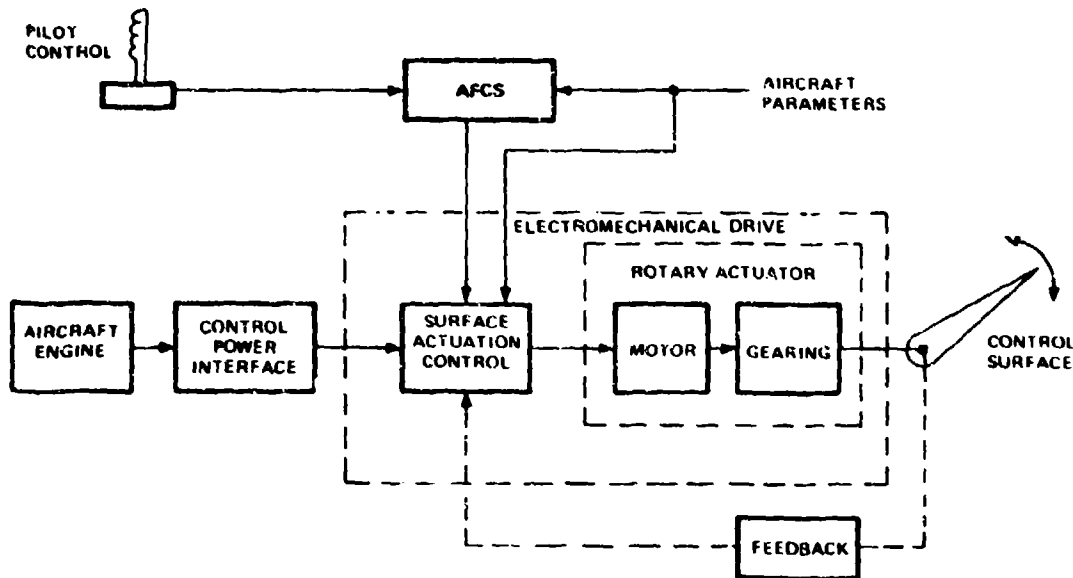


Figure 3. Generalized Electromechanical Actuation System,
(Does not Include Redundancy)

TABLE 1
 BASELINE ACTUATION SYSTEM PERFORMANCE REQUIREMENTS

Parameter	Requirement	Reference
<u>Aircraft Interfaces</u>		
Available aircraft power	115/200 v, 3-phase, 400 Hz, ac power. Compliance with MIL-STD-704.	4
Aircraft control input	Digital or analog	4
Control surface inertia	17,894 lbe-in. ² (46.6 lbf-in.-sec ²)	3
<u>Actuation Performance</u>		
Power level (approx.)	1 to 3 hp (sufficient to meet rate and torque)	1, 3, 4
Control surface no-load rate	80 deg/sec	3
Maximum stall hinge moment	37,575 lbf-in.	3
Control surface stroke (minimum)	+20 deg	3
Frequency response	See Figure 4	3
Phase lag	See Figure 5	3
<u>Installation</u>		
Actuator type	Rotary actuator of the integrated hinge type	1, 4
Maximum diameter	4-in. OD	4
Stiffness of structure	40,000 lbf/in.	3
<u>Reliability/Maintainability</u>		
Flight safety	Fail-safe	4
Redundancy	Two channel, with degraded operation after single failure allowable. Both channels normally in operation.	4
Redundant channel isolation	Motor brakes prevent a loose control surface after two failures.	4
MTBF	2500 hr (goal)	3

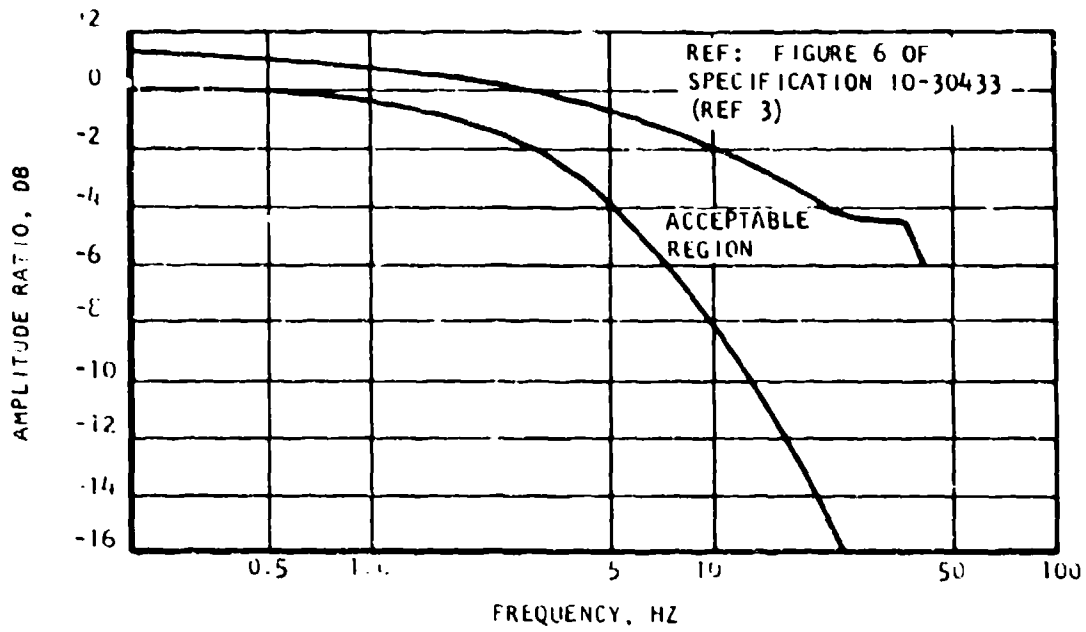


Figure 4. Amplitude Ratio

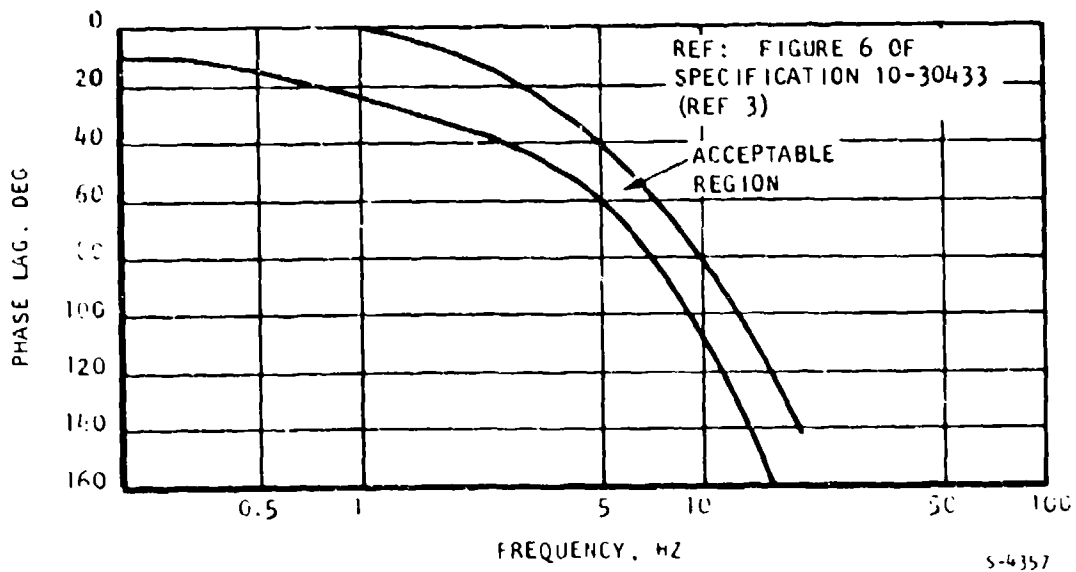


Figure 5. Phase Lag

4. ACTUATION SYSTEM REQUIREMENTS ANALYSIS

This section analyzes the critical actuation performance requirements and describes the impact of specific requirements upon the design characteristics of a control surface servosystem.

4.1 REQUIREMENTS REVIEW

Aircraft performance requirements can be translated into control surface actuation requirements. The most fundamental of these are acceleration, stall load, velocity, and stroke. The acceleration capability is generally a function of the torque-to-inertia ratio. The selection of a gear ratio is a factor in evaluating the motor torque in terms of the equivalent system inertia. Evaluation of the equivalent inertia includes the terms for the motor, geartrain, and control surface. The gear ratio also establishes the fundamental relationships of torque and velocity between the control surface and the motor.

Based upon practical constraints of motor design, a low gear ratio is associated with high control surface rate and acceleration, but will result in low output torque. To determine a motor/gear ratio combination that can provide rotor acceleration and torque suitable for a primary flight control system requires an optimum gearing arrangement based upon the characteristics of the motor and the control surface, or load. An additional aircraft operating parameter useful in evaluating actuation requirements is duty cycle.

Electromechanical actuation concepts can be categorized as demand systems (i.e., systems that use power only upon demand and only in proportion to the load requirements). Therefore, the sizing and arrangement of components in these systems are affected by the duty cycle of the applications. Applications requiring intermittent operation (trim tabs) will be designed for sustained load-holding capability (including continuous stall), but for relatively few operating cycles. A more active control surface (aileron) will require an actuation system with relatively high cycle life capability, but which normally operates at only 10 to 30 percent of stall and rate capability.

4.2 BASELINE ACTUATION SYSTEM PROBLEM STATEMENT

The electromechanical actuation system analyses and example calculations presented in this report were derived based upon review of the following representative aircraft actuation requirements.

- F-100 aileron, rudder and elevator (see Appendix A)
- B-52 rudder and elevator (see Appendix B)

- 1-15 rudder (see Appendix C)
- 1-8 rudder (see Appendix D)

The performance characteristics of at least these control surfaces satisfy the ground-rules of this study, and are viable candidates for application of electromechanical actuation systems.

After review of the actuation requirements for each control surface, the B-52 elevator was selected as the baseline problem statement because it is representative of past and expected future requirements. The baseline problem statement is presented in Table 2.

4.3 ANALYSIS OF ACTUATION SYSTEM REQUIREMENTS

4.3.1 Acceleration

Performance requirements for power servosystems can be expressed by representations of velocity and torque. Figure 6 shows this relationship for the baseline problem statement, Curve B. The particular relationship of torque and speed between these two design points could take any form (Curves A or C). Special performance might be dictated by requirements such as high acceleration (torque) while operating at a substantial rate. This condition is shown in Curve A of Figure 6, where additional torque is available at a given rate compared to Curves B and C. The relationship expressed by curve A is similar to the parabolic form expected from a hydraulic actuation system, while curve C is more nearly a constant-horsepower relationship.

The versatility of the electromechanical actuation approach discussed in this report allows scheduling of torque and velocity to satisfy particular actuation requirements.

TABLE 2
BASELINE CONTROL SURFACE PERFORMANCE REQUIREMENTS

Stall hinge moment	37,575 lbf-in.
No-load rate	80 deg/sec
Bandwidth	4 to 12 Hz (8 Hz nom.)
Load inertia	46.6 lbf-in.-sec ²
MTBF	2500 hr
Redundancy	fail-safe
Duty cycle	Continuous operation at 20 percent peak power
Stroke	up to 90 deg

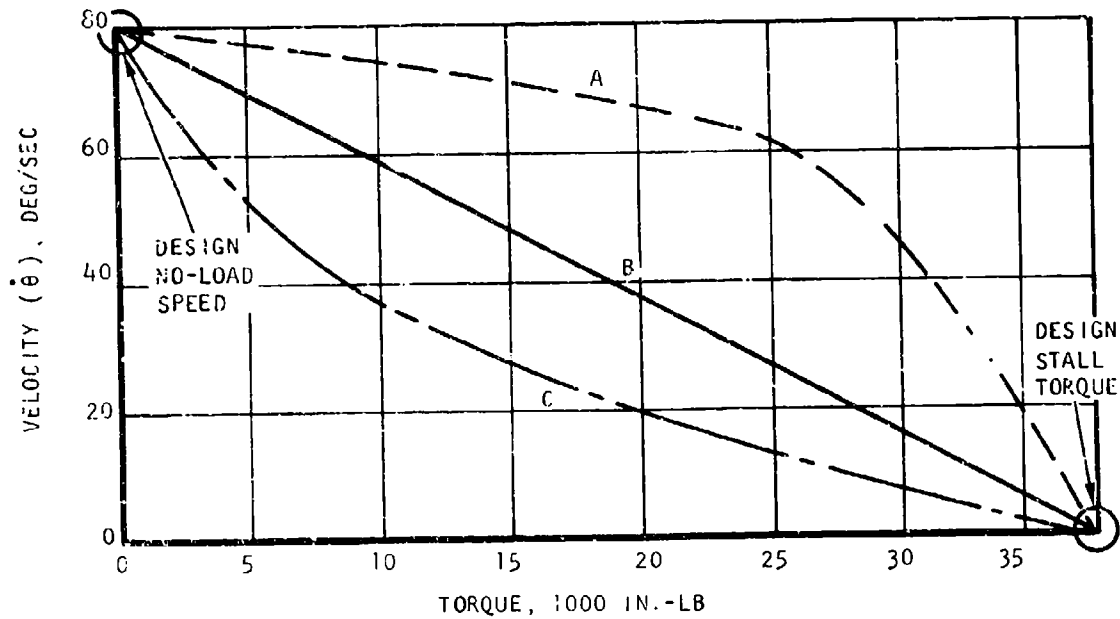


Figure 6. Characterization of Control Surface Velocity and Torque

To evaluate the dynamic relationships and characteristics of a control surface, the following example is presented using the appropriate numerical values from the baseline problem statement. Angular velocity of the control surface is determined by:

$$\omega = 2\pi f$$

$$\omega = 2\pi \times 8 = 50.3 \text{ rad/sec}$$

and the time constant by:

$$\begin{aligned} \tau_c &= \frac{1}{\omega} \\ &= \frac{1}{50.3} = 0.02 \text{ sec} \end{aligned}$$

The time constant also can be expressed as:

$$\tau_c = \frac{\dot{\theta}}{\ddot{\theta}} = \frac{\text{velocity}}{\text{acceleration}}$$

For the baseline problem statement where:

$$\dot{\theta} = 80 \text{ deg/sec} = 1.39 \text{ rad/sec};$$

$$\ddot{\theta} = \frac{\dot{\theta}}{\tau_c} = \frac{1.39}{0.02} = 70 \text{ rad/sec}^2$$

For a sinusoidal output operating into an inertial load only, the peak amplitude at which both velocity and acceleration saturation occurs is:

$$A = \frac{\dot{\theta}}{\omega}$$

$$= \frac{1.39}{50.3} = 0.027 \text{ rad or } 1.58 \text{ deg}$$

or:

$$A = \frac{\ddot{\theta}}{\omega^2} = \frac{70}{(50.3)^2} = 0.027 \text{ rad or } 1.58 \text{ deg}$$

Response for other amplitudes, with or without concurrent loads, can be calculated using the same relationships. For this example, the frequency response is not affected by changing the value of the aerodynamic load because the ratio $\dot{\theta}/\ddot{\theta}$ remains constant. Figure 7 shows the relationship of acceleration to load, as defined by frequency response and stall load. Between these two points, the acceleration capability could take any form (as shown for Figure 6). Referring to the baseline problem statement (Curve B, Figure 7), the acceleration is 70 rad/sec² when the actuator is operating into the specified inertial load. The control surface also will have to operate with non-inertial loads. As the control surface operates into other loads (such as aerodynamic and friction loads), the acceleration capability decreases. The curve marked A in both figures 6 and 7 shows an actuation system designed to provide additional torque for acceleration loads compared to either Curves B or C.

4.3.2 Gear Ratio

An electric motor is connected to the control surface by gearing that simultaneously provides torque multiplication and speed reduction. For flight control applications, the motor is used with a rather large gear reduction to reduce the typical motor no-load speed of 5000 to 30,000 rpm to an output speed of 10 to 40 rpm (60 to 240 deg/sec). The large gear reduction minimizes the effect of load inertia on the frequency response of the motor. For typical applications, the load inertia reflected to the motor shaft amounts to less than 10 percent of the motor inertia, and thus causes less than a 10 percent increase in the mechanical time constant.

The motor speed and torque and the gear ratio can be selected to deliver the peak control surface rate, torque, and acceleration required. For the motor shown in Figure 16, the output gearing to meet the requirements is defined by the following relationships.

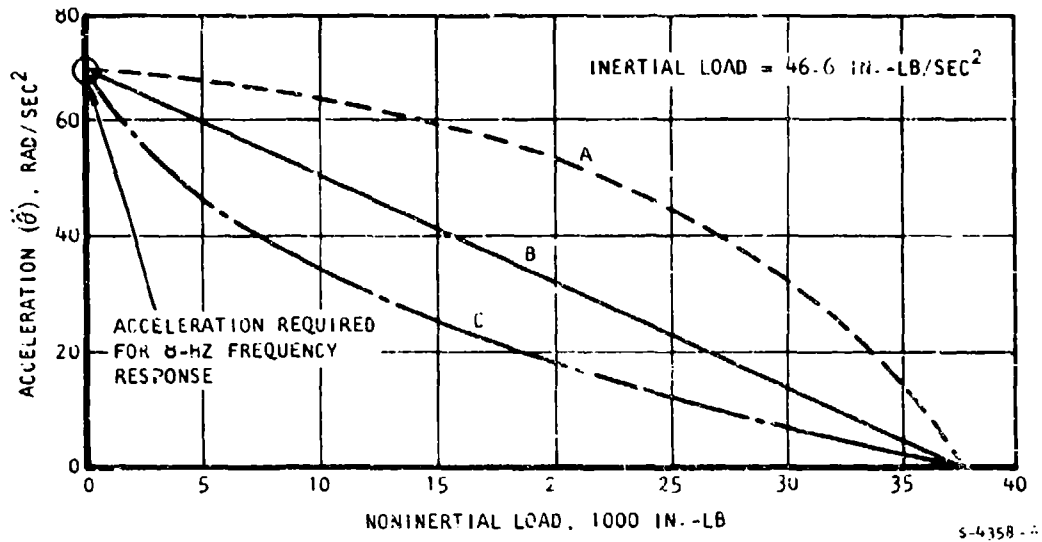


Figure 7. Load Acceleration Capability (operating with Prescribed Load Inertia)

$$\text{Output no-load speed} = \frac{\text{motor no-load speed}}{\text{gear ratio}}$$

$$\text{Output stall torque} = \text{motor stall torque} \times \text{gear ratio} \times \text{gear efficiency}$$

$$\text{Output acceleration} = \frac{\text{motor acceleration}}{(\text{gear ratio})}$$

$$\text{Motor acceleration} = \frac{T_m - \frac{T_o}{G}}{i_m + \frac{I_l}{G^2 \times \text{Eff}}}$$

Where T_m = motor torque

T_o = output torque

G = gear ratio

i_m = motor inertia

I_l = load inertia

EFF = gear efficiency

Based upon the following conditions:

$$i_m = 1.638 \times 10^{-3} \text{ lbf-in.-sec}^2$$

AFFDL-TR-76-42

$$I_L = 46.6 \text{ lbf-in.-sec}^2$$

$$\eta = 0.9$$

$$G = 600$$

The effective load inertia reflected to the motor is

$$\frac{I_L}{G^2 \times \eta} = \frac{46.6}{(600)^2 \times 0.9} = 0.00014 \text{ lbf-in.-sec}^2$$

Compared to the motor rotor inertia, I_m , the load inertia is seen as only a 9 percent increase in effective rotor inertia.

The gear ratio and motor no-load speed can be selected to minimize power (current) from the servo amplifier. One method includes selecting motor no-load speeds and actuator gear ratios such that no additional current above that required to provide the desired output torque and speed is needed to meet frequency response (acceleration) requirements. Conversely, no additional current beyond that required to meet frequency response requirements is needed to provide the required output torque and rate. Then since

$$T_m = I_m \ddot{\theta}_m$$

and motor acceleration torque equals:

$$T_m = \frac{T_{T0} - (T_{TL} + T_C)}{G \eta}$$

and

$$\ddot{\theta}_m = \ddot{\theta}_o G$$

then

$$\frac{T_{T0} - (T_{TL} + T_C)}{G \eta} = I_m \ddot{\theta}_o G$$

or

$$I_m G^2 \ddot{\theta}_o \times \eta = T_{T0} - (T_{TL} + T_C)$$

$$\text{or } G = \left(\frac{T_{T0} - (T_{TL} + T_C)}{I_m \ddot{\theta}_o \times \eta} \right)^{1/2}$$

where:

T_{T0} is the maximum output torque, and is the larger of

1. $2(T_{TL} + T_C)$ (load + concurrent load)
2. T_s (stall)
3. T_r (running)

$\ddot{\theta}_o$ = output acceleration required (rad/sec²)

I_m = motor rotor inertia (in.-lb-sec²)

η = gear efficiency

The use of a current limiter in the servoamplifier allows the motor to be operated in the high efficiency region of the torque speed curve, with the current limited to that needed to provide the maximum output torque as well as desired motor acceleration.

The theoretical maximum power efficiency of the motor is the ratio of the operating speed to no-load speed. Therefore, at 1/2 no-load speed, the maximum theoretical power efficiency is 50 percent. To operate efficiently, the motor should run at speeds near no-load. This is accomplished by designing a motor with a stall torque capability far in excess of that required, and limiting the applied current to control torque output. The motor is therefore operated at a fraction of stall capability, and in a region near no-load speed, therefore, the region of highest efficiency.

4.3.3 Motor Sizing

Motor power output is a function of voltage and current. To maintain current at values consistent with low cost and state-of-the-art transistor switch capability (50 amp), the practical output power can be related to supply voltage as follows:

28-v system, 0 to 1.0 hp

56-v system, 0 to 2.5 hp

90-v system, 0 to 5.0 hp

270-v system, 0 to 15.0 hp

To exceed these general ranges of power values, the electronic amplifier, cables, and noise filter become too large, and other approaches may be preferable. For servosystem requirements within this horsepower range, the direct-coupled electric system may offer significant advantages in terms of size, weight, accuracy, resolution, and predictability of performance compared to other approaches.

4.3.4 Stroke

The control surface stroke capability is an important advantage for the rotary hinge-line actuator compared to the conventional linear actuator. The linear actuator must be designed (and the weight penalty accepted) for a particular maximum stroke required of the output. The major design parameters which size a rotary actuator are load, stiffness, and life. The rotary actuator is not affected by the stroke requirement except for the operating range of the feedback mechanism. This design consideration is minimal, however, and does not significantly affect the actuator weight.

4.3.5 Duty Cycle

To interpret and evaluate control surface actuation duty cycle requirements for a particular application, it is helpful to compare the design requirements to the actual flight data. In Table 3, the specification performance requirements for the B-52 elevator actuator are summarized. Flight simulator data also are given. As arbitrary evaluation criteria, the performance requirement and simulation data can be compared using horsepower. Based upon peak horsepower calculated using one-half no-load speed and one-half stall torque (a linear torque speed relationship), the maximum required power for the specified performance is 2 hp and for the simulated flight is 0.064 hp. The resulting power ratio (average/maximum), or apparent equivalent duty cycle, is therefore 3.2 percent.

The specified performance of control surfaces of the F-100 is compared in Table 4 to documented performance data that represent various operating conditions of the aircraft. Depending upon the specific operating mode, the apparent duty cycle can be summarized as follows:

Highest Duty Cycle--Aileron during combat, 86 percent.

Lowest Duty Cycle--Rudder during cruise, 0 percent.

The aileron and rudder experience a duty cycle in the range of 10 to 20 percent during combat, and approximately 3 to 7 percent during cruise. The flight control duty cycle is therefore a function of the control surface considered and the flight operating mode. High percentage duty cycles are generally associated with short operating times, such as shown for combat. A reasonable duty cycle is therefore estimated to be 20 percent for most flight control surfaces.

TABLE 3
B-52 ELEVATOR PERFORMANCE

<u>Specification Requirements</u>	
80 deg/sec rate	
8 Hz	
37,575 lbf-in. hinge moment	
<u>+20</u> deg stroke	
<u>Data from Simulator*</u>	
Nominal stroke, +5 to -3 deg	*340,000 to 360,000 lb gross weight
Nominal hinge moment (1000 lbf-in.)	350 klbs
<u>+2</u> deg amplitude	500 ft above highest terrain, Barksdale.
1.25 Hz minimum	
2.00 Hz average	
3.33 Hz maximum	
<u>+4</u> deg amplitude	
2 Hz average	

TABLE 4
F-100 CONTROL SURFACE PERFORMANCE

Condition	Surface	Rate, deg/sec	Hinge Moment, in.-lb	Power, hp
Design Requirement	Aileron	11.5	132,000	1
	Stabilizer	20.0	500,000	6.6
	Rudder	10.0	4,300	0.03
Ground Checkout				
Maximum	Aileron	50	Inertial and friction only	
	Stabilizer	20		
	Rudder	50		
Flight				
Combat	Aileron	10	132,000	0.86
	Stabilizer	4	500,000	1.32
	Rudder	1	4,300	0
Cruise	Aileron	0.2	60,000	0.01
	Stabilizer	0.25	100,000	0.02
	Rudder	0.0	0	0.0
Landing	Aileron	3.33	10,000	0.02
	Stabilizer	5.0	20,000	0.07
	Rudder	1.0	800	0.00

5. ACTUATION SYSTEM STUDIES

This section presents design data used in conducting trade studies of various electromechanical actuation system concepts. Initial screening of candidate approaches is used to eliminate marginal and low-potential systems. Detailed characteristics of viable candidates are presented and used in tradeoff comparisons. The results of the tradeoffs are used to synthesize an aircraft actuation system and define the preferred approach to control surface actuation. The actuation system studies and options are presented in parts as follows:

Power Source--Includes engine-mounted electrical generation and initial conditioning equipment.

Actuation Drive--Includes electronic controller, power switching, and servomotor elements.

Actuation Elements--Includes mechanical rotary hinge and mechanization of redundancy.

Reliability Considerations--Considers redundancy management for future high-performance aircraft.

Aircraft Actuation Integration--Evaluates interrelationships of components and summarizes total system characteristics.

5.1 POWER SOURCE OPTIONS

5.1.1 Initial Screening

The power for control surface actuation of an aircraft such as the F-100 will be in the range of 4 to 10 hp (peak for each control surface). Assuming nine control surfaces, the total power required is between 36 and 90 hp. Therefore, the aircraft electrical power source must be sized in the approximate range between 30 and 70 kw. A number of power types can be derived from the basic power source as shown in Figure 8. A program ground rule is use of an alternator producing 115/200-vac power. Three principal options are available.

- (a) Use of the power at a constant, 400-Hz, fixed frequency, which requires a constant-speed drive for the alternator, or a suitable power conditioning system.
- (b) Use of the power at a variable frequency, eliminating the weight, complexity, and unreliability of a constant-speed drive.
- (c) Converting the ac power (either variable or fixed frequency) to dc using a rectifier, allowing operation of dc motor drive systems.

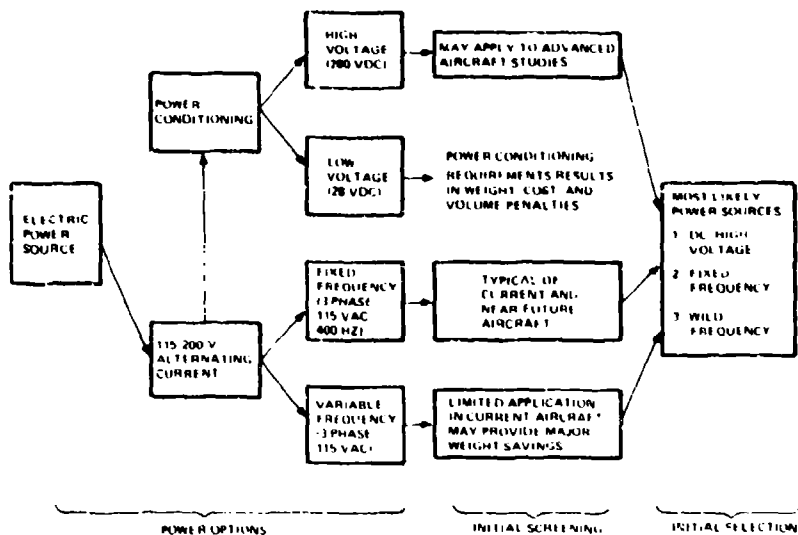


Figure 8. Initial Screening of Power Options

Upon closer examination, it is apparent that operation of either an ac or a dc drive system requires that the primary power be conditioned by adjusting frequency, voltage, or both prior to use in the electric motor, Reference 5. Figure 9 shows the similarities of the ac and dc motor drive systems in terms of requirements for the power source. Either drive concept can function equally well from fixed-frequency ac or variable-frequency ac because of the commonality of the dc link. Thus, the most likely power sources for operation of a drive system are (1) high-voltage dc available from rectification of a 115/200-v alternator output, (2) 400-Hz ac power, or (3) ac power provided at a frequency dependent upon operating speed.

5.1.2 Component Characteristics

The power source for an electromechanical actuation system comprises an alternator (with or without a constant speed drive), a rectifier, and power distribution lines. These components are discussed in the following paragraphs.

5.1.2.1 Alternators

The characteristics of airborne alternators and permanent magnet generators are presented in parametric form in Figure 10. Usually, the optimum magnetic configuration for an alternator at any speed is in the range of six to ten poles. Fewer poles require excessive back iron and end turn copper, and the machine must operate at relatively low electric loading. A greater number of poles permits excessive flux leakage between poles. Therefore, the rated speed of an alternator would be determined by

$$\text{RPM} = \text{FREQ} \times 120/\text{POLES}$$

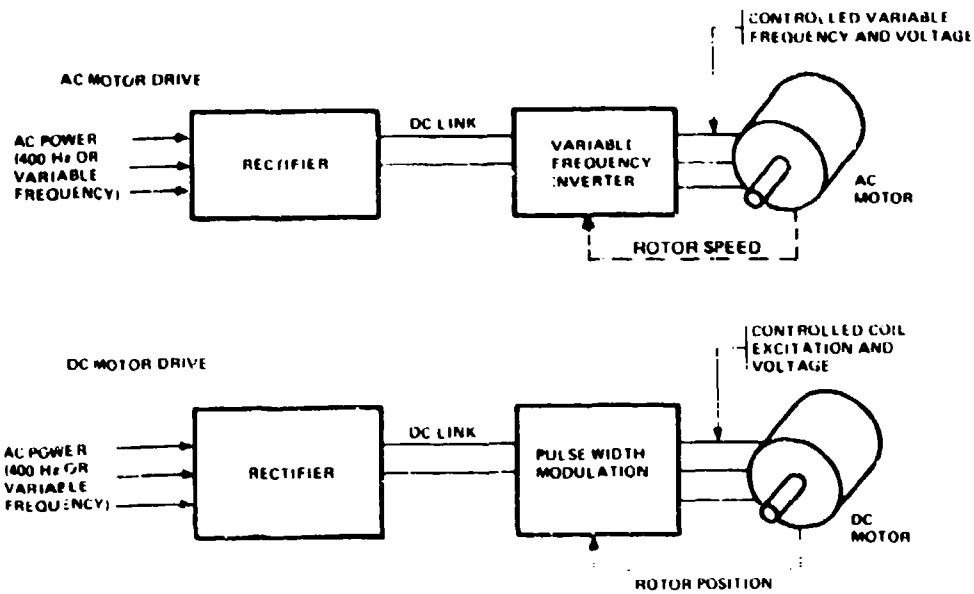


Figure 9. Control Approach Similarity

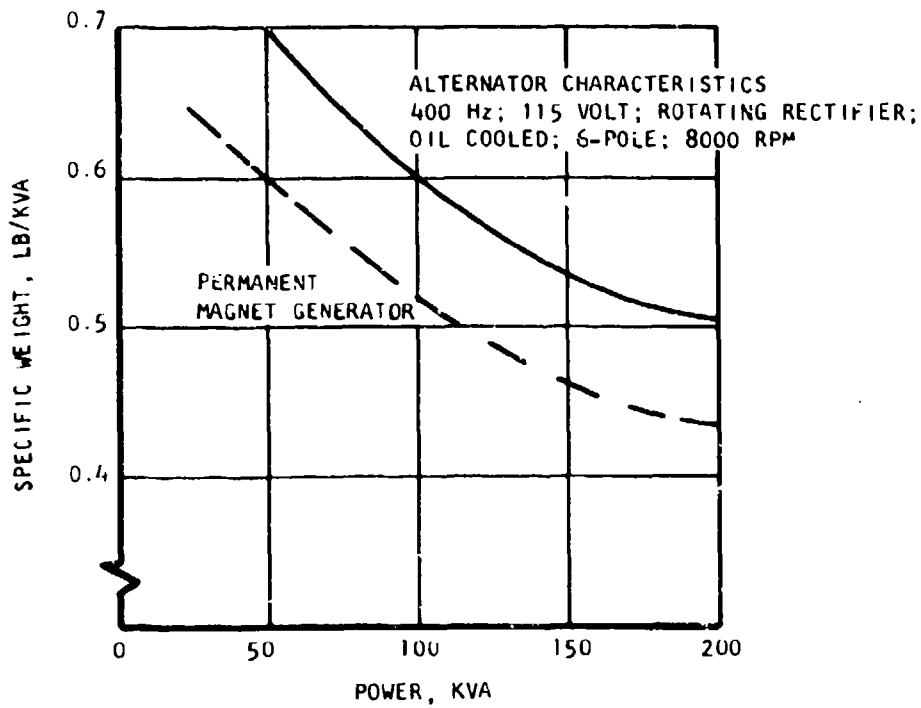


Figure 10. Power Source Characteristics

The rotor tip speed parameter reflects state-of-the-art capability. Figure 11 shows the relationship of alternator specific weight to rotor tip speed. Projected advances in machine design will reduce machine weight by 30 percent by increasing the tip speed from 275 to 400 ft/sec. The permanent magnet generator (PMG) uses a rare-earth-cobalt rotor and a wound stator; no slip rings are necessary in this design. Because the output of the alternator can be varied by rotor excitation, the alternator can provide two times the rated output for very short periods (5 sec). However, the PMG provides a very flat voltage characteristic as a function of current demand, without the complexity of field control, slip rings, rotating rectifiers, and associated complexities and unreliabilities.

5.1.2.2 Rectifiers

The rectification of the primary power source can be accomplished using solid-state devices manufactured by numerous suppliers for similar airborne applications. Parametric weight and volume characteristics for rectifiers operating from a 3-phase, 115/200-v supply and providing output power at 270 vdc are presented in Figure 12.

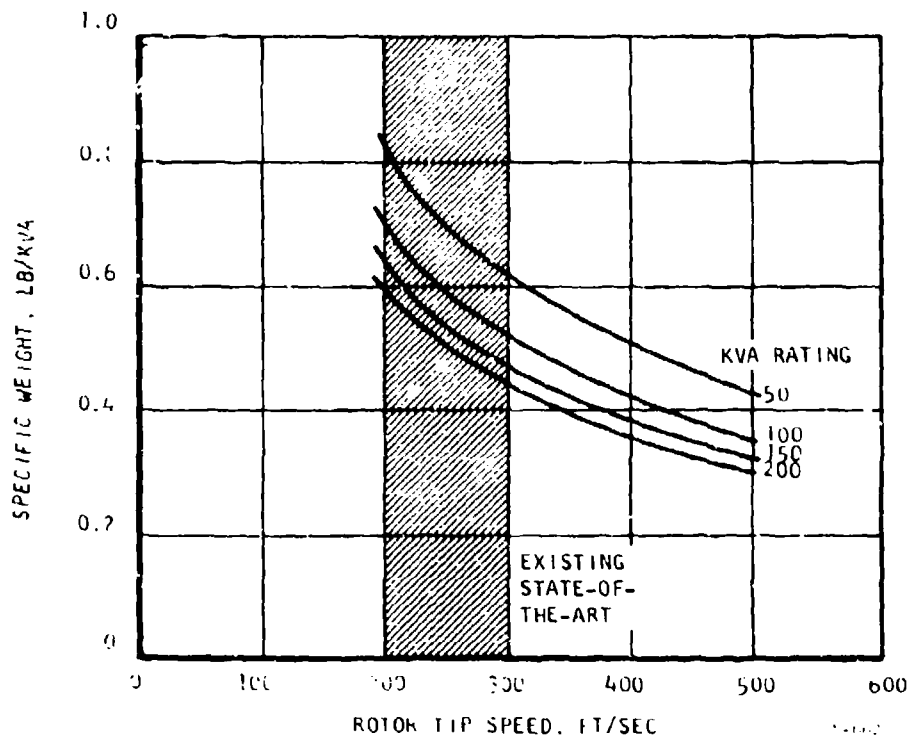


Figure 11. Alternator Characteristics

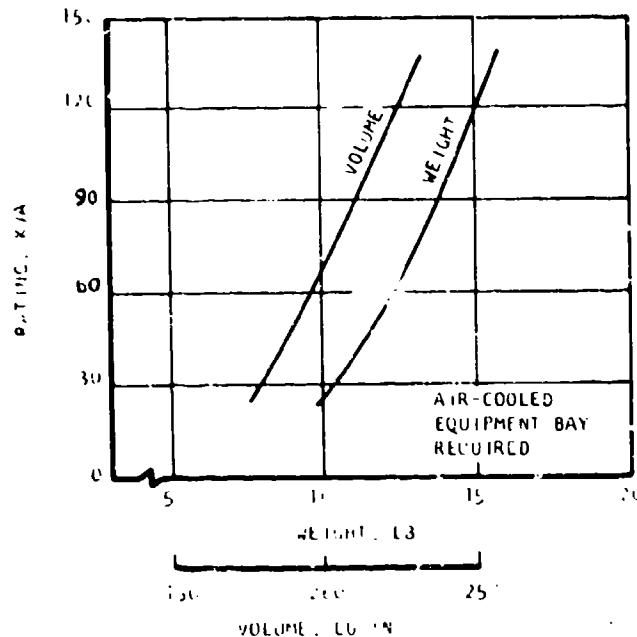


Figure 12. Rectifier Characteristics

5.1.2.3 Electrical Power Distribution

Electrical power will be distributed in the aircraft using a dual redundant bus. Figure 13 presents the specific weight of a 3-phase, ac, nonredundant electrical bus. A reference weight for a 9.5-hp hydraulic transmission line is included. The apparent weight saving using an ac bus is 3 to 1 compared to the hydraulic line. Figure 13 also presents the weight of a 200-ft-long, 270-vdc transmission line. It results in a 30 percent weight saving compared to the ac power distribution bus. The use of aluminum conductors results in an approximate weight saving of 50 percent compared to copper.

5.1.3 Power Source Tradeoffs

The power source tradeoff is a function of power quality required by the motor controller. Because of the dc link, a variable frequency from the electrical generator is entirely suitable for an actuation system. High quality power for airborne electronics and communications systems can be obtained from an auxiliary alternator designed for that particular application. The weights for nonredundant concepts to provide electrical power to the control surface actuation subsystems are compared in Table 5. As shown, the PMG is the lightest power generator. The comparison of power distribution throughout the aircraft is based upon ac and dc power buses using both copper and aluminum conductors. The weight of a single rectifier is included in the dc distribution system configuration. Since the rectifier is located at the PMG, the dc motor controller comprises only the control logic and the required transistor switches for commutation. The ac distribution system will require a rectifier and a control at each motor drive location.

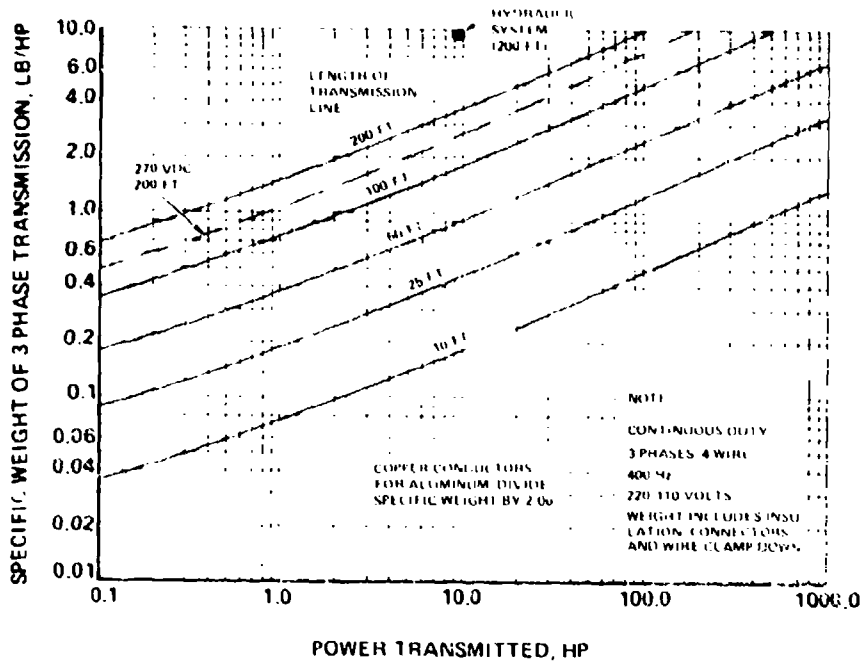


Figure 15. Power Transmission, Continuous Duty

Table 5

POWER SOURCE TRADEOFFS

SUBSYSTEM ELEMENT	POWER SOURCE OPTION			
	CONSTANT SPEED DRIVE (CSD) AND ALTERNATOR, 88 LB (CSD = 47) (ALTERNATOR = 41)		PERMANENT MAGNET GENERATOR, 35 LB	
ELECTRIC SOURCE 60 KVA				
POWER DISTRIBUTION	3 PHASE AC		270 VDC	
50 FT, 60 KVA	COPPER CONDUCTORS	ALUMINUM CONDUCTORS	COPPER CONDUCTORS	ALUMINUM CONDUCTORS
100 FT, 15 KVA	142 LB	67 LB	114 LB	55 LB
POWER CONDITIONING 60 KVA	36 LB (9 RECTIFIERS)	36 LB (9 RECTIFIERS)	13 LB (1 RECTIFIER)	13 LB (1 RECTIFIER)
TOTAL WEIGHT, LB (NON REDUNDANT)	266	191	162	103

5.1.4 Power Source Selection

Based upon the component data and the weight comparison of Table 5, the selected approach is the use of a PMG as the electrical source, a rectifier to provide 270-vdc power, and distribution of the power through the aircraft using aluminum conductors. The total nonredundant system weight for the configuration is 103 lb.

5.2 ACTUATOR DRIVE OPTIONS

Electric direct-coupled dc position servosystems are being considered for a variety of new applications, including missile control fin positioning, thrust vector nozzle control, primary and secondary aircraft flight controls, valve positioning, etc. The new interest in this approach results primarily from increased power rating and frequency response made possible by the advent of new rare-earth-cobalt, permanent magnet materials for field excitation of PM servomotors, coupled with advancements in transistor switching technology. This section discusses the options of drive assemblies and the characteristics of individual components in those assemblies. A drive assembly comprises a motor and a controller. The controller, in turn, comprises an electronic servo, electrical power switching circuits, and any necessary feedback devices.

5.2.1 Initial Screening

The drive options for power-by-wire are summarized in Figure 14, which shows that the high voltage brushless dc motor with a permanent-magnet rotor and pulse-width modulation control provides better performance than either brush-type dc motors or stepper motors. The selection is based primarily upon consideration of the combination of lower weight and reduced thermal design problems associated with the brushless dc motor drive. Also shown is that the preferred ac motor drive is the induction motor with an inverter that provides variable frequency drive to the motor as a function of motor shaft speed. To minimize losses, the voltage also is programmed as a function of applied frequency (motor speed).

5.2.2 Component Characteristics

The pertinent component characteristics for the candidate motors and controllers are discussed below. The basic requirements for the motor and control are:

- (a) 1 to 3 hp peak output capability in a 4.0-in.-dia maximum frame. (The typical flight control actuator problem statement requires this power output capability to drive the load at the desired rates, irrespective of frequency response requirements.)
- (b) A frequency response capability of 4 to 16 Hz.
- (c) Capable of maintaining a 50 percent duty cycle at a torque level corresponding to that produced at the peak output horsepower (one-half no-load rate and one-half stall torque.)
- (d) Capable of providing static torque in accordance with a program representing aerodynamic trim loads.

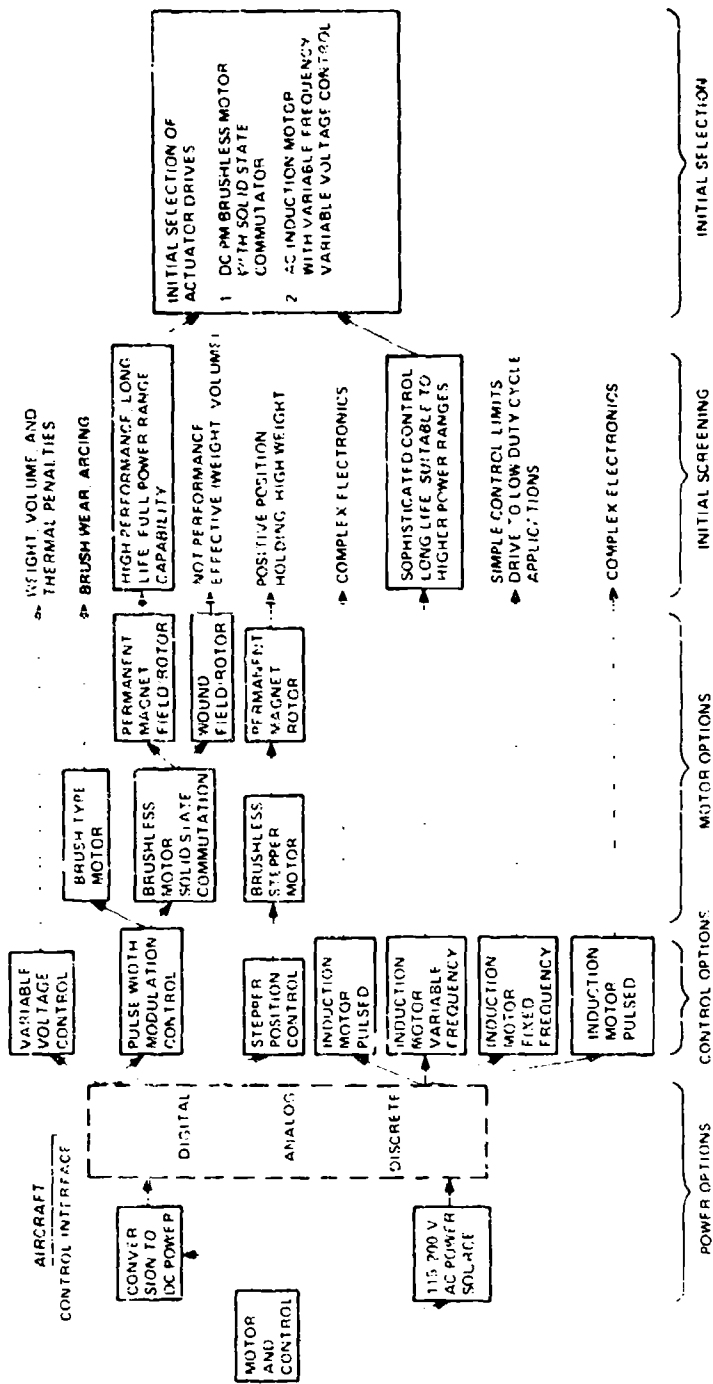


Figure 14. Candidate Drive Options

In support of the initial screening described above, a number of candidate motor types were evaluated. The motors selected for evaluation represent types that can operate as part of a power servosystem and that have the potential to meet the requirements listed above. The motors evaluated are:

- (a) Permanent magnet and variable-reluctance steppers
- (b) Flex spline steppers
- (c) Variable-frequency, variable-voltage induction motors
- (d) Rare-earth-cobalt, permanent-magnet, brushless dc motors

5.2.2.1 Permanent Magnet, Variable-Reluctance, and Flex Spline Steppers

5.2.2.1.1 Power Output

Figure 15 shows typical torque speed and power output curves for the three-stepper types in the general size range of interest for this requirement. The data were obtained from manufacturer's catalog literature. The stepper motors respond to programmed, pulsed, dc voltages, causing rotation of the output. The permanent magnet (PM) stepper comprises a permanent magnet rotor and a wound stator. The PM unit offers holding or detent torque capability. The variable-reluctance (VR) stepper design operates on the reaction between an electric field generated in the stator and a soft iron toothed rotor. The VR machine is generally capable of higher speed than the PM design.

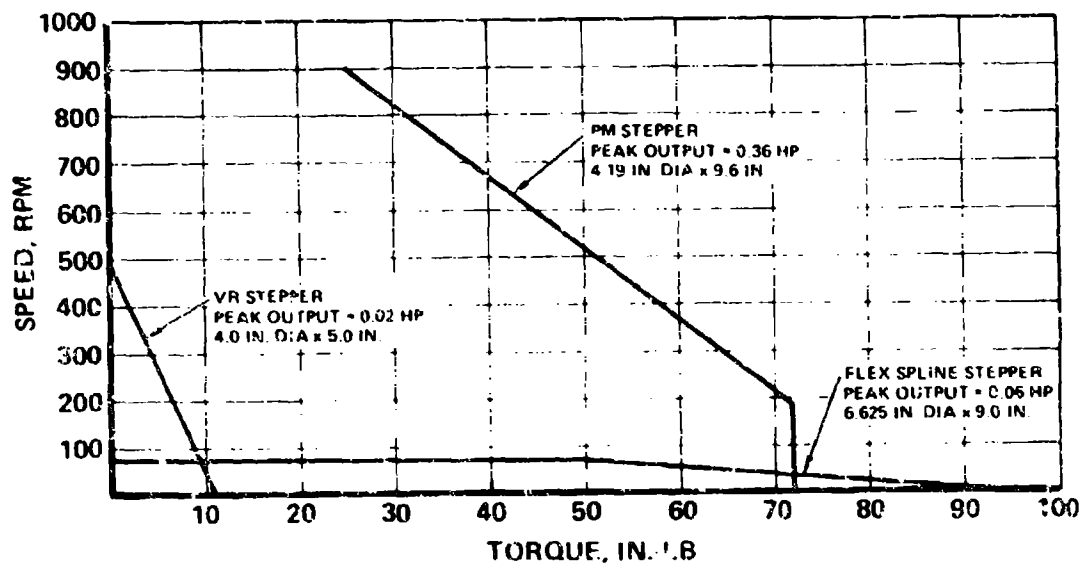


Figure 15. Power Capability of Stepper Designs

Although the relationship of digital (pulsed) input to discrete steps at the output appear to offer advantages in the area of integration with a digital control actuation system, the basic stepper designs are not competitive with other forms of electromagnetic machines in terms of providing both the required torque and the required rate. The units are not suitable for the application because the maximum power output capability is about an order of magnitude below that required.

The flex spline stepper (Reference 6) is a device that offers exceptionally high acceleration capability. Compared to the PM and VR steppers, the flex spline machine can provide output acceleration 100 times greater. This characteristic is not realized as an advantage, however, for the following reasons:

- (a) The acceleration requirements of a flight control system can be met with stepper or conventional servomotor components.
- (b) The mechanization of high acceleration results in excessive weight, and is not capable of substantial power, rate, or stiffness.

5.2.2.2 Rare-Earth-Cobalt, Permanent-Magnet, Brushless dc Motor

Optimization of the number of motor poles involves both the theoretical and practical aspects of design. Machine weight becomes excessive as the number of poles is reduced below six or eight because of the increase in back iron required to accommodate the flux return path. As the number of poles is increased above six or eight, the motor becomes lighter, and the winding end losses become lower since the ends constitute a smaller percentage of the total. Small motors with many poles can be difficult to manufacture, however, and there is less magnet length available to develop the required air gap flux. The motor stator is wound for a three-phase input. A two-phase winding configuration results in a less uniform torque field and approximately a four percent lower torque output compared to a three-phase machine. The three-phase winding, however, requires six solid-state switches compared to four for the two-phase approach. Based upon these considerations, a motor with six poles and a three-phase stator winding was used as the baseline design.

5.2.2.2.1 Power Output

Figure 16 shows a typical performance curve for a rare-earth-cobalt, permanent-magnet, brushless dc motor designed for servo applications. The motor has a peak output, corresponding to maximum speed and current limit, of 8 hp. The extremely high power output for this small unit results from two basic design features. First, the use of rare-earth-cobalt magnets, which offer high energy products, and second, the arrangement of the magnet in the rotor and using brushless commutation of the coils in the wound stator (References 7 and 8). This latter feature results in improved thermal control of the motor. The motor losses (copper losses in the stator) can be readily transferred to the motor casing, as compared to a wound-rotor configuration.

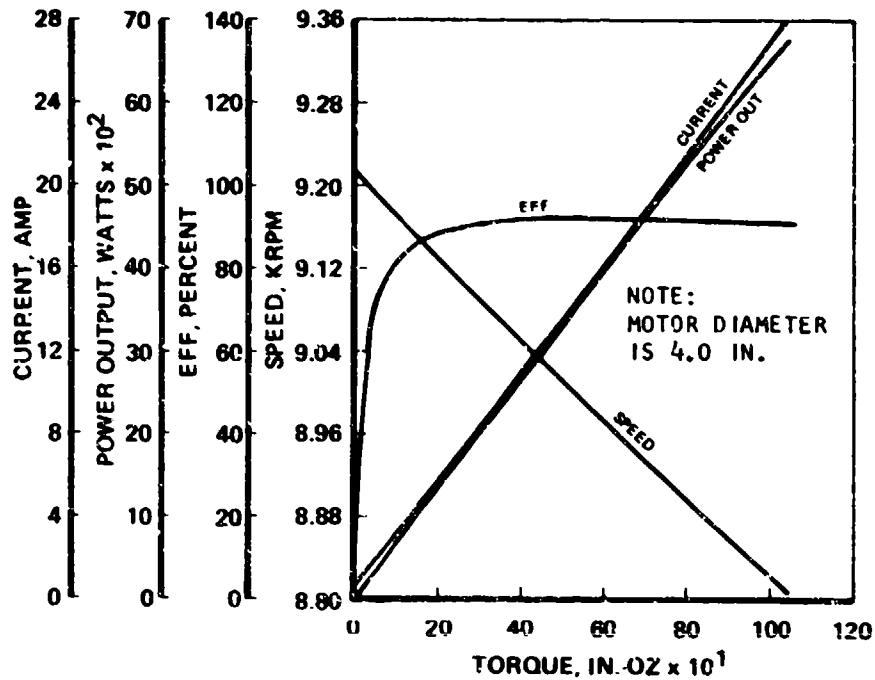


Figure 16. Typical Motor Performance

The energy product relationships of currently available magnet materials are presented in Figure 17. As shown, the samarium-cobalt magnets (SM-CO) exhibit a BH product 3 to 4 times greater than Alnico magnets (Reference 9); the benefit derived from this parameter is that the Sm-Co unit will provide the same torque and faster acceleration than the equivalent Alnico unit, but will weigh 40 percent less and will be one-half the size of the motor using the magnets with the lower energy product. Recently, magnet materials having energy products in the range of 40 to 50 $\times 10^6$ Gauss-Oersteds have been produced in laboratory quantities. As these materials become commonly available for servomotor applications, they will have the following impact upon flight control servo actuators.

- (a) Smaller rotors, yielding faster response and lower weight
- (b) New construction techniques and magnet/stator arrangements that will reduce overall cost. The potential configuration changes are as follows:
 - (1) Tangential vs radial magnet arrangements (See SA71060, Section 6).
 - (2) Toothless stators, resulting in lower cost of manufacture
- (c) Improved resistance to demagnetization due to high magnetic flux fields from electrical sources, lightning, and electromagnetic pulses.

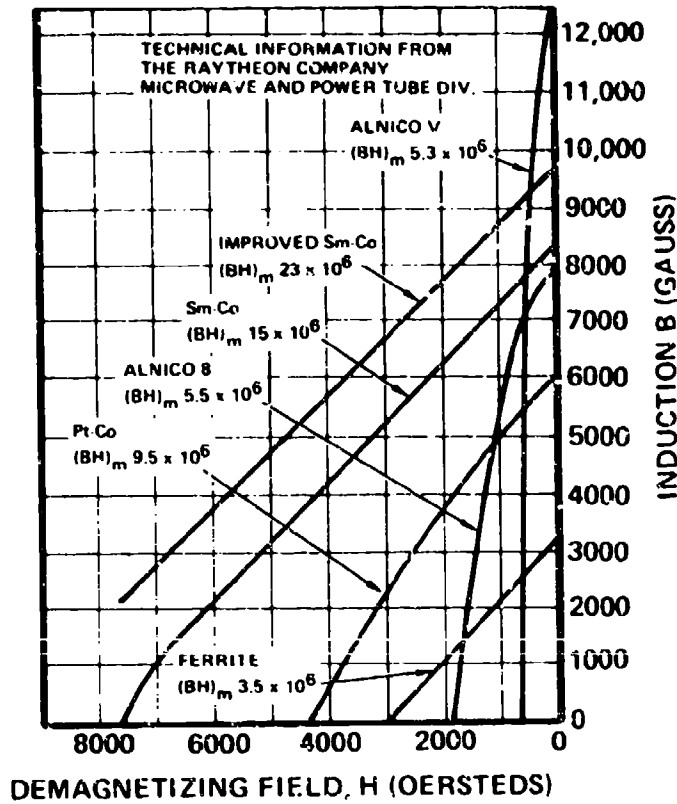


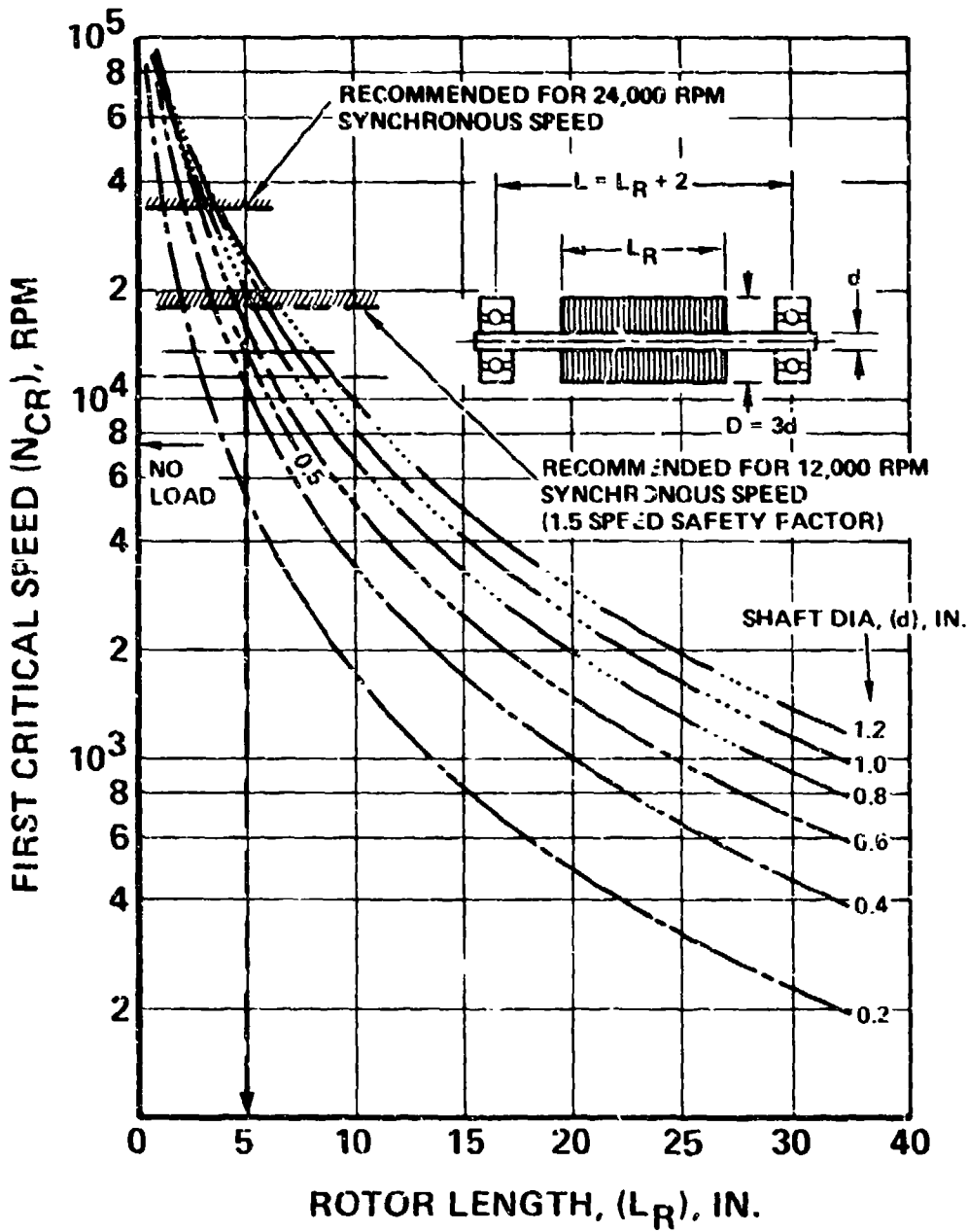
Figure 17. Comparison of Magnet Materials

5.2.2.2 Thermal Capability

The motor is not normally capable of operating continuously at stall unless the motor is designed for a very low speed and used with little or no gear reduction (a torquer design). However, a similar result can be achieved without sacrificing power output capability by using a servoamplifier with a current-limiting feature. Using a current limiter, high acceleration and rate performance can be realized along with a stall capability adequate for flight control applications, (see Section 4).

5.2.2.3 Ac Induction Motor

The characterization of the ac induction motor is based upon the same set of operating characteristics as the dc brushless. The motor diameter was set at 4-in. maximum, with a 1.5-in.-dia rotor, which is the same as the dc motor presented earlier. Rotor inertia for a design using copper conductors and a rotor length of 5 in. was determined to be $0.002187 \text{ lbf-in.-sec}^2$. The relationship of rotor geometry to critical speed is shown in Figure 18. Because the



S-98070 - B

Figure 18. Rotor Critical Speed

ac motor is designed as a servo, the time constant of the motor is low. For commands requiring slew of the control surface, the motor will be operating at no-load speed for a short period of time. The use of first critical speed as a criterion for rotor design is therefore a conservative approach. Other characteristics of the machine are presented below.

Load inertia torque:

$$T_{IL} = I\ddot{\theta}$$

$$T_{IL} = (46.31 \text{ lbf-in.-sec}^2) (52.55 \text{ rad/sec}^2) = 2433 \text{ lbf-in.}$$

From the relationships of Section 4, gear ratio (gearbox efficiency = 93 percent):

$$G = \sqrt{\frac{37575 - 2433}{(0.002187)(52.55)(0.93)}} = 573$$

Motor no-load speed at = 255 Hz, four-pole motor:

$$\theta_{MNL} = \frac{1.396 \frac{\text{rad}}{\text{sec}} \times 573 \text{ gear ratio} \times 60 \frac{\text{sec}}{\text{min}}}{2\pi \text{ rad/revolution}} = 7643 \text{ rpm}$$

Maximum motor stall torque required:

$$T_{MS} = \frac{37575}{(573)(0.93)} = 70.51 \text{ lbf-in. (assume 72 lbf-in. to allow for motor internal mechanical losses)}$$

Establish current limit of 30 amp/phase during acceleration:

$$\text{Torque/amp} = \frac{72}{30} = 2.40 \text{ lbf-in./amp}$$

Maximum theoretical torque/amp at 0.80 PF and 7500 rpm (100 percent efficiency), 100 v is calculated as:

$$\begin{aligned} \text{Torque/amp} &= \frac{(3\phi)(100 \text{ v})(0.8 \text{ PF})}{(746 \frac{\text{W}}{\text{HP}}) \times (7500 \text{ rpm})} \times 63025 \frac{\text{lbf-in.}}{\text{rad} \times \text{min} \times \text{HP}} \\ &= 2.70 \text{ lbf-in./amp} \end{aligned}$$

The power characteristics of the ac induction motor are shown in Figure 19 for the condition of an applied frequency of 255 Hz and 100 volts. This torque-speed plot shows a stall torque of approximately one-half the peak torque value. To provide a more uniform torque from stall to near-synchronous speed and to limit rotor heating (which occurs at high slip), the motor is driven by a variable frequency. The generator frequency is a function of motor speed. Therefore, the motor drive frequency is continuously variable from synchronous speed at full-rated no-load speed down to approximately 10 percent of maximum synchronous speed.

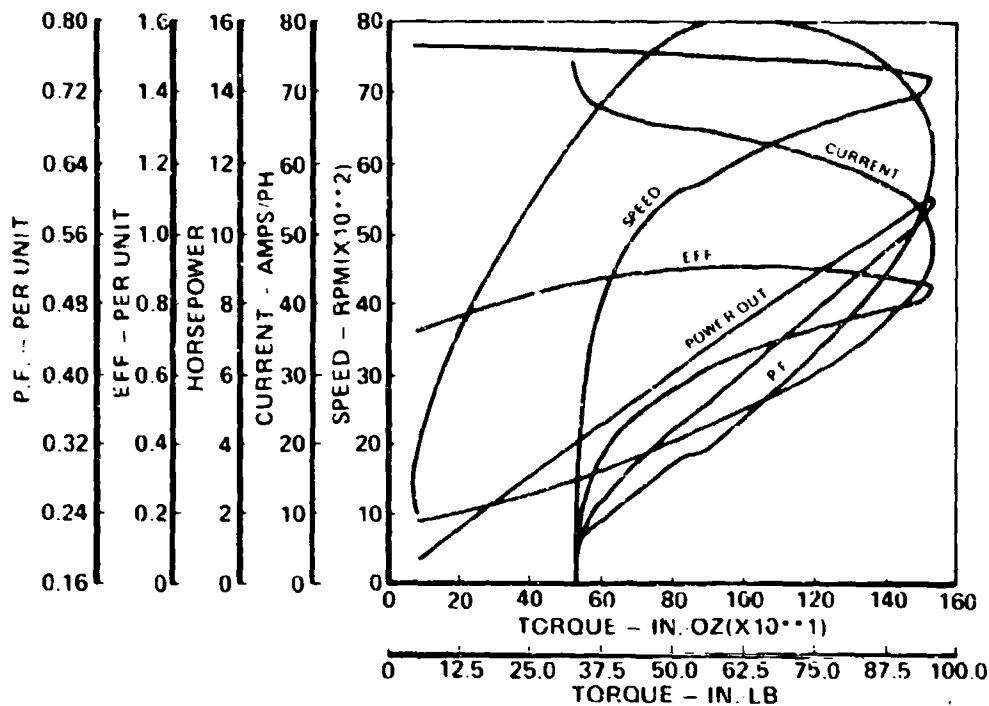


Figure 19. Motor Power Characteristics

Five selected torque-speed curves from the continuously variable family of relationships are shown in Figure 20. As frequency is adjusted, so is the applied voltage. Figure 21 shows the relationship of voltage and slip to the applied drive frequency. Table 6 presents performance as the motor increases in speed.

The losses calculated for the ac machine are presented in Table 7. The thermal management of electrical losses is the key to servomotor design. Experience has shown that a temperature rise of 175°F measured at the end bell is the maximum practical temperature rise for long bearing and lubricant life. Similarly, a winding temperature of 430°F is the maximum value for state-of-the-art ML-type insulations. Practical design experience shows these maximum temperature levels to be experienced with a thermal watt density of 2.5 watts per sq in. of total motor surface area (including the end bells). The allowable maximum duty cycle of high-performance servomotors is therefore a direct function of the cooling available. Using the aircraft structure as a motor heat sink will obviously extend the duty cycle. The use of forced air, fluid cooling, or submerged motor components is not considered for thermal management. The savings in motor size and weight resulting from the cooling is less than the associated pumps, heat exchangers, fluid loops, and controls. Complexity of such an approach also makes it unattractive.

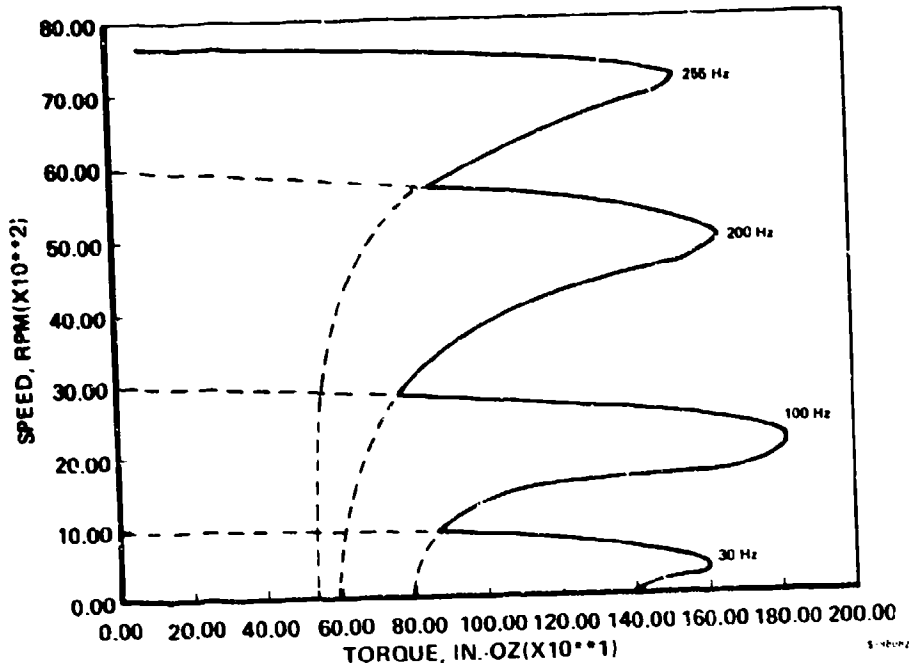


Figure 20. Variable Frequency Motor Drive

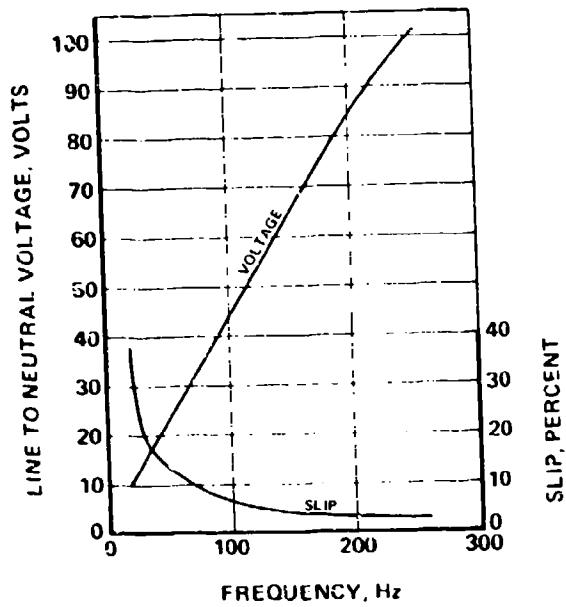


Figure 21. Ac Inverter Voltage Schedule

TABLE 6

AC INDUCTION MOTOR PERFORMANCE DURING STARTUP

Voltage	Frequency, Hz	Current, amp	Torque, lb.-ft.	Speed, rpm	Power Factor	Voltage Schedule, v/Hz	Specific Torque, in.-lb/amp		Efficiency, P ₀ /P _i , Percent
							Theoretical	Design	
10	20	29.2	72	370	0.87	0.5	5.96	2.466	41
15	30	26	72	720	0.83	0.5	4.38	2.769	64
45	100	26.2	72	2820	0.8	0.45	3.24	2.75	81
85	200	27	72	5800	0.79	0.425	2.953	2.667	69
100	252	28.8	72	7300	0.79	0.397	2.74	2.50	90
102	255	28.5	72	7450	0.795	0.4	2.759	2.53	90

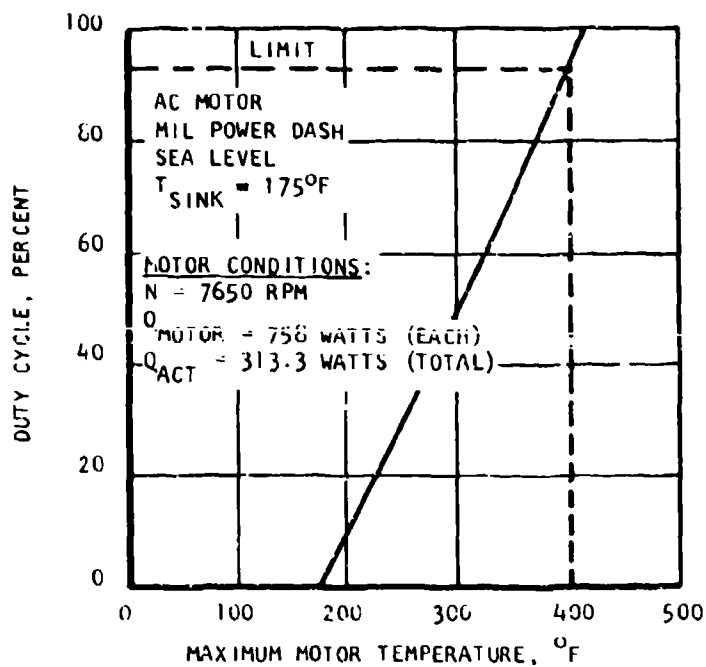
TABLE 7

AC INDUCTION MOTOR LOSSES

Condition		Power, Watts	Slip		Losses, Watts				Total
Voltage	Frequency, Hz		rpm	percent	Stator Copper	Rotor Copper	Total Core	STRAY (Stator Copper)	
10	20	309	230	38	230	3	213	16	462
15	30	665	180	20	237	213	7	27	484
45	100	2501	180	6	191	162	38	81	472
85	200	4923	200	3.3	185	168	100	148	600
100	252	6266	260	3.4	230	225	115	190	758
102	255	6341	200	2.6	206	215	120	190	731

RUNNING CONDITION AT LOAD POINTS	
Power	Total Losses
1492 (2 hp)	396 (η = 79 percent)
2238 (3 hp)	491 (η = 82 percent)
2984 (4 hp)	485 (η = 86 percent)

Figures 22 through 24 show the results of thermal analyses of the motor shown in SK71068. The analytical thermal model included the heat sink effects of the actuator and the aircraft structure. The thermal model of the structure was determined from a typical installation for the F-100 alleron. The analysis indicates that the actuator duty cycle is not severely limited by the environment except for ground operation on a hot day. However, since this condition represents a checkout operation, the 40 percent duty cycle limitation may not be an over-riding constraint.



5-670

Figure 22. Motor Thermal Analysis for MIL Power Dash

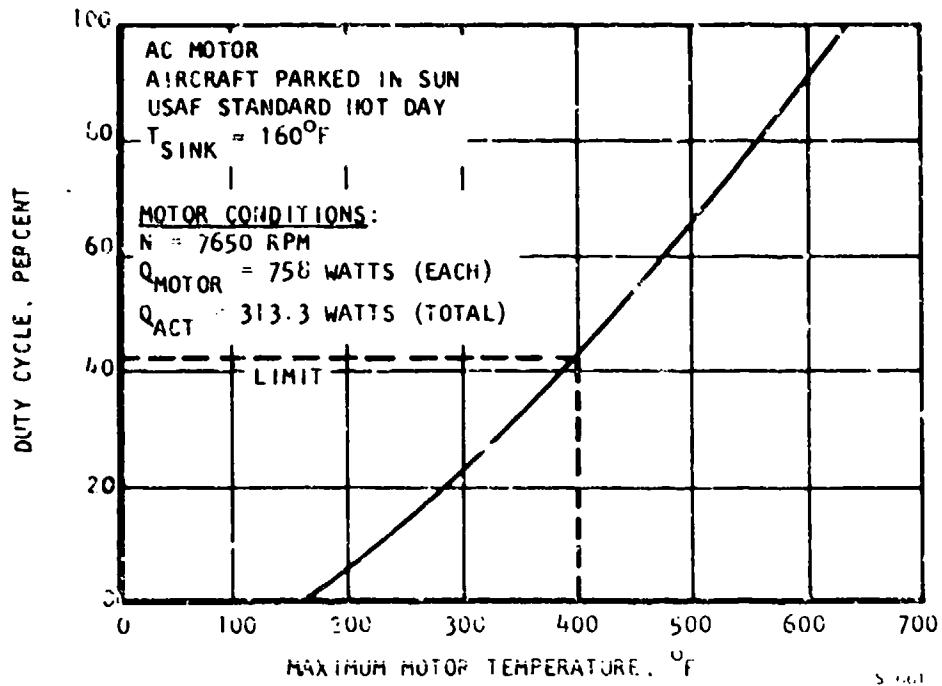


Figure 23. Thermal Analysis Results for Parked Aircraft on USAF Standard Hot Day

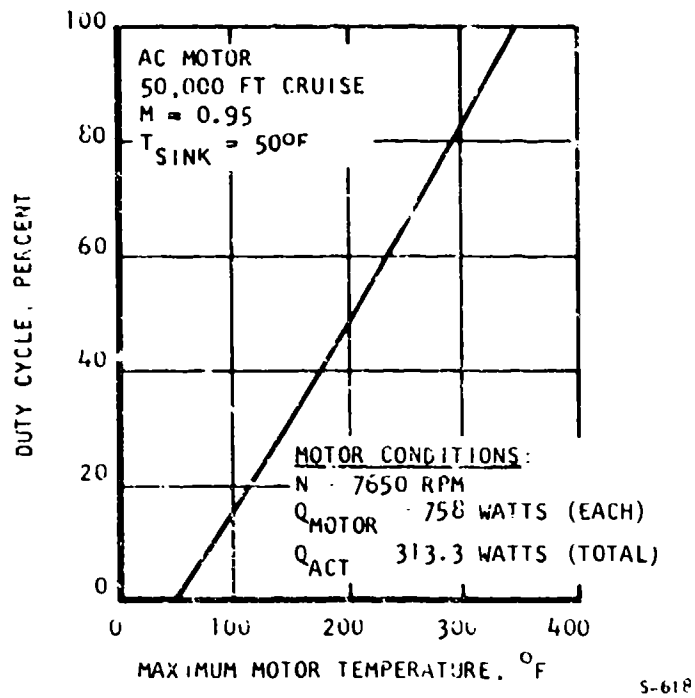


Figure 24. Thermal Analysis Results for 50,000-ft Cruise

5.2.2.4 Controller Characteristics

5.2.2.4.1 Servo Design Considerations

Servoloops may be analyzed using frequency or time domain analysis techniques. For a frequency domain design, the specifications are usually given by gain margin, phase margin, peak resonance, and bandwidth. These criteria are related to time domain specifications such as rise time, delay time, settling time, and overshoot. Two common methods of stability analysis and design are the bode diagram and the root locus. The bode diagram is a plot of gain and phase shift versus frequency. It is obtained from the loop transfer function by replacing S by $j\omega$, where ω is the angular frequency of excitation. The root locus is an S plane plot of the locus of the poles of the feedback transfer function as the loop gain is increased from zero to infinity. The main advantage of the bode diagram is ease of use, and of the root locus, the ability to closely estimate the loop time and frequency responses directly from the S -plane plot.

A proportional type control system develops a correcting signal that is proportional to the magnitude of the actuating signal. If the rate of change and magnitude of the error signal is detected, the system is a proportional plus rate system. The proportional plus rate system may be realized with a simple lead network. The main advantages of this system are faster response and high accuracy. A proportional plus integral compensating network may be a more desirable system, and can be realized by using a lag network. This system will produce a feedback network with high accuracy.

The steady-state error of the feedback control system may be determined by computing the position, velocity, and acceleration error constants. The error constant is defined as the desired output divided by the steady-state error. The steady-state error is the error in displacement at the servo loop output due to a step, ramp, or acceleration input. If a pure time lag exists in a servosystem, the output will not begin to respond to a transient input until after a given time interval. Because of the time lag effect, the transfer function of the system is not a quotient of polynomials; it consists of the term e^{-TS} where T denotes the time lag or transportation lag. For a servoloop with transport delay, the compensation network may be designed with two parts, the first part to cancel the effects of e^{-TS} and the second part to equalize the controlled system without delay.

The servo techniques discussed above can be used with both analog and digital controller systems. For an analog system, the input-output relation of both parts of the system can be described and analyzed with the Laplace transform and the bode diagram. For a digital control system, the motor controller is considered to be a closed-loop sampled data system. The digital system can be analyzed with the Z transform. The loop compensation network can be realized with a digital filter. Use of the bilinear transform allows digital controller design using the Bode diagram method.

For the analog system, the compensation network can be realized with a simple resistance and capacitance network. The circuit synthesis can be obtained by equating like coefficients of the transfer function of the RC

network with the transform function of the proportional plus rate or integral system. For a digital compensation system, the digital filter can be implemented with either the recursive (feedback) or nonrecursive method. The advantages and disadvantages of both methods are listed below.

Recursive Filter

Advantages--Infinite memory, fewer terms to describe a sharp cutoff filter, and more complex processing capability

Disadvantages--Insufficient word length may cause instability

Nonrecursive Filter

Advantages--Excellent linear phase characteristics, and no stability or limit cycle problems

Disadvantages--Large number of terms required for sharp cutoff filter

5.2.2.4.2 Current Limiting

Current limit controls provide needed protection for the motor and the semiconductors in the power unit and limit the electrical demand from the power bus. Two commonly used current limit techniques are the spillover and the current minor loop method. In the spillover current-limit circuit, the armature current is compared with the limit point value I limit. When the armature current I_a exceeds I_a limit, the error correction signal changes in the direction to decrease the current. This current-limit circuit is implemented in a minor feedback control loop. The correction signal is scaled such that the magnitude of the change is proportional to the amount by which I_a exceeds I_a limit. If the gain of the limit circuit is high, the circuit may be unstable in limit. Overshoot is also a design consideration for this approach.

A tighter control over armature current is provided with the current minor-loop approach. The current minor-loop method is a continuous feedback system that prevents overshoot by clamping the error and the rate of change of the error to adjustable values. The method is implemented by incorporating a zener diode current limit clamp around the error correction amplifier in conjunction with a current rate-of-change limiter in the forward path of the servoloop.

5.2.2.4.3 Power Switch Selection

The switching devices in the commutator may either be silicon control rectifiers (SCR's) or transistors. In either case, the devices have diodes connected across them in inverse parallel. Until recently, most commutators have used SCR's as the switching element because they were the only devices available with the necessary high voltage and current ratings. One of the drawbacks in using SCR's is the requirement for a commutation circuit to turn off the device. Figure 25 shows a typical SCR commutation circuit. The AUX SCR is turned on and discharges the capacitor to provide a reverse

bias in the main thyristor. The turnoff time is proportional to the size of the commutation capacitors and the voltage to which they are charged, and inversely proportional to the current to be commutated. Darlingtons with high voltage and current ratings now provide an alternative in the design of the power stage of the inverter circuit. The Darlington circuit (shown in Figure 26) produces a power stage that is significantly smaller than SCR commutators in size and weight. PWM requires that the switching transistors be operated at a frequency several times higher than the signal frequency; switching losses in SCR's become appreciable at frequencies above 1 kHz, while the Darlington transistors can be operated easily to 20 kHz.

5.2.2.4.4 Brushless Dc Motor Control

The torque in an electric motor is produced by the interaction between the magnetic fields in the rotor magnets and the stator conductors. The axis of the magnetic field established by the stator current is displaced at some angle

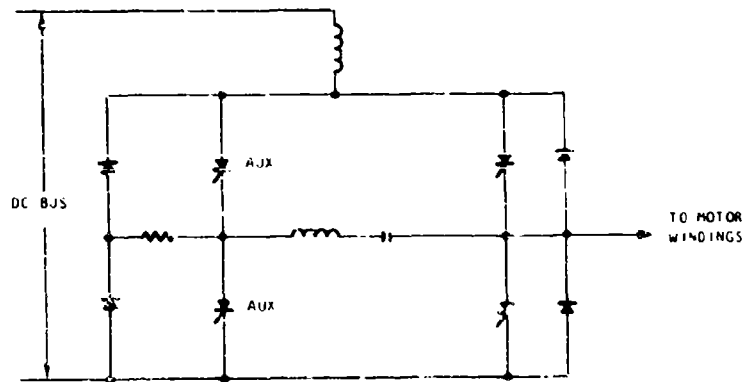


Figure 25. SCR Commutation Circuit

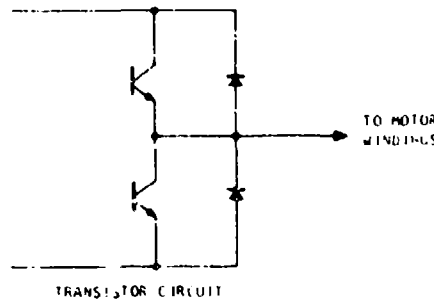


Figure 26. Transistor Commutation Circuit

from the axis of the rotor flux field. The torque generated by the interaction of the two fields is given by

$$T = \pi F_{PK} B_{PK} L r \sin \delta$$

where T = torque

F_{PK} = maximum stator MMF (assume sine wave)

B_{PK} = maximum air gap flux density

L = rotor length

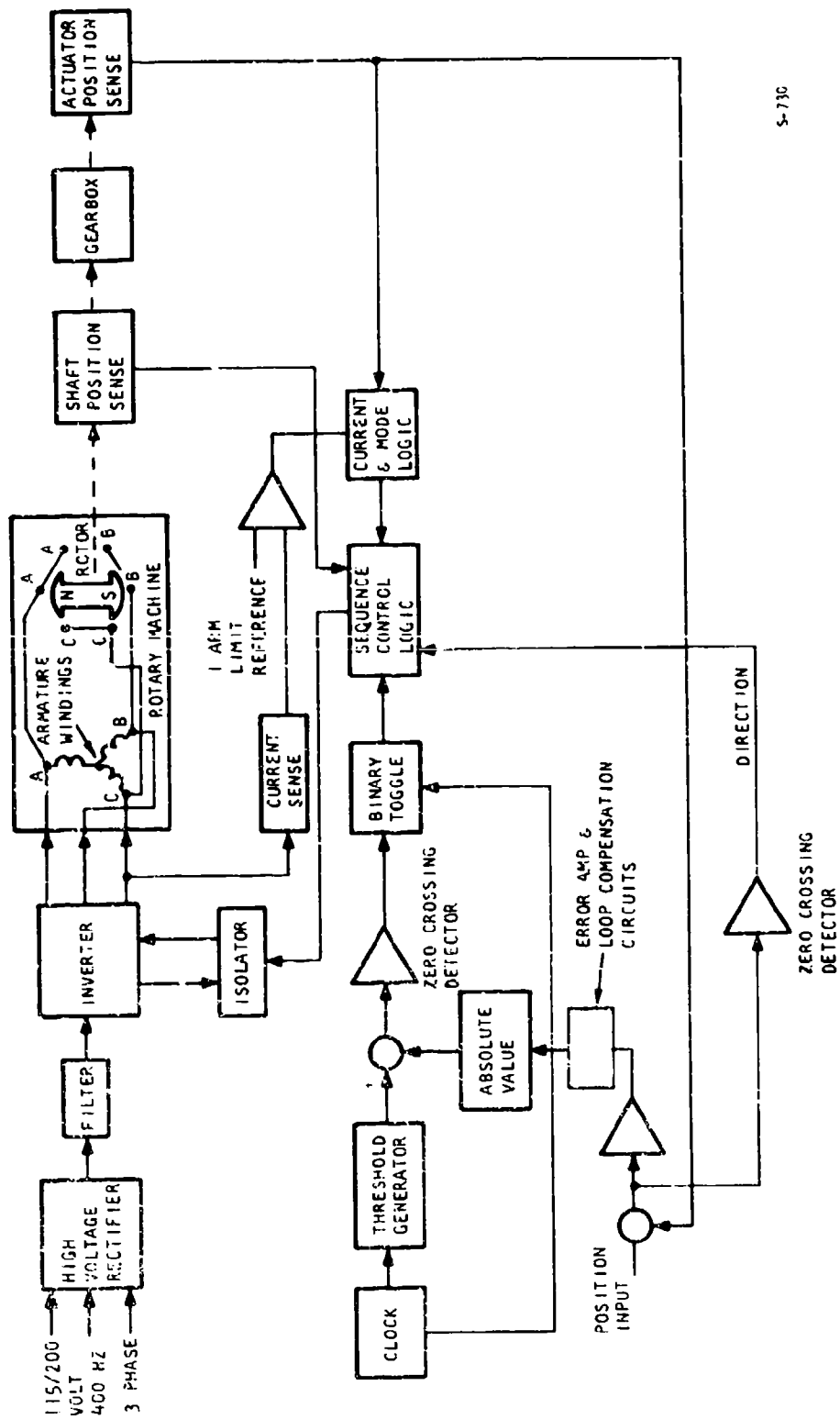
r = rotor radius

δ = angle between stator MMF and rotor flux field

To maximize torque, δ must be maintained close to 90 deg. In a brush-type dc motor, this relation is obtained by the position of the brush axis with respect to the main rotor axis. In a brushless dc motor, this relationship is controlled using a rotor position sensor. Therefore, torque control corresponds to controlling the magnitude of stator current for any fixed value of δ , the angle between the stator and rotor magnetic fields.

The stator consists of several discrete stator windings. Current is supplied to the proper stator windings by an electronic commutator, as a function of sensed rotor position. The commutator consists of solid-state switches used to connect selected stator windings to the dc bus as a function of rotor position. The current wave form, frequency, and phase are determined by switching times, and the amplitude by pulse-width modulation of the dc bus voltage (Reference 10). For the 3-phase stator winding being considered, two switches are conducting at any one time; every 60 deg of rotation one switch is turned off and a new one is turned on to obtain the required current pattern and resulting rotating magnetic field in the stator. The rotor position sensor controls the limits of the turn-on and turn-off points of the commutation switches to provide the maximum torque per amp ($\delta = 90$ deg). The duration of switch on-time provides the control of current magnitude necessary to control output torque.

The use of a digital shaft encoder will simplify the machine-circuit interface. For example, absolute optical encoders are available which require less torque to turn the shaft; operate faster than mechanical encoders; provide long life; and exhibit a memory such that power outages will not affect the output when power is restored. In the brushless dc motor, the torque is controlled by adjustable average current supplied through the electronic commutator. Either phase (δ) control or PWM techniques may be used to generate the required voltage. A coil will be required as a smoothing reactor to suppress the ripple current if a phase control circuit is used to generate the voltage. Figure 7 is a functional block diagram of a dc drive system. Its basic features are: (1) power circuits and line isolation technique identical to ac drive, (2) PWM control for a simplified voltage control circuit, and (3) adaptable to digital implementation.



5-730

Figure 27. DC Drive functional Block Diagram

5.2.2.4.5 Ac Induction Motor Control

When sinusoidal input power (neglecting excitation losses and stator voltage drops) is applied to the stator windings of the ac induction motor, a rotating magnetic field is produced in the stator with angular speed

$\omega_s = \frac{2\omega}{P}$, where P is the number of poles and flux $\phi_s = \frac{V}{\omega}$. If the rotor speed is ω_r , the slip speed will be $\omega_d = \omega_s - \omega_r$.

The difference in speed between the rotor conductors and the rotating magnetic field generates the rotor voltage $V_r = \phi_s \omega_d$. The rotor current will be

$$I_R = \frac{V_r}{\sqrt{R_r^2 + (\omega_d L_r)^2}}$$

where R_r = rotor resistance and L_r = rotor reactance. The rotor flux is given by $\phi_R = I_R \frac{\phi_s \omega_d}{\omega}$. The rotor flux lags the stator flux by $\theta = \frac{\pi}{2} + \tan^{-1} \frac{\omega_d L_r}{R_r}$, and the motor torque is given by

$$T = \left(\frac{V}{\omega}\right)^2 \frac{\omega_d R_r}{R_r^2 + (\omega_d L_r)^2}$$

The torque is dependent only on slip ω_d in the constant torque speed range if $\frac{V}{\omega}$ is held constant. $\omega_{ds} = kr/L_r$ is defined as the breakdown point. Operation

below breakdown will yield high efficiency and high power factors. The results are comparable to dc machines. The speed of the motor can be varied by adjusting the stator frequency if the flux is maintained at a level high enough to prevent saturation. The direction of slip relative to the stator determines the direction of power flow, while the voltage determines the level of torque.

A functional block diagram of a variable-voltage, variable-frequency ac drive system is shown in Figure 28. Salient features are:

- (a) Direct line rectification to minimize weight (no transformer input in power circuit).
- (b) High-voltage mode for increased efficiency
- (c) Darlington transistor commutator to simplify turnoff
- (d) Use of optical couplers to protect the control interface
- (e) Torque control with slip $\left(\frac{V}{f} = \text{constant}\right)$ to minimize heating
- (f) PWM drive for low harmonic content
- (g) Digital implementation for versatility

Inverter circuits are generally employed to generate the desired excitation signal. The inverter circuits associated with a variable-speed ac drive may be classified into two groups: (1) amplitude modulation or (2) PWM. For six-step amplitude modulation, the line-to-neutral applied sine wave signal is approximated by a six-step waveform. A phase-controlled dc source or a chopper may be used to generate the dc source required for the six-step modulation circuit. A smoothing filter is required to minimize the beating of the motor currents caused by the difference in inverter output and the rectified line or chopper frequency. The use of the chopper with a full-wave bridge will produce a faster voltage response due to the smaller LC filter time constant.

The PWM inverter is a simple control circuit that generates both frequency and voltage. The output voltage waveform is a constant amplitude pulse train whose polarity changes periodically to provide the motor fundamental frequency. The magnitude of the fundamental is varied through pulsewidth control. The inverter is modulated to a sine wave envelope, and the modulating frequency is set high enough to be rejected by the motor.

When induction motors are driven by PWM inverters, both the magnitude and frequency of the harmonics must be carefully controlled. The presence of large-amplitude harmonics will increase motor heating and peak currents and may affect torque production. The harmonic contents of the PWM waveform may be analyzed with the Fourier series. Figure 29 shows a plot of the Fourier coefficient of a 5f waveform. From odd-half symmetry considerations, the even harmonics are zero. Trap circuits can be used to reduce the eleventh and thirteenth harmonics. In general, as the number of pulses approach a large number, the harmonic content approaches the value for an equivalent square wave: one-fifth for the fifth harmonic, one-seventh for the seventh harmonic, etc.

PWM harmonic control schemes may use a carrier-to-signal frequency ratio which is either fixed or adaptive. The harmonic content in a fixed-ratio system will cause losses and unnecessary temperature rise. In one adaptive modulation scheme, the number of pulses per half-cycle increases as the signal frequency decreases. The pulsewidth is then varied to obtain voltage control. In a second method, the carrier is identified as a triangular wave with a fixed frequency. Both the amplitude and frequency of the sine wave is varied to generate the inverter control signal. The use of many pulses per half-cycle reduces the harmonic content, but requires fast turn-off switches, and commutation losses may be significant if SCR's are used.

5.2.3 Tradeoffs

5.2.3.1 Motor

The comparison of the motor performance is presented in Table 8. The thermal management characteristics of the two machines are described in Figure 30. The allowable duty cycle for the dc machine is higher than the ac machine because of the higher efficiency and the preferable loss distribution in the stator. A minor consideration in favor of the ac machine is the relatively lower cost compared to the dc motor. The magnet material and the rotor construction costs are more expensive than for the ac rotor. The stator, end bells, and housings for the two motors are very similar in cost. Total system costs will be very similar when including the actuator and controller.

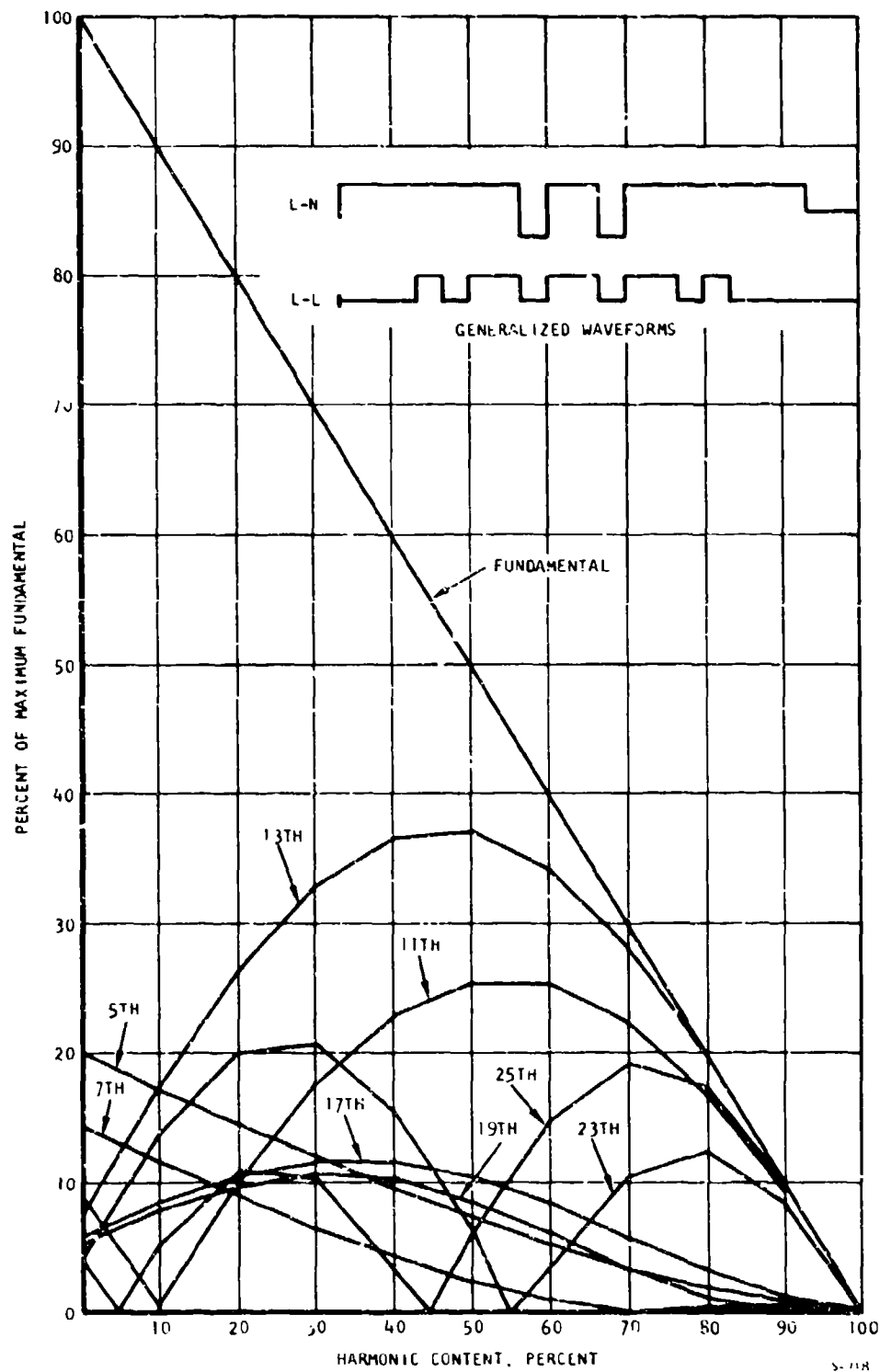


Figure 19. Harmonic Content of 5-Phase Inverter (Motor Center at 75 Deg)

TABLE 8
MOTOR COMPARISON

Parameter	Ac Motor	Brushless Dc Motor
No-load speed, rpm	7643	9200
Motor accelerator, rad/sec	30,369	35,510
Current limit, amp	30	29
Actuator gear ratio	573	670
Maximum output acceleration, rad/sec ²	53	53
Outside diameter, in.	4	4
Overall length, in.	8-3/4	7-1/2
Weight, lb	19	18
Rotor diameter, in.	1.5	1.5
Rotor length, in.	5	4

5.2.3.2 Controller

Analog and digital power servo concepts are compared in Table 9. The microprocessor provides the desirable operational characteristics of flexibility, versatility, and low cost. The hardware design can be fixed, while the functional characteristics can be tailored to meet modified performance requirements. The microprocessor motor control versatility is further illustrated in Table 10. By changing only software, the microprocessor can operate either on an ac or dc servomotor. The processor capability to monitor and fault isolate is an additional advantage. The implementation of control for the ac and dc motors is summarized in Table 11, which shows the similarities in the basic drive requirements for the two approaches. The quantitative method of handling these requirements is accomplished by software changes for the microprocessor as opposed to hardware changes for an analog servosystem.

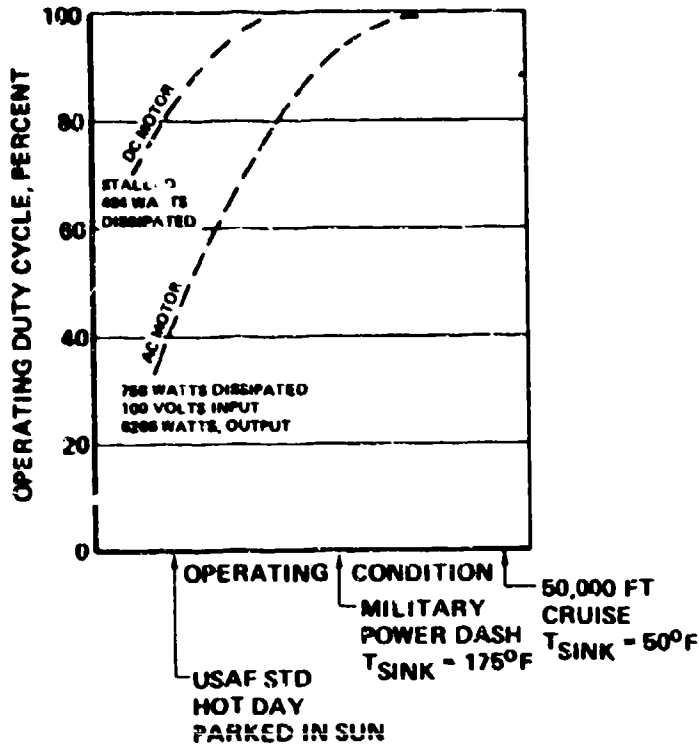


Figure 30. Ac and Dc Motor Thermal Management Comparison

TABLE 9

COMPARISON OF CONTROLLER TYPES

	Advantages	Disadvantages
Analogy	<ul style="list-style-type: none"> ● Simplicity 	<ul style="list-style-type: none"> ● Precision components required in feedback loop ● Not adaptable to changes in system requirements ● Unreliable
Microprocessor	<ul style="list-style-type: none"> ● Versatility ● Simple hardware ● Adaptable to failure and redundancy monitoring ● Adaptive servo capability ● Cost competitive 	<ul style="list-style-type: none"> ● Software design required

TABLE 10
COMPARISON OF DRIVE SYSTEM

	Brushless DC Drive System	AC Drive System
Sensor Requirements	Angular position info required - digital code with magnetic or optical coupling	Shaft angle revolution frequency and applied voltage information to stator
Modulation	Variable dc may be generated with PWM or phase control	PWM inverter is an efficient means of generating a variable voltage and frequency in a single circuit
Power Circuits	Transistor preferred with PWM control because of high frequency switching	SCR requires forced commutation circuit to start
Performance	Wide range of speed control with voltage control; current limit used to reduce stator heating	Comparable to dc motor if slip is constrained to values below breakdown
Microprocessor Control	Simple software and hardware control	Simple hardware - slightly more complex software than dc controller

TABLE 11
SIMILARITIES IN MOTOR CONTROL CONCEPT APPLICATION

AC DRIVE

- Constant torque
- PWM or amplitude modulation
- Torque control with slip and current
- Adaptable to digital implementation

DC DRIVE

- Constant torque
- Phase control, chopper, PWM dc source
- Optical, magnetic shaft encoders
- Commutation approach adaptable to digital implementation

5.2.4 Selected Drive Approach

The selected drive approach for the hinge-line actuator is a dc. brushless, permanent-magnet motor controlled by a digital microprocessor. The drive system selected for preliminary design is summarized in Table 12. A schematic of the selected drive system is presented in Figure 31. The features listed in this figure emphasize the versatility of the selected approach, which is the principal consideration in selection of the microprocessor for a primary flight control component.

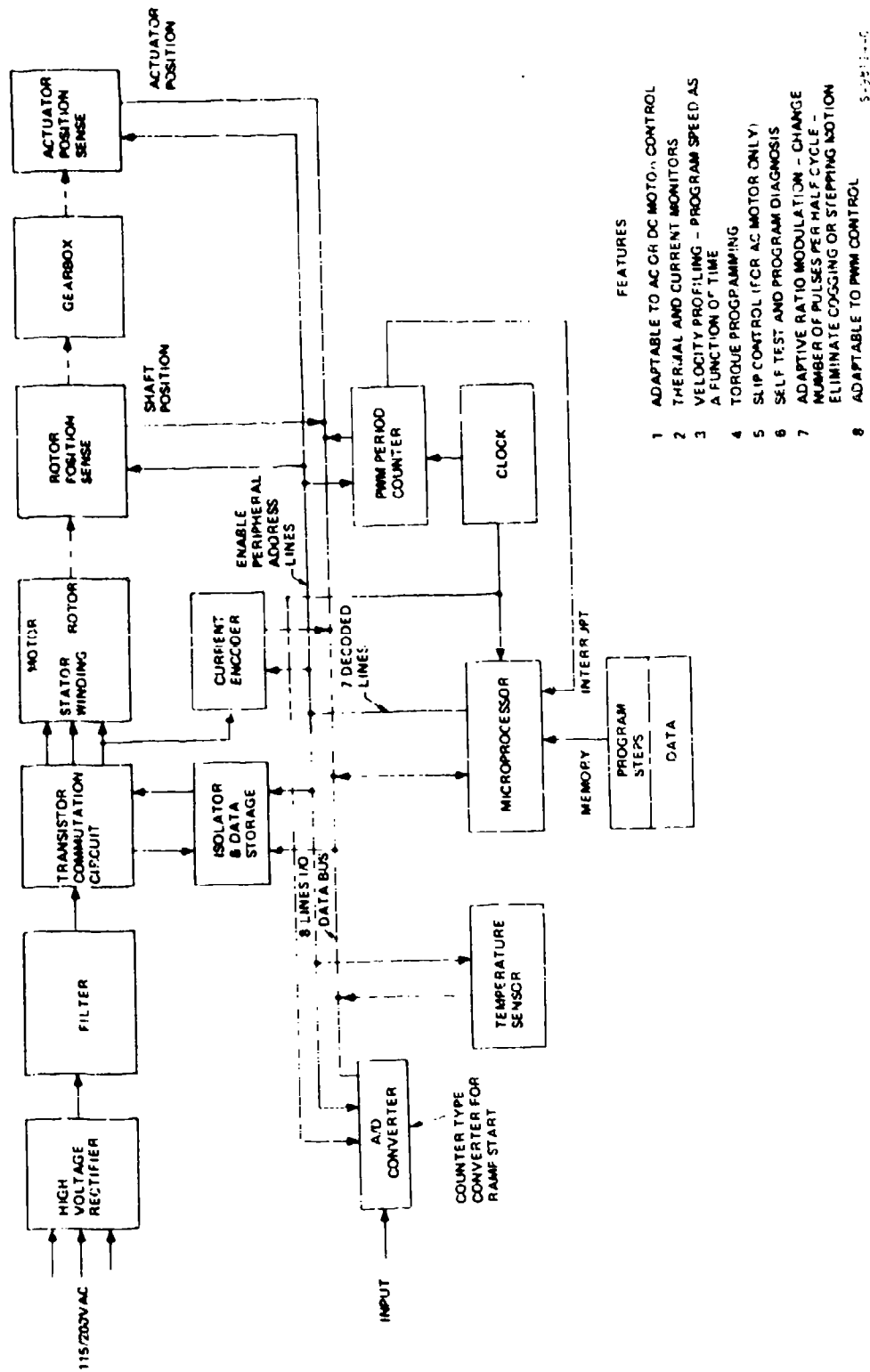
5.3 ACTUATOR ELEMENT OPTIONS

5.3.1 Initial Screening

The options for the mechanical elements of an actuator are shown in Figure 32. The linear actuator is eliminated from further consideration because the baseline design approach (ground rule) is to be a rotary, hinge-line actuator. Within the general category of actuators having a rotary output, there are many implementation techniques. A continuous-running electric drive can be mechanically controlled to provide variable rate by use of intermittent clutching (spring, electromagnetic), or by use of continuously variable toroidal transmission type drives. Intermittent clutching devices are eliminated from the study because of serious limitations of life, repeatability, and reliability.

TABLE 12
DRIVE SYSTEM FOR PRELIMINARY DESIGN

1. PROGRAMMABLE MICROPROCESSOR CONTROLLER
2. EMPHASIS ON BRUSHLESS DC MOTOR CONTROL
3. DIGITAL FILTER COMPENSATION
4. NON-ADAPTIVE PWM CONTROL
5. OPTICAL POSITION AND FREQUENCY ENCODERS
6. TRANSISTOR POWER SWITCHING
7. USE OF CURRENT AND TEMPERATURE MONITOR
8. USE OF AIRCRAFT PARAMETERS FOR TORQUE LIMITING



FEATURES

- 1 ADAPTABLE TO AC OR DC MOTOR CONTROL
- 2 THERMAL AND CURRENT MONITORS
- 3 VELOCITY PROFILING - PROGRAM SPEED AS A FUNCTION OF TIME
- 4 TORQUE PROGRAMMING
- 5 SLIP CONTROL (FOR AC MOTOR ONLY)
- 6 SELF TEST AND PROGRAM DIAGNOSIS
- 7 ADAPTIVE RATIO MODULATION - CHANGE NUMBER OF PULSES PER HALF CYCLE - ELIMINATE COGGING OR STEPPING MOTION
- 8 ADAPTABLE TO PWM CONTROL

5-2211-100

Figure 31. Selected Drive System

even though they may provide good frequency response. Continuously variable output devices using constant running inputs include the toroidal transmission and the opposing differential types. The toroidal transmission (shown in Figure 33) is not included as a principal candidate because of the limited life of the rolling mechanical elements and low frequency response capability (see Appendix E).

A direct-drive servo offers both reversible and nonreversible operation. The high-efficiency reversible approach is limited to applications where redundancy of actuation is not required. The irreversible approach using brakes or no-backs for position holding is superior to the low efficiency approach because less power is consumed in moving the surface, and the surface is positively locked even in the presence of vibration and periodically reversing loads, which can cause an irreversible geartrain to creep. The most promising actuation system elements are therefore:

Actuator Type--Rotary

Drive Type--Direct-drive servo

Geartrain Efficiency--High (>50 percent)

Position Holding--Motor brake (used on servomotor to lock a standby

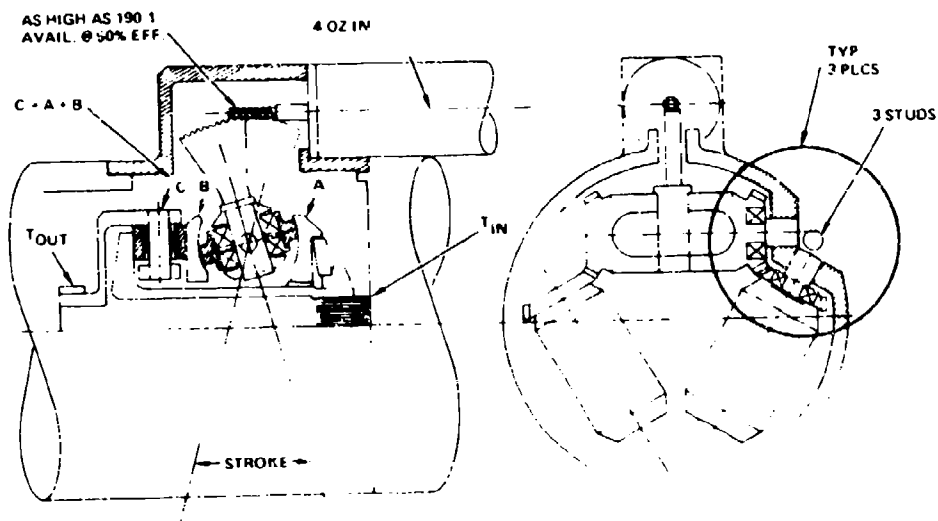


Figure 33. Harmonic Drive

5.3.2 Component Characteristics

5.3.2.1 Rotary Actuator

The characteristics of a planetary geared, rotary, hinge-line actuator of the type shown in Figure 34 are presented in Figure 35, which relates weight, torque, spring rate, and cycle life to the actuator diameter. For example, the 4-in. OD actuator sized for 37,500 in.-lb torque and 100,000 life cycles will have the following characteristics.

- Torque per unit length: 6,000 lbf-in./in.
- Spring rate per unit length: 600,000 lbf-in./rad-in.
- Weight per unit length: 2 lb/in.

The length of the actuator is obtained by dividing the specific torque value into the load torque required, as follows:

$$\text{Actuator length} = \frac{37,500 \text{ lbf-in.}}{6,000 \text{ lbf-in./in.}} = 6.25 \text{ in.}$$

Based upon this length, the other characteristics are determined as follows:

Actuator spring rate:

$$600,000 \frac{\text{lbf-in.}}{\text{rad-in.}} \times 6.25 \text{ in.} = 3.75 \times 10^6 \frac{\text{lbf-in.}}{\text{rad}}$$

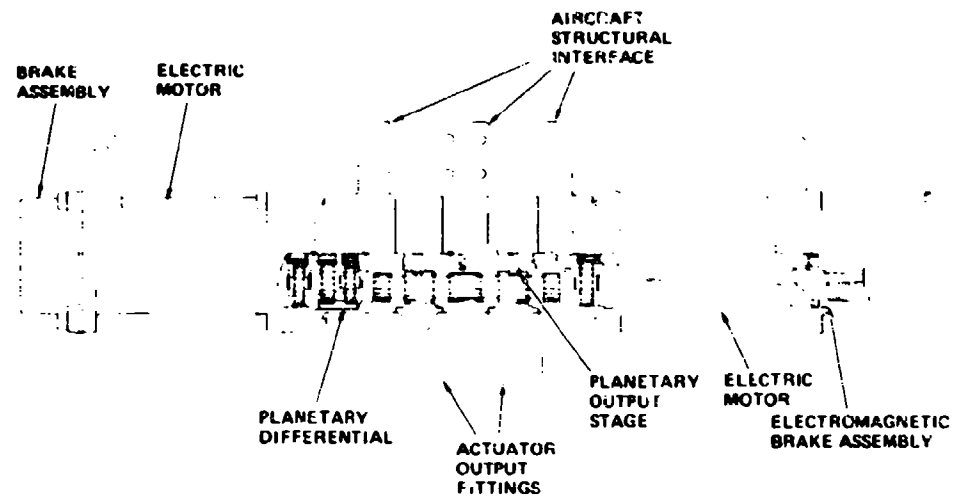
Actuator weight:

$$2 \text{ lb/in.} \times 6.25 \text{ in.} = 12.5 \text{ lbs}$$

The parametric data are extrapolated data from the following aircraft systems which use rotary actuators.

- F-16 leading edge flap
- F47 leading edge flap
- SST flap
- B-1 bomb bay door

A harmonic drive of the type shown in Figure 36, was sized to provide the 37,500 lbf-in. torque corresponding to the example problem situation. Figure 37 compares the characteristics of the harmonic drive and the planetary gear actuator. Also included are catalog data obtained for a pancake harmonic drive.



1-98-30

Figure 34. Hinge-Line Actuator

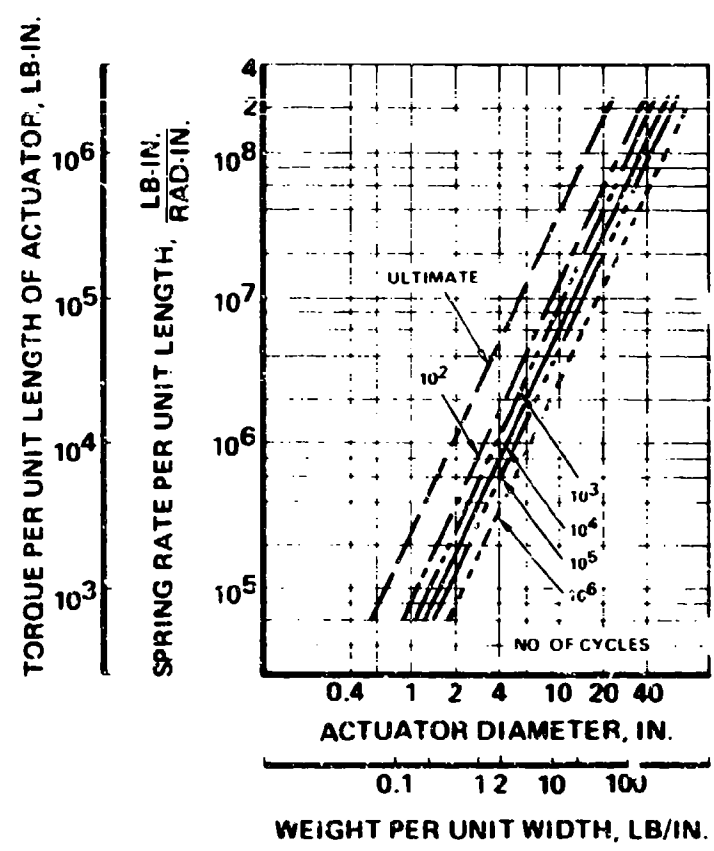


Figure 35. Parametric Rotary Actuator Data

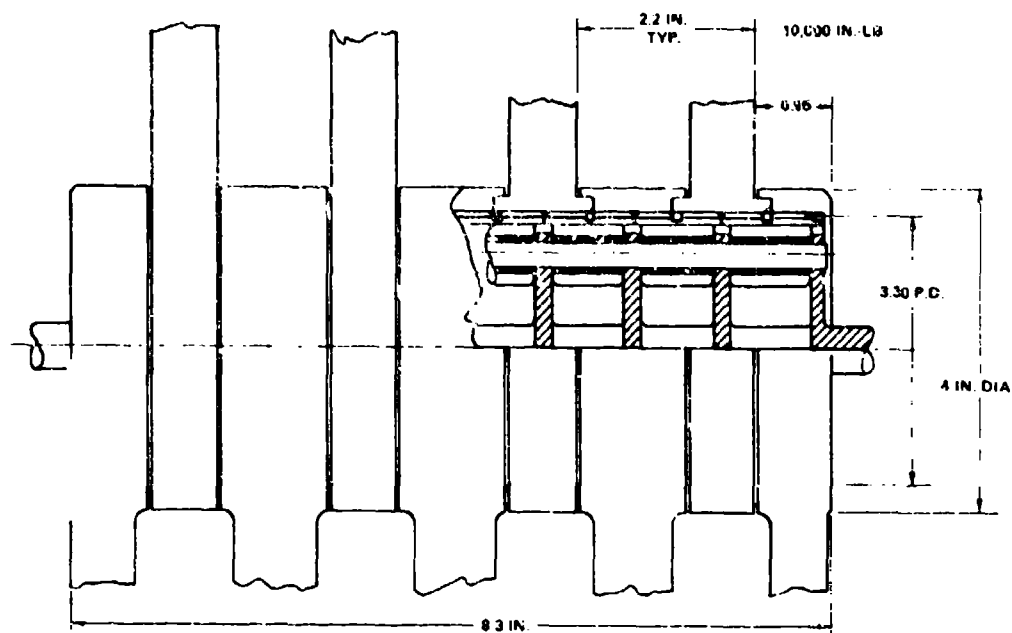


Figure 36. Harmonic Drive

TABLE 13
ACTUATOR COMPARISON

Characteristic	Planetary Geared Drive	Harmonic Drive	Pancake Harmonic Drive
Diameter, in.	4.0	4.0	4.33
Length, in.	6.25	8.5	29(1)
Weight, lb	12.5	13	83(2)
Volume, cu in.	78.5	104	421
Efficiency, percent	90	85	53

(1) 36 "pancake" slices in parallel

(2) Configuration is not weight-optimized for aircraft application

5.3.2.2 Velocity Summing Differential

A velocity summing differential is required when redundant electric motor drives are used. Since the actuator provides a gear ratio of approximately 250 to 1, the torque rating of the differential is as follows:

$$\frac{37500 \text{ lbf-in.}}{250} = 150 \text{ lbf-in.}$$

The resulting weight of the mixing differential is 2 lbm. Added to the actuator weight, the total weight of the mechanical drive is 14.5 lbm.

5.3.2.3 No Backs and Brakes

A no-back is a device that allows power to pass from the input to the output with high efficiency, and which acts as a positive brake to prevent power from being transmitted from the output back to the input. The characteristics of a no-back are shown in Figure 37. The major features of the device are:

- (a) No motion when the point of operation determined by the input and output torque falls in the cross-hatched area of Figure 37.
- (b) The input must be driven to produce motion at the output.
- (c) A friction drag of 1 to 3 percent is experienced when driving an opposing load.

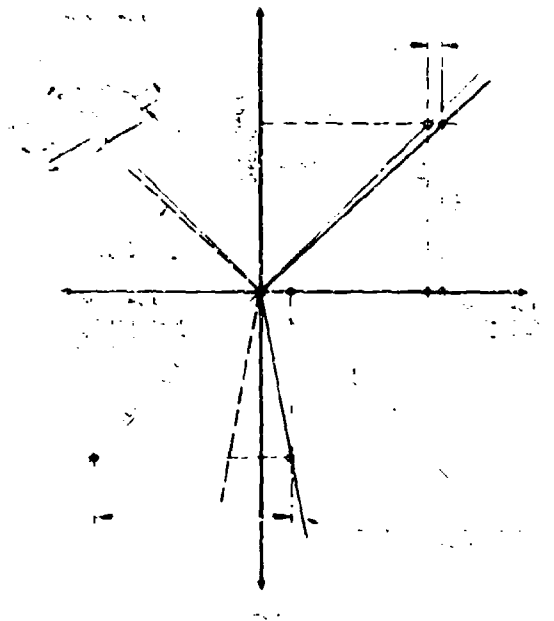


Figure 37. Mechanical No-Back Characteristics

- (d) To move an aiding load, the input required may range from approximately 5 percent to more than 100 percent, depending upon the design and the coefficient of friction.

A no-back is used in a system that primarily performs a trim function. This results in less motor heating because the no-back holds the load. In the aiding load mode of operation, the motor is only required to provide sufficient torque to unlock the no-back.

The principal methods of achieving a no-back function are divided into the following classifications; some are illustrated in Figure 38.

Irreversible components

Thrust collars

Capstan Coils

Ramp (load weighing) activated no-backs.

Components such as screw threads and gearing achieve irreversibility by a design efficiency of less than 50 percent. The simplicity gained by this approach is at the expense of power input required due to the low operating efficiency. Management of the power dissipated also can be a major disadvantage.

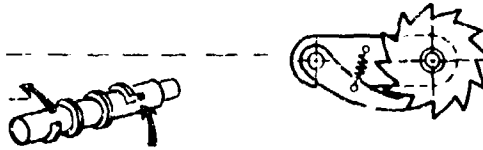
The thrust collar device is based upon the principle that an axial (or equivalent) force produces sufficient friction at the thrust collar to prevent back driving. In the opposing load mode, the thrust collar is allowed to ratchet, and thus nullify the friction torque. The principal disadvantage of the thrust collar type of no-back is that the power demand from the motor during aiding load operation varies with the coefficient of friction on the collar. Therefore, the aiding load usually sizes the power unit rather than the opposing load case. A power penalty results. The capstan coil device is generally not used for applications requiring energy absorption. The heat generated by friction occurs in limited small surfaces and complicates the thermal design of the unit. The simplicity of the device is attractive for parking-brake applications (non-energy absorbing).

The ramp-activated no-back is shown in Figure 39. Schematics of the no-back are shown in Figures 40 and 41, which show all normally rotational motion converted to linear motion. When the motor drives the load, the ball-ramps are in phase, and only the small bias brake is engaged. The bias brake serves as a damping device to achieve jitter-free operation during aiding load conditions. Figure 40 shows operation of the device when the output attempts to drive the input. Here, the ball-ramps become out-of-phase, applying braking forces upon the disc brake assembly and directing all torque to the outer fixed housing structure.

NON ENERGY ABSORBING

- RATCHETS

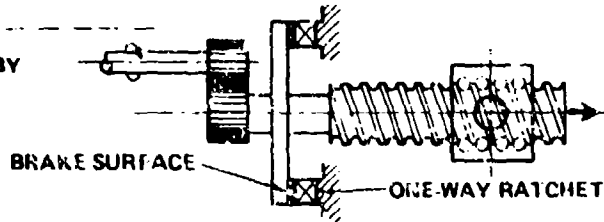
- CAPSTAN COIL



- IRREVERSIBLE COMPONENTS - GEAR BOX $\eta < 50\%$; WORM GEAR

- THRUST COLLARS

POWER SIZED BY
AIDING LOAD



ENERGY ABSORBING

- LOAD WEIGHING

HIGH EFFICIENCY
ENERGY ABSORBING
NON-CHATTERING

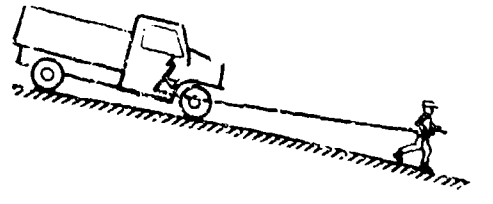


Figure 38. Mechanical No-Backs

INPUT DRIVING AGAINST AN OPPOSING TORQUE

NOMENCLATURE

1. LOAD BRAKE SPRING
2. LOAD BRAKE DISCS-ROTATING PLATES-STATIONARY
3. OUTPUT RAMP
4. DRIVE DOGS
5. INPUT RAMP
6. CONTROL BRAKE PLATE
7. CONTROL BRAKE SPRING
8. LOCK PIN
9. RAMP

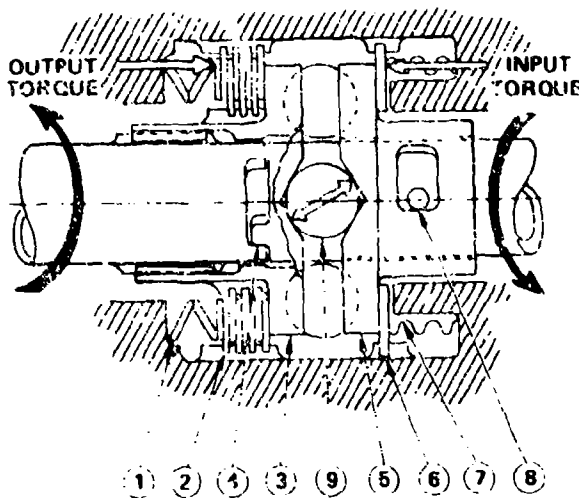
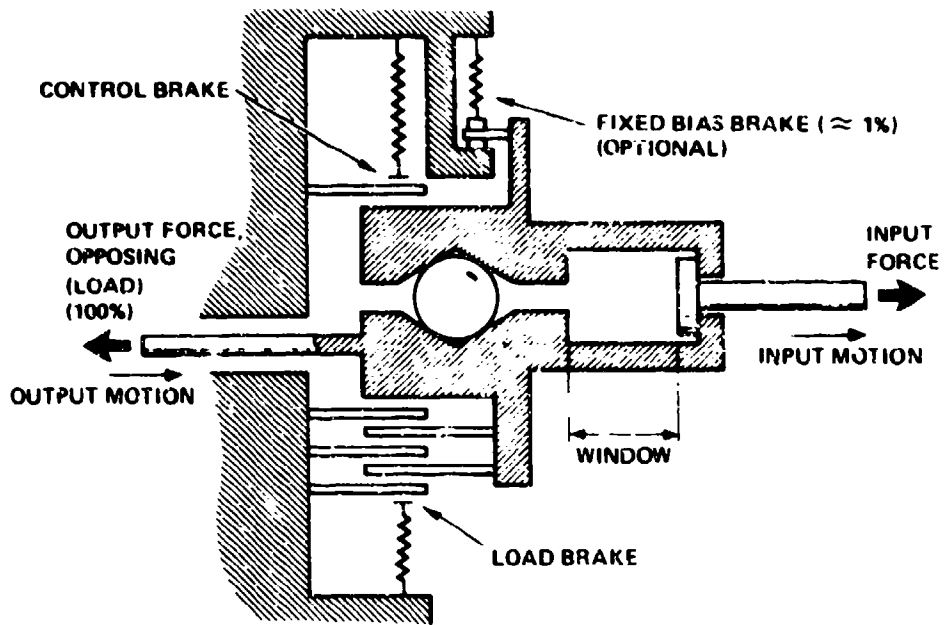
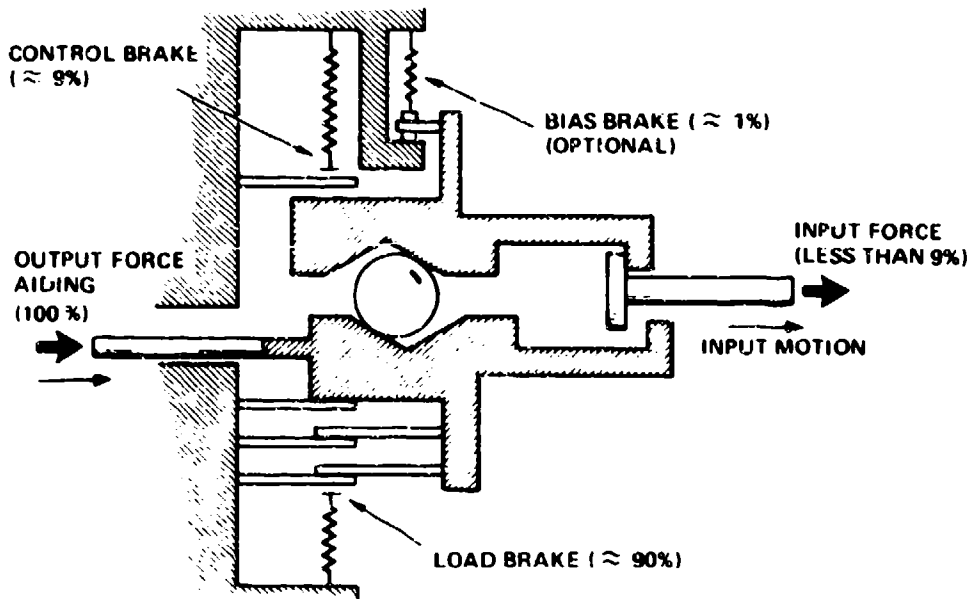


Figure 39. Ball Pump Type of No-Lock



5.191

Figure 40. Energy Absorbing No-Back: Input Driving an Opposing Load



5.192

Figure 41. Energy Absorbing No-Back: Input Driving an Aiding Load

5.3.2.4 Load-Limiting Devices

Two approaches to load limiting are considered: mechanical and electronic. Mechanical load-limiting devices are sensitive to variations in coefficient of friction due to wear, temperature, and velocity, and exhibit wide tolerance in meeting load requirements. The load limiter should be placed at the input, where torque levels are low, reducing the weight of the device. This requires that the device have high sensitivity to conducted torque and a narrow operating tolerance band. The characteristics of the unit are also a function of the output gear efficiency. For example, the F-100 aileron has a load limit of 150,000 lbf-in. torque and a minimum load requirement of 132,000 lbf-in. The hydraulic actuation system uses a load relief valve across the actuator to limit the control surface hinge moment. The characteristics of a mechanical device to provide the required load limiting of the F-100 aileron are given in Figure 42. The curve shows that a minimum output gear efficiency of 94 percent and an input drive torque of 141,000 lbf-in. is required to provide a 132,000 lbf-in. torque at the output. The curve also shows that a back-driving torque of 150,000 lbf-in. operating through the 94 percent efficient gearbox yields a torque of 141,000 lbf-in. at the input. For this case, therefore, the load limiter must hold full load up to 141,000 lbf-in., and then provide full release of the load at all greater levels of torque. There is no tolerance band available for manufacturing or other variations. For gear stages that exhibit higher efficiencies, a tolerance band exists. Current limiting of the motor provides a torque limit applied to the load. The current applied to a motor can be accurately monitored and controlled. The torque generated for a particular current value is not affected by the operating temperature of the motor, and is therefore predictable and repeatable.

5.3.3 Tradeoffs

The hinge-line actuator configuration selection is made on the basis of weight. The differential planetary geared actuator is the lightest in weight and has the smallest volume, thus easing installation and structural interface problems. To select between a no-back and a motor shaft brake to hold a load requires a definition of the cyclic frequency, duty cycle of the load, and particular actuation concept. Figure 43 shows that energy can be usefully extracted from the actuator/motor by the technique of regeneration when the control surface experiences sinusoidal oscillation at frequencies of 2.5 Hz or less. At higher frequencies, power from the motor to the surface is required to achieve the desired surface acceleration. If electric regeneration is not used, an energy-absorbing no-back could be considered as a means of load holding and also braking of control surface. As discussed earlier, thermal management during periods of high loads and duty cycles is a major design problem.

5.3.4 Selected Actuator Approach

The baseline configuration for the actuator is the differential compound hinge-line geared unit. For applications requiring redundant power inputs, the actuator will include a planetary differential for velocity summing of the two motor inputs. Also required when using redundant drive inputs are separately excited dc brakes for redundancy management. The brakes are provided to hold the motor shaft stationary in the event that the drive channel is determined to be inoperative for any reason. Thus, the brake is not a part of the system dynamics.

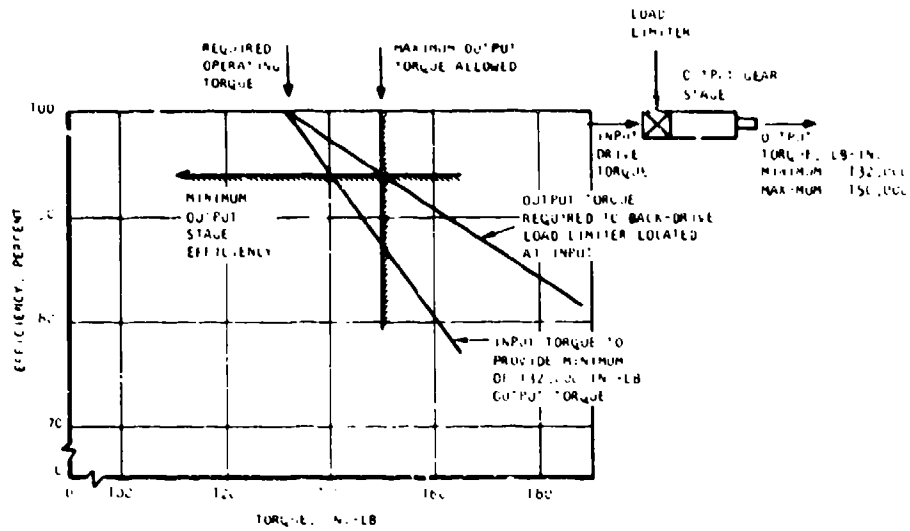


Figure 42. Output Torque Limiting of F-100 Aileron

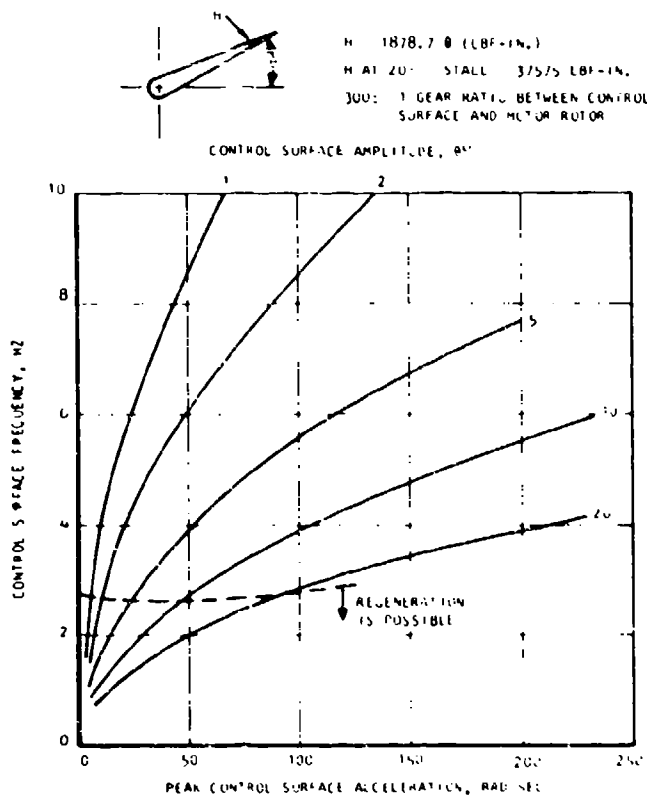


Figure 43 Power Regeneration

The energy absorbed in the no-back appears as friction heating in the disc plates. Figure 44 shows the limitation of the no-back related to the example problem statement. A transient condition of 100 cycles at ± 8.5 deg can be handled by the thermal capacity of the no-back, and does not require heat transfer to the structure or other thermal sink. Also, a control surface deflection of 2.0 deg and a steady-state cycling frequency of 0.1 Hz can be accommodated, and the required energy dissipated from the unit as heat. Within these operational constraints, the brake plate temperature will not exceed 460°F. The weight of the no-back is based upon providing sufficient surface area for heat rejection during steady-state energy dissipation, and to provide sufficient mass to accommodate transient friction heating. The size of the unit is larger than needed to handle the 1150 ozf-in. braking torque required at the motor shaft.

By comparison, a motor brake is not designed for power dissipation. It is designed for holding torque. For this reason, motor brakes will generally provide position holding at a lower weight penalty than the use of a no-back. Actuation of the brake to the on position, however, may require control logic and actuation. Typically, the motor brake is actuated off by the same power circuit that operates the motor. A short time delay can be built into the brake coil circuit to hold it in the off position for a period of time following motor shutoff. This feature offers the advantage of increased brake life. A part of the fault detection and isolation circuitry also can be used to continuously hold the brake off when the control servo circuits are active. When the fault monitoring logic signals shut down a drive channel, the brake would be actuated on. If energy dissipation is required, a combination of regeneration and motor brakes may have application. This must be considered in conjunction with duty cycle and total energy dissipated and regenerated.

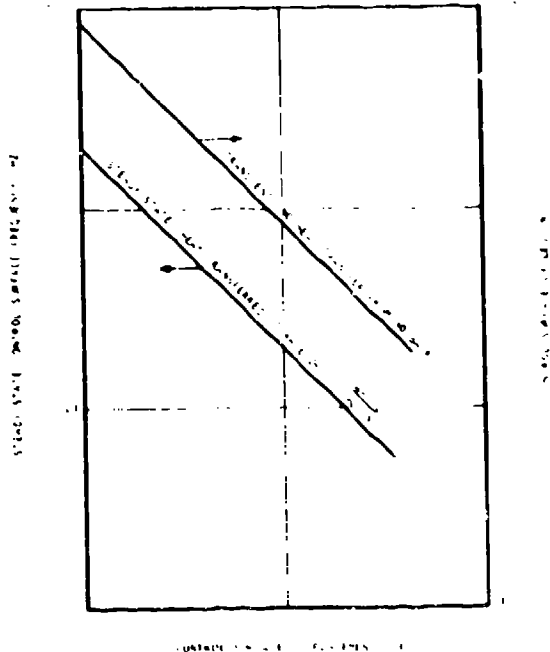


Figure 44. Thermal Capability of Energy Absorbing No-Back

5.4 RELIABILITY CONSIDERATIONS

Because all actuation systems have a degree of unreliability, it is necessary to establish ground rules by an iterative process of evaluating acceptable and unacceptable failure modes, and resulting failure effects. Some flight control surfaces are more important to safe (get-home) capability of an aircraft than others. For example, complete loss of rudder control will not endanger the safety of the aircraft, especially if the control surface fails centered and locked, because minimum yaw control can be achieved using aileron control. Therefore, the significance of any single failure must be evaluated based upon (1) the probable condition of the failed control surface and (2) the degree of aircraft control lost due to the failure of that surface. The condition of a failed surface could be (1) fail trail, (2) return to center and lock, (3) lock where failed, or (4) actuation by an alternate control mode at either full or reduced capability.

Allowable failure modes are determined by the criticality of the control surface to provide the get-home (or safe) operation of the aircraft, and the basic mission requirements. Particularly for a military aircraft, the requirement to accept at least one control system failure and still provide full control indicates a dual- (or even triple) redundant system approach. This redundancy can be provided by selected combinations of redundant control signal paths, multipowered actuators, and split or multiple control surfaces. For example, the ailerons of the F-100 are split into an inboard and an outboard section. These two sections are coordinated mechanically and driven by a dual tandem hydraulic cylinder.

An alternate concept is to drive each aileron panel of the F-100 from a separate actuation system. In normal operation, the inboard and outboard panels are driven by common input commands and panel motion coordinated by the servo control. In the event of a control system failure on one panel, adequate control is available from the remaining three panels. This type of split control surface redundancy is ideally implemented by electromechanical actuation devices. The actuation hardware for a particular control surface does not interface with other surfaces; all control interfaces are electrical.

5.4.1 Approach

Reliability apportionment and redundancy provisions are determined based upon the ground rule that an aircraft must be capable of getting home after a minimum of any one failure in the total flight control system. To maintain a cost-effective, operational system, minimum redundancy and/or backup provisions are indicated. Therefore, it is necessary to define which elements of the control system must be backed up and to what degree. Table 14 lists typical control surfaces of an aircraft, the criticality of the control surface to the aircraft safety, and methods of providing backup for required functions. Active-standby redundancy is assumed for all backup systems. It is unrealistic to expect the pilot to perform remedial action (switchover) and/or to activate redundant control systems following a failure.

TABLE 14
TYPICAL CONTROL SURFACES
AND BACKUP REQUIRED

Surface	Control Provided/ Criticality	Probable Failure Mode	Performance Required For Safety	Backup Option
Loading edge flap	Performance improve- ment, not critical	Unstable, tree-running	Lockup	<ol style="list-style-type: none"> 1. Alternate actua- tion source 2. Return surface to neutral and lock with auxiliary control
Flaperon/ aileron	Roll (lateral), critical	Trailing	Stable, return to neutral	<ol style="list-style-type: none"> 1. Use surface on neutral and lock with auxiliary control 2. Split control surfaces 3. Full capability backup actuation system
Trailing edge flap	Performance improve- ment, not critical	Trailing	Stable (no flutter)*	<ol style="list-style-type: none"> 1. None 2. Alternate actua- tion source
Horizontal	Pitch (longitudi- nal), critical	Trailing	Stable, return to neutral	<ol style="list-style-type: none"> 1. Full capability backup actuation system 2. Split control surfaces (stabilator)
Rudder	Yaw (directional), critical	Trailing	Stable, return to neutral	<ol style="list-style-type: none"> 1. None 2. Alternate actua- tion source

*Motor rotor inertia (0.001658 in.-lb-sec²) reflected through gearbox gear ratio is equivalent to a damper weight of 44 lb at a distance of 7 in. from the hinge line.

To implement the use of an alternate actuation system (redundant components or backup systems) requires that a failure be detected and isolated. Instrumentation usually available as part of the servocontrol feedback is used to determine adequate system functioning. Independent sensors and/or additional performance monitoring devices may be required to satisfy built-in-test equipment (BITE) requirements and to also serve operational fault detectors.

Mechanization of redundant mechanical drive channels may be handled in several ways, as shown in Figure 45. For example, a method of mixing multiple actuator drive inputs for use at the control surface is to use a velocity summing device such as a differential gearbox. Since both motors drive at all times, the output from the differential is the sum of the input velocities. In the event of a failure in one drive channel (not in the differential), the differential output velocity is reduced to one-half, while the output torque remains unchanged. To maintain output torque during this mode of operation requires that the input to the differential on the failed side be locked. This is implemented by either a mechanical no-back or a motor brake.

5.4.2 Requirements

The reliability requirements and goals for an electromechanical system for primary flight control surface actuation are based upon known data of aircraft operations. Information relating aircraft failures to the control system and the actuation system is summarized in Table 15, which shows a total failure rate of nearly 9×10^{-6} failures per hour for fighter aircraft and a minimum rate of 1×10^{-6} for the 680J, one of the most recent fly-by-wire aircraft. To be compatible, therefore, a goal for the electromechanical actuation system is 1×10^{-6} failures per hour. This includes the power source, flight control, and actuation system elements.

The reliability model is shown in Figure 46. A parallel redundant electrical supply is assumed including redundant electrical distribution within the aircraft. At each of the nine control surfaces, it is assumed that a two-channel drive is used. The output of each drive assembly is mixed in a velocity summing differential to operate the control surface. Table 16 gives the numerical values of reliability for the various components based upon the reliability model (Figure 46); Figure 47 shows the failure rate improvement achieved by the use of simple active standby redundancy. Failure rates are given for individual system components, subassemblies, and the total actuation system based upon a total of nine control surfaces. The system failure rate of 1×10^{-6} failures per operating hour appears to be reasonable and achievable.

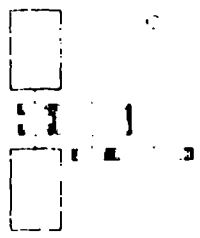
SCHEMATIC	CONCEPT	COMMENTS
	<p>SINGLE DRIVE</p>	
	<p>DUAL DRIVE DIRECT</p>	
	<p>DUAL DRIVE WITH VELOCITY SUMMING</p>	

Figure 45. Control Surface Drive Redundancy Arrangement

TABLE 15
AIRCRAFT RELIABILITY DATA*

AIRCRAFT	FAILURES PER 10 ⁶ HOURS		
	FLIGHT CONTROL	ACTUATION SYSTEM	TOTAL
CAB/FAA COMMERCIAL TRANSPORT HISTORY, 1949 TO 1962 AS COMPILED BY AFFDL (EARLY GOAL FOR ELECTROMECHANICAL CONTROL SYSTEM)			0.23
680 J AIRCRAFT			1.0667
AIR FORCE FIGHTER AIRCRAFT	5.46	3.51	8.97
AIR FORCE LARGE COMBERS (1964 TO 1973)			0.55
AIR FORCE ROTARY WING AIRCRAFT (1964 TO 1973)	1.92	0.96	2.88
NAVY (1960 TO 1970)	5.5	3.47	8.97

*REFERENCE: FLIGHT CONTROL SYSTEM ADVANCES FOR NEAR FUTURE MILITARY AIRCRAFT.
PAUL E. BLATT

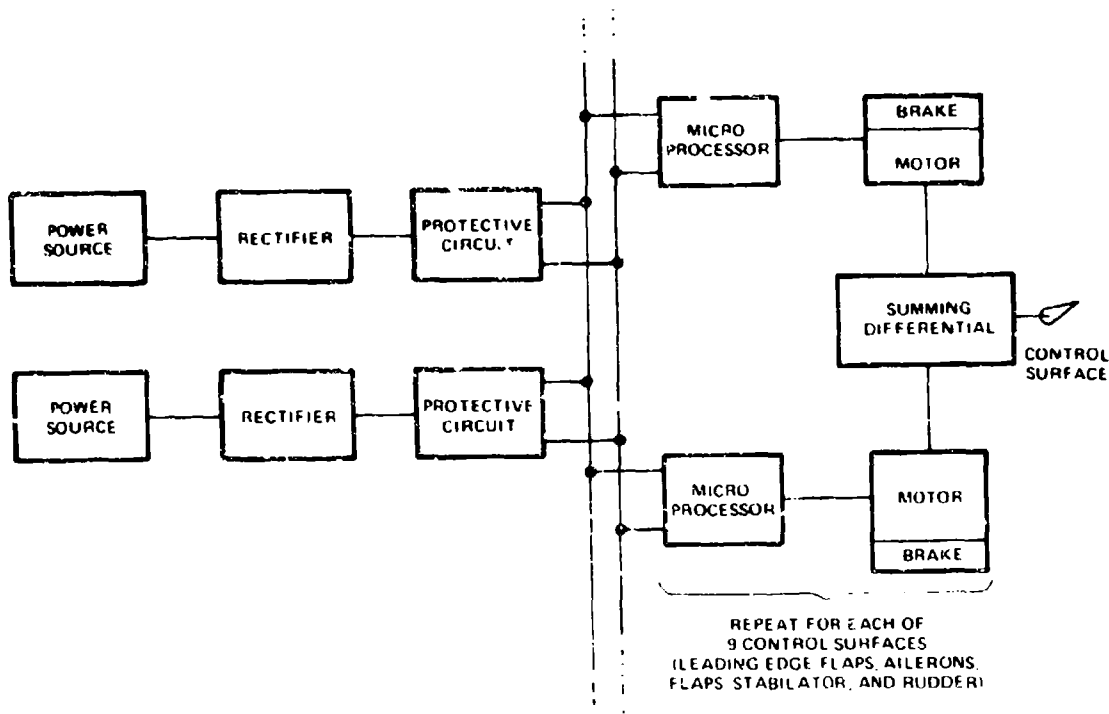


Figure 46. Reliability System Model

TABLE 16

RELIABILITY ESTIMATES

Component	Failures per 10^6 hr		
	Lower Limit	Upper Limit	
PMG	*94.5	71.0	Estimate for subsonic aircraft data source, FARADA
Rectifier/ power supply	40.0	25.0	Assumed switching regulator to minimize power (F-14 CADC)
Microprocessor (digital control)	8.33	4.44	Assumed average ambient operating temperature around 40°C . (F-14 AICS)
Dc/brushless motor	29.5	7.3	Data source, Farada
Gearbox	5	0.1	DC-10; 418,395 fleet hours reported.

*Based on DC-9, both Series 10 and 30; fleet size was 371 aircraft with 2,648,858 engine-on hours.

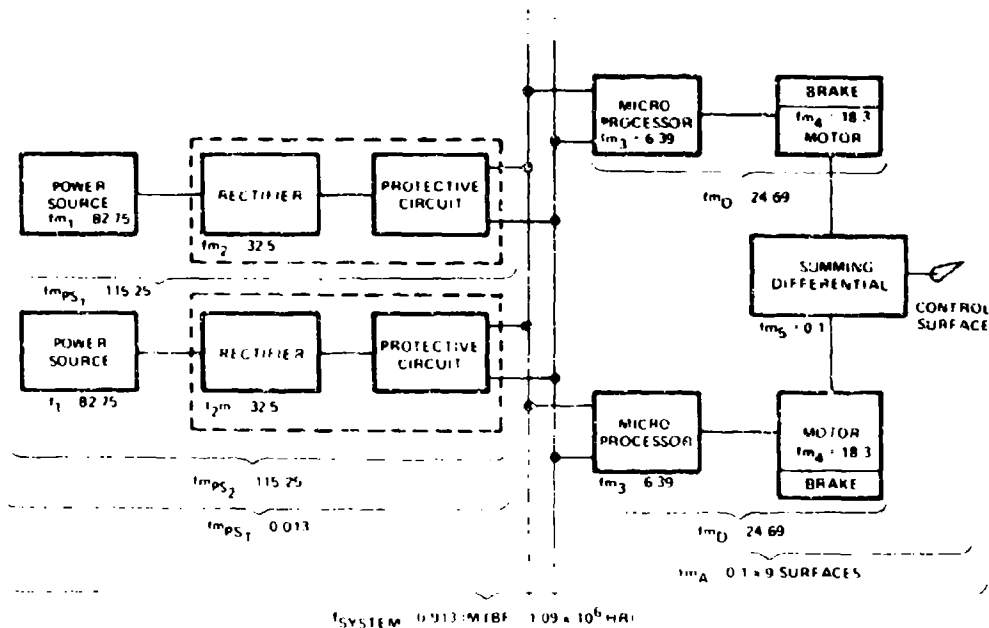


Figure 47. Study Concept

5.4.3 Redundancy for the F-100

Using the F-100 as an example of redundancy management, Table 17 gives the electric actuation system drive tradeoff to meet the performance requirements. A drive unit consists of the motor(s), actuator, and controller(s), as indicated in the table. The minimum requirements for control surface actuation can be achieved with a drive weight of 378 lb. An additional 52 lb (14 percent increase) provides sufficient redundancy in the control surface drive to provide full operational capability after any single failure. A 25-lb weight penalty results when reduced performance is acceptable following a failure. The table shows that the minimum weight system without redundancy is the same weight synthesized for minimum control for get-home capability.

5.5 AIRCRAFT ACTUATION SYSTEM INTEGRATION

The component parametric data presented earlier in this section are used to compare the electromechanical actuation system to the current hydraulic system for the F-100 aircraft. Individual electromechanical component characteristics are shown in Table 18. The total weight shown includes the motor, differential gearbox (if used), and the final actuator output stage gearing.

The summary of the system weight for an all electromechanical F-100 flight control system is presented in Table 19. The actuator configuration corresponding to the weight summary is shown in the block diagram of Figure 48. The total system weight including the redundant power source and electrical distribution is 966 lb. The hydraulic system weight for flight control actuation is presented in Table 20. The total weight is 971 lb.

Based upon the data shown, the electromechanical and hydraulic approaches are weight competitive. An approach to installation of the electromechanical actuator into the F-100 outboard aileron is shown in Figure 49. The figure shows damper weights used to prevent flutter of a control surface in the event of loss of the redundant hydraulic circuits. The electromechanical actuation concept would not require damper weights because of the equivalent inertia resulting from the motor rotor reflected through the relatively high gear ratio.

The potential for weight reduction made possible by eliminating the outboard panel damper weights is therefore an additional 73.4 lb for both panels. The electromechanical actuation system, with redundancy equivalent to the hydraulic system, weighs 893 lb, for a total weight reduction of 76 lb compared to the hydraulic system, or an 8 percent weight reduction.

As an additional point of comparison, the electro-hydraulic actuation system for the B-52 elevator has been evaluated against the equivalent electromechanical approach. Table 21 presents the comparison. The B-52 unit represents technology eight years old, but is representative of actuation system concepts based upon power-by-wire and fly-by-wire versatility and adaptability.

TABLE 17
 REDUNDANCY MANAGEMENT TRADEOFF

Control Surface	Min. Drives Required for Full Control		Drives Required for Full Control After 1 Failure (Note 1)		Reduced Capability (Half-Rate) After 1 Failure (Note 2)		Min. Control for Get-Home Capability After 1 Failure	
	No. of Motors	Drive Weight, lb	No. of Motors	Drive Weight, lb	No. of Motors	Drive Weight, lb	No. of Motors	Drive Weight, lb
Rudder	1	27	2	52	2	52	1	27
Stabilizer	2	179	3	206	2	179	2	179
Aileron								
Inboard	2	95	2 Note 4	95	2 Note 3	95	2	95
Outboard	2	77	2 Note 4	77	2 Note 3	77	2	77
Total weights, lb		378		450		403		378

- NOTES: 1. Assumes redundant drive is actuated on after failure of primary drive.
 2. Assumes active standby redundancy.
 3. Assumes split control surfaces; loss of one panel out of 4 is not critical.
 4. Surface fails trailed.

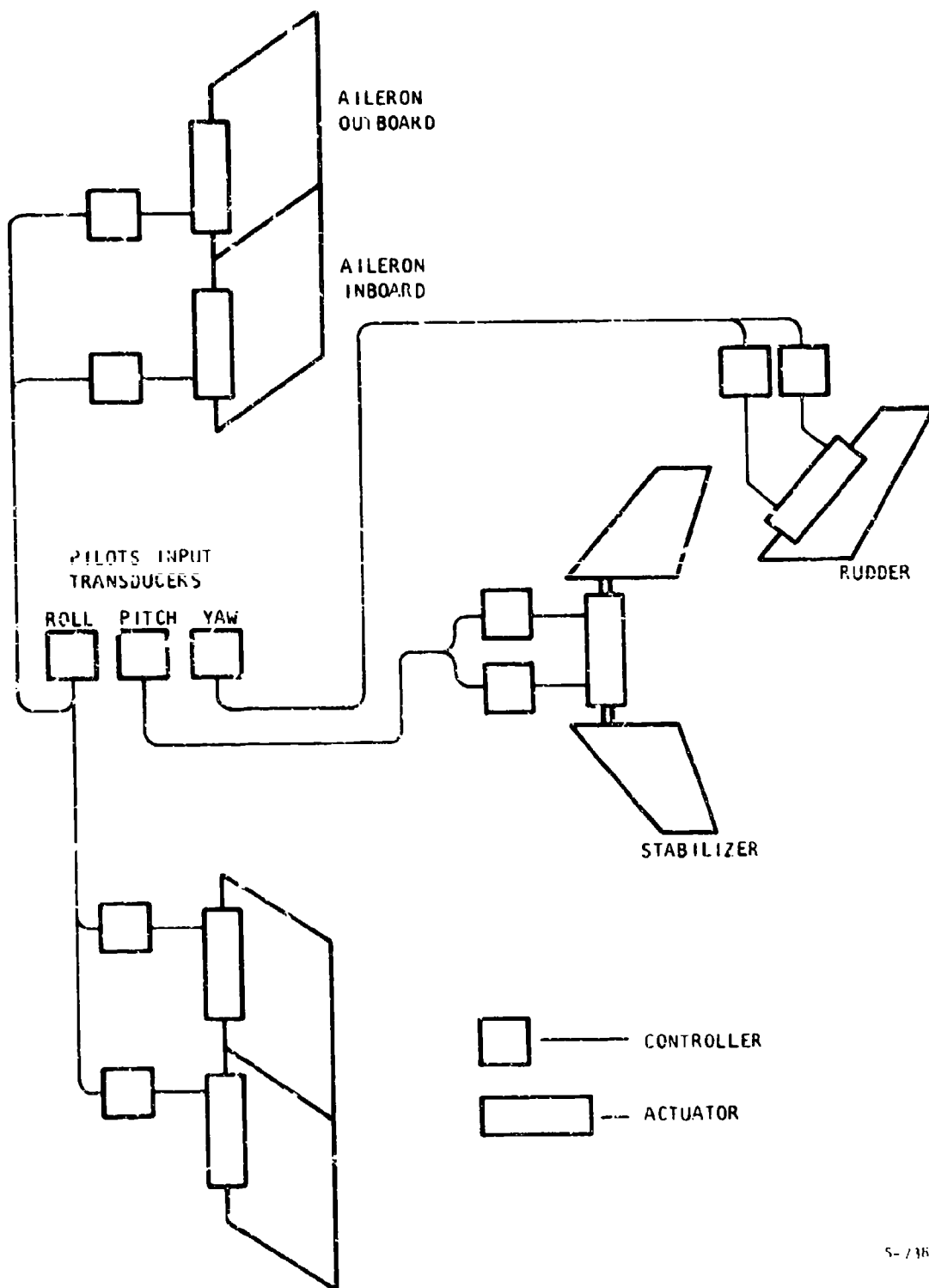
TABLE 18
 ELECTROMECHANICAL COMPONENTS SIZED FOR F-100 APPLICATION

	No. of Motors	Motor Weight, lb	Actuator Weight, lb	Minimum Hinge Weight, lb-in	Minimum No-load Rate, Deg/sec	Total Weight, lb
Rudder	2	9 x 2 = 18	4	4500	50	22
Stabilizer	2	18 x 2 = 36	155 0-in. 18	50,000	6 (with both motors)	169
Aileron*						
Inboard	1	18	27	80,600	31	45
Outboard	1	18	14	51,400	58	50

*Redundancy gained by split panels

TABLE 19
F-100F ELECTROMECHANICAL SYSTEM WEIGHTS

	Number of Units	Unit Weight, lb	Total Weight, lb
Aileron actuators			
Inboard	2	45	90
Outboard	2	36	72
Aileron control boxes	4	5.25	10.5
Stabilizer actuator	1	169	169
Stabilizer control boxes	2	5.25	10.5
Rudder actuator	1	22	22
Rudder control boxes	2	0.3	10.5
Pilot input transducer	3		1
Aileron mounting structure			75
Stabilizer mounting structure			75
Rudder mounting structure			15
Input transducer mounting			10
Aircraft power source			
Permanent magnet generator	2	35	70
Conditioning and power distribution			135
Electrical generating system (standby)			200
Total			966



5-716

Figure 48. F-100 Electromechanical Actuator Block Diagram

AFFDL-TR-76-42

INBOARD AILERON
AIL. STA 165.617

— OUTBOARD AILERON

— DEPTH--UPPER ML TO L
AT AILERON HINGE PL
AILERON STATION 168.
3.963

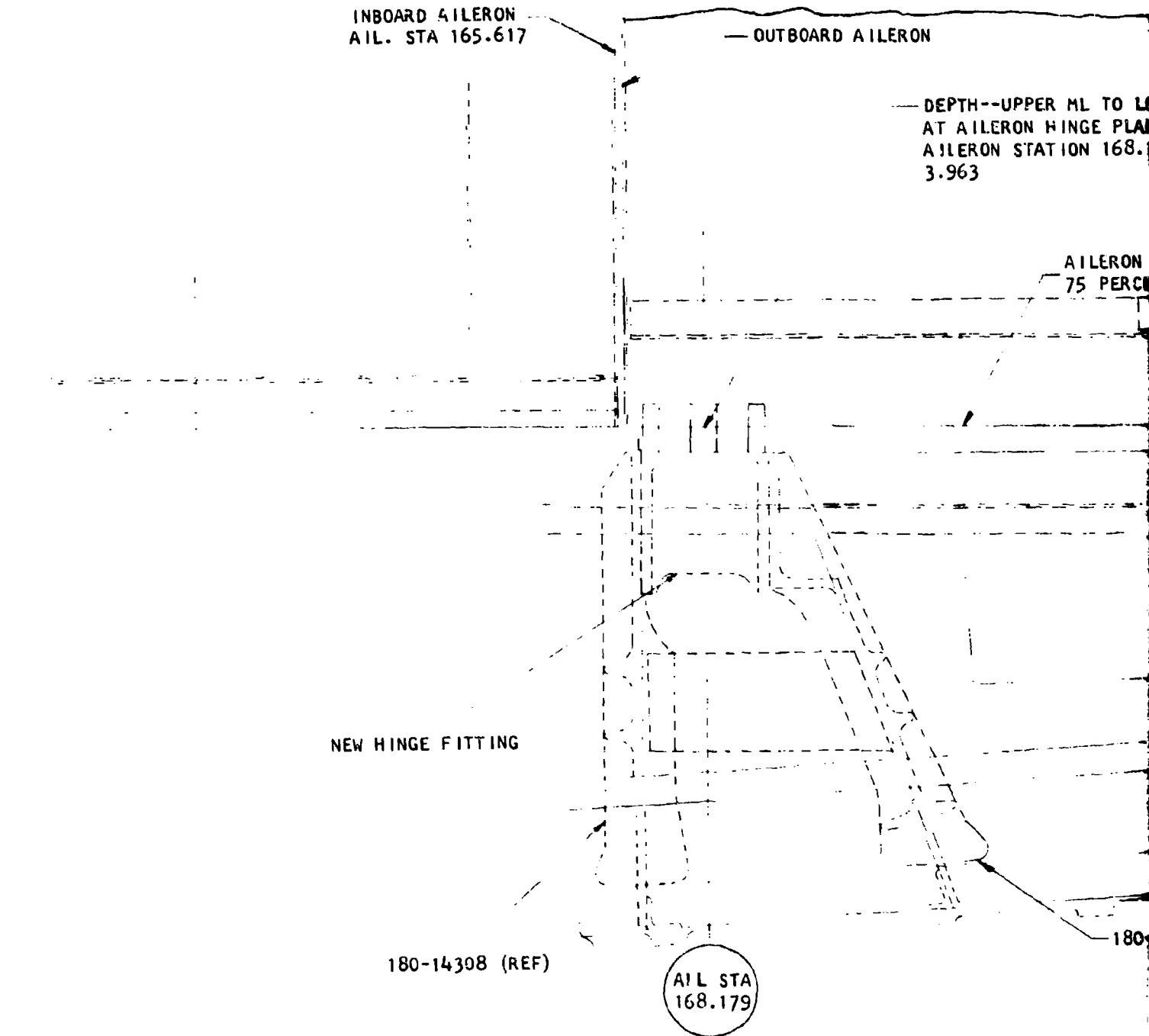
AILERON
75 PERC

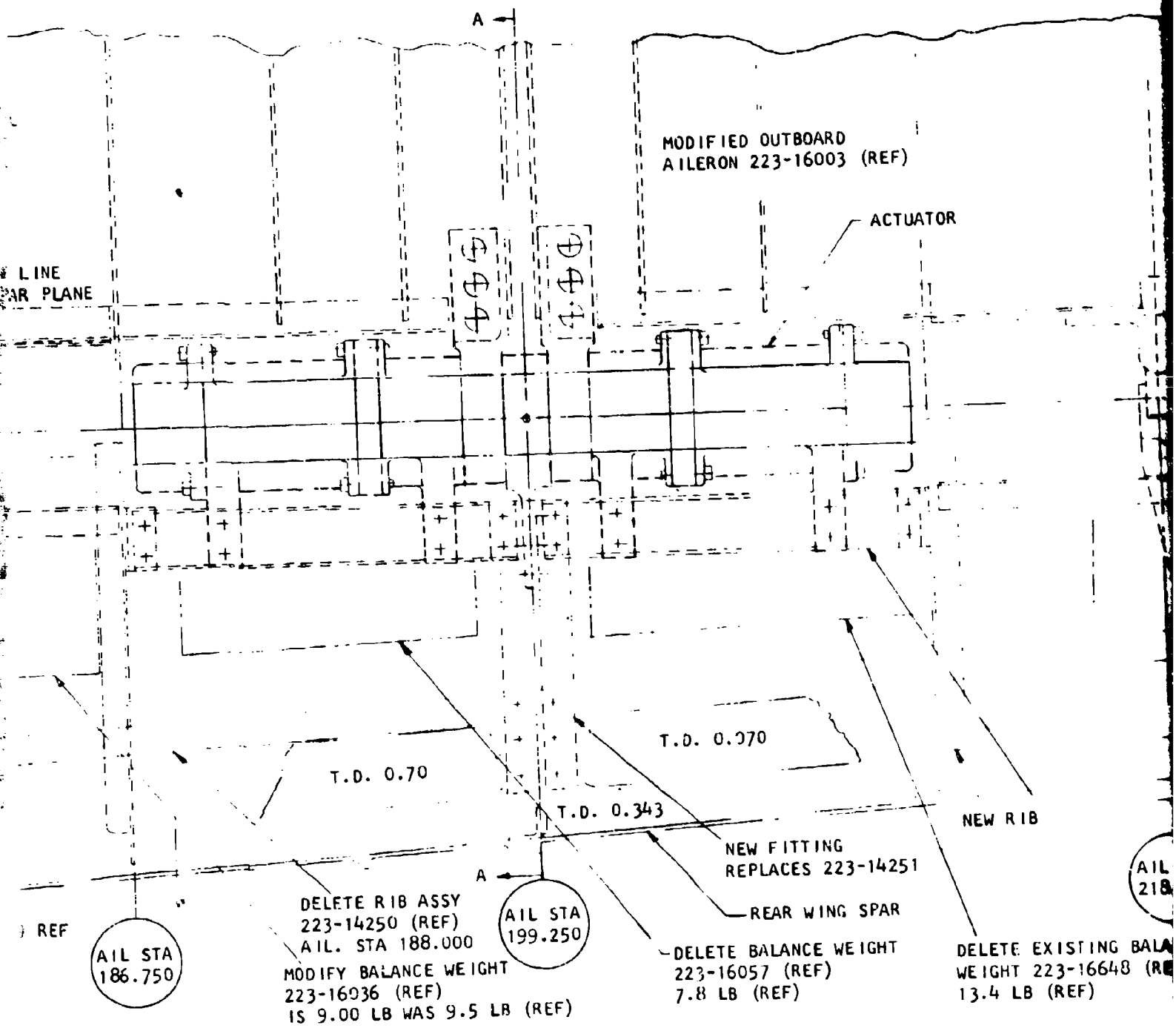
NEW HINGE FITTING

180-14308 (REF)

AIL STA
168.179

180





MODIFIED OUTBOARD
AILERON 223-16003 (REF)

ACTUATOR

LINE
SPAR PLANE

T.D. 0.70

T.D. 0.070

T.D. 0.343

NEW RIB

NEW FITTING
REPLACES 223-14251

REAR WING SPAR

DELETE RIB ASSY
223-14250 (REF)
AIL. STA 188.000
MODIFY BALANCE WEIGHT
223-16036 (REF)
IS 9.00 LB WAS 9.5 LB (REF)

DELETE BALANCE WEIGHT
223-16057 (REF)
7.8 LB (REF)

DELETE EXISTING BALANCE
WEIGHT 223-16648 (REF)
13.4 LB (REF)

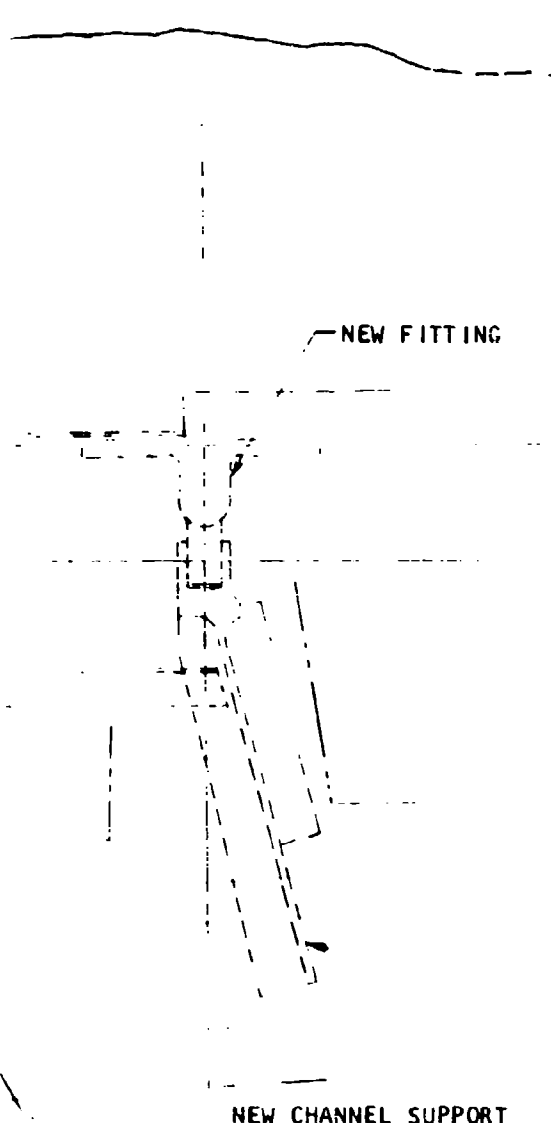
AIL STA
186.750

AIL STA
199.250

AIL
218

REF

A



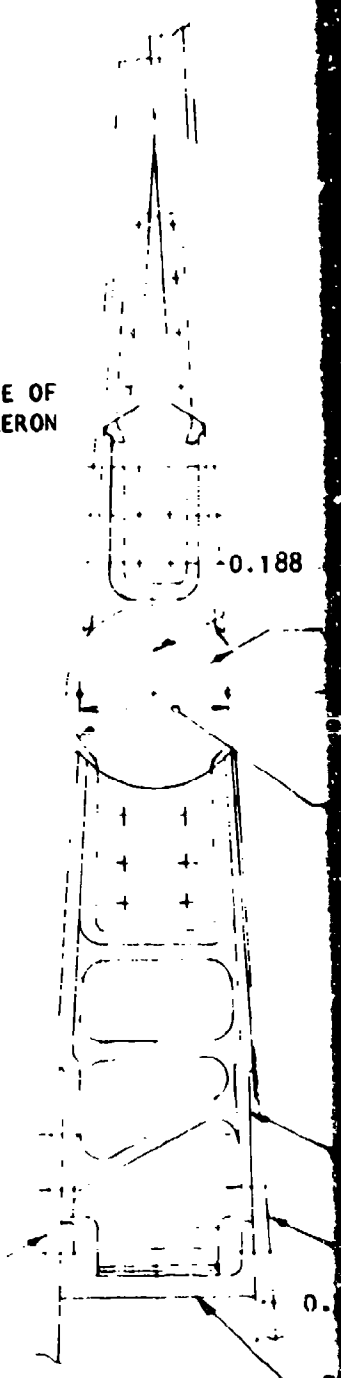
OUTBOARD EDGE OF
OUTBOARD AILERON

AILERON HINGE PLANE

EXISTING BALANCE WEIGHT
192.16531 (REF)
6 LB (REF)

NEW HINGE FITTING
REPLACES 223-14242

UPPER WING SKIN



SECTION A-A

AIL STA
218.875

AIL STA
229.250

EXISTING BALANCE
223-16648 (REF)
(REF)

Figure

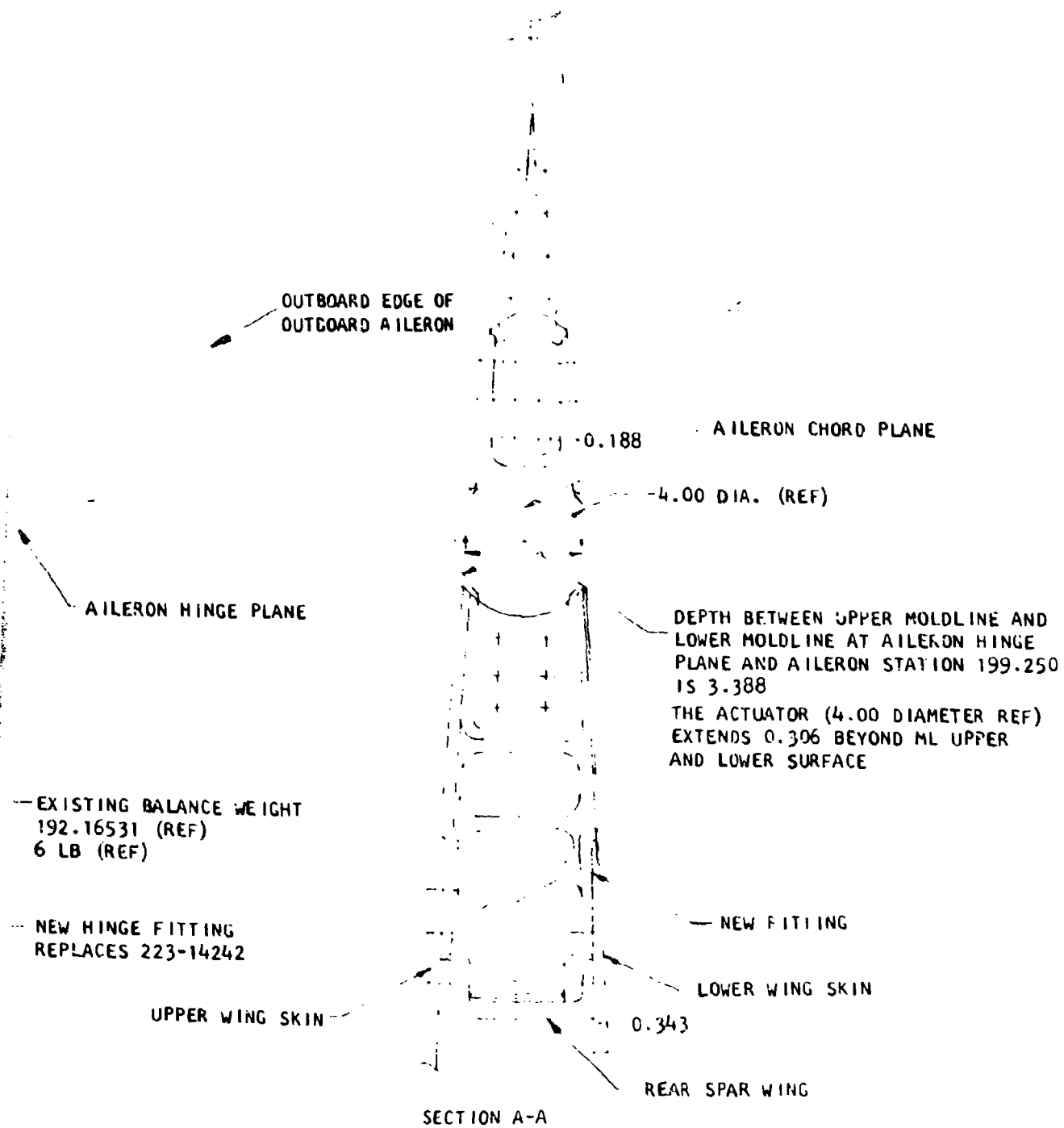


Figure 49. F-100 Electromechanical Actuator Installation at Aileron Station 199.250

TABLE 20

F-100F HYDRAULIC FLIGHT CONTROL SYSTEM WEIGHT REDUCTIONS

	Weight, lb
Component	
Flight controls	
Auto flight controls	43
Servos	34
Plumbing and fluid	9
Aileron controls	(243)
Mechanical	28
Hydraulic	206
Artificial feel	9
Horizontal tail controls	(224)
Mechanical	49
Electrical	21
Hydraulic	90
Artificial feel	64
Rudder controls	(80)
Mechanical	27
Hydraulic	31
Artificial feel	14
Vibration damper	6
Power control system	(242)
Pumps	31
Accumulators	41
Reservoirs	24
Valves, filters, etc.	23
Plumbing	68
Fluid	24
Emergency system	31
Structure	(139)
Aileron hinges	88
Rudder hinges	4
Rat door and mechanization	47
Total deletions	971

TABLE 21
 WEIGHT COMPARISON OF EM AND HYDRAULIC SYSTEM
 FOR B-52 ELEVATOR PROBLEM STATEMENT

<u>ELECTROMECHANICAL WEIGHT, LB</u>		<u>ELECTROHYDRAULIC WEIGHT, LB</u>	
MOTOR (2)	36 LB	POWER UNIT	
BRAKES	3	MOTOR/PUMP	35 LB
*ACTUATOR	14.5	RESERVOIR	23
CONTROL (2)	10.5	ACTUATOR	57
TOTAL	<u>64 LB</u>	TOTAL	<u>115 LB</u>

*64 LB TOTAL WEIGHT FOR ACTUATOR SIZED FOR 100,000 CYCLE LIFE; WEIGHT INCREASES TO 76 LB FOR ACTUATOR SIZED FOR 500,000 CYCLE LIFE.

6. PRELIMINARY DESIGN

This section presents the preliminary design of the selected approach to electromechanical flight control actuation. The elements of the selected approach are listed below:

- 115/200-vac, 3-phase power source
- Rectifier
- Microprocessor motor control
- Brushless dc motor with magnetic shaft encoder
- Magnetic brake
- Velocity summing planetary differential
- Rotary, hinge-line output

6.1 DESIGN

The following paragraphs present the preliminary design of the system and discuss major components that meet the baseline problem statement given in Table 22.

TABLE 22
BASELINE PROBLEM STATEMENT

Voltage	270 vdc
Stroke	<u>+19</u> deg
Frequency response	8 Hz (90 deg phase shift)
(Inertial load only) at <u>+1.19</u> deg amplitude	
No-load speed	80 deg/sec = 1.397 rad/sec
Stall torque	37,575 lbf-in.
Inertial load	17,894 lbf-in. ² = 46.6 lbf-in.-sec ²
Ambient temperature	-65° to +160°F at 60,000 ft
Open loop gain	One degree error generates a control surface rate of 45 deg/sec

The actuation system approach is presented in the functional diagram of Figure 50. The interfaces with the aircraft flight control system, the servomotor, redundancy management monitoring and fault isolation provisions, and adaptive control inputs are shown. The design rationale and characteristics for the major components of the system are discussed below.

6.1.1 Brushless Dc Motor

6.1.1.1 General Design Characteristics

The normal torque-speed curve of the rare-earth-cobalt servomotor is a straight line from no-load to stall. As the applied current (voltage) is varied, a family of parallel torque-speed curves is generated, with the stall torque and no-load speed proportional to the applied current and voltage. Also, for a given voltage, the motor no-load speed can be adjusted by means of selecting the appropriate number of coils and wire size in the stator windings. This flexibility is subject to certain restrictions related to practical wire sizes, whole number of coils and maximum rotor speed limitations.

Since this motor will be used in a gear reduction actuator, the slope of the torque-speed curve at the actuator output can be selected as a function of the motor speed-gear ratio combination. However, the general characteristic of decreasing speed as a function of load is inherent in the direct-coupled servosystem. Other characteristics independent of the gear reduction are:

- (a) Theoretical maximum torque that can be obtained for a given current is determined as follows:

$$T/A (\text{maximum}) = \left(\frac{1352 \times \text{voltage}}{\text{no load speed (rpm)}} \right) \text{ in.-oz/amp}$$

where the dimensions of the factor 1352 are: $\frac{\text{in.-ozf-rpm}}{\text{amp-volt}}$

- (b) For a given voltage, the current required to obtain a given torque, or force, at the output shaft is directly proportional to the no-load speed of the output shaft.
- (c) The current required to obtain a given torque, or force, at the output shaft is inversely proportional to the minimum power supply voltage.
- (d) The theoretical maximum efficiency of the system at any load is the percentage of the output shaft loaded speed to the no-load speed.

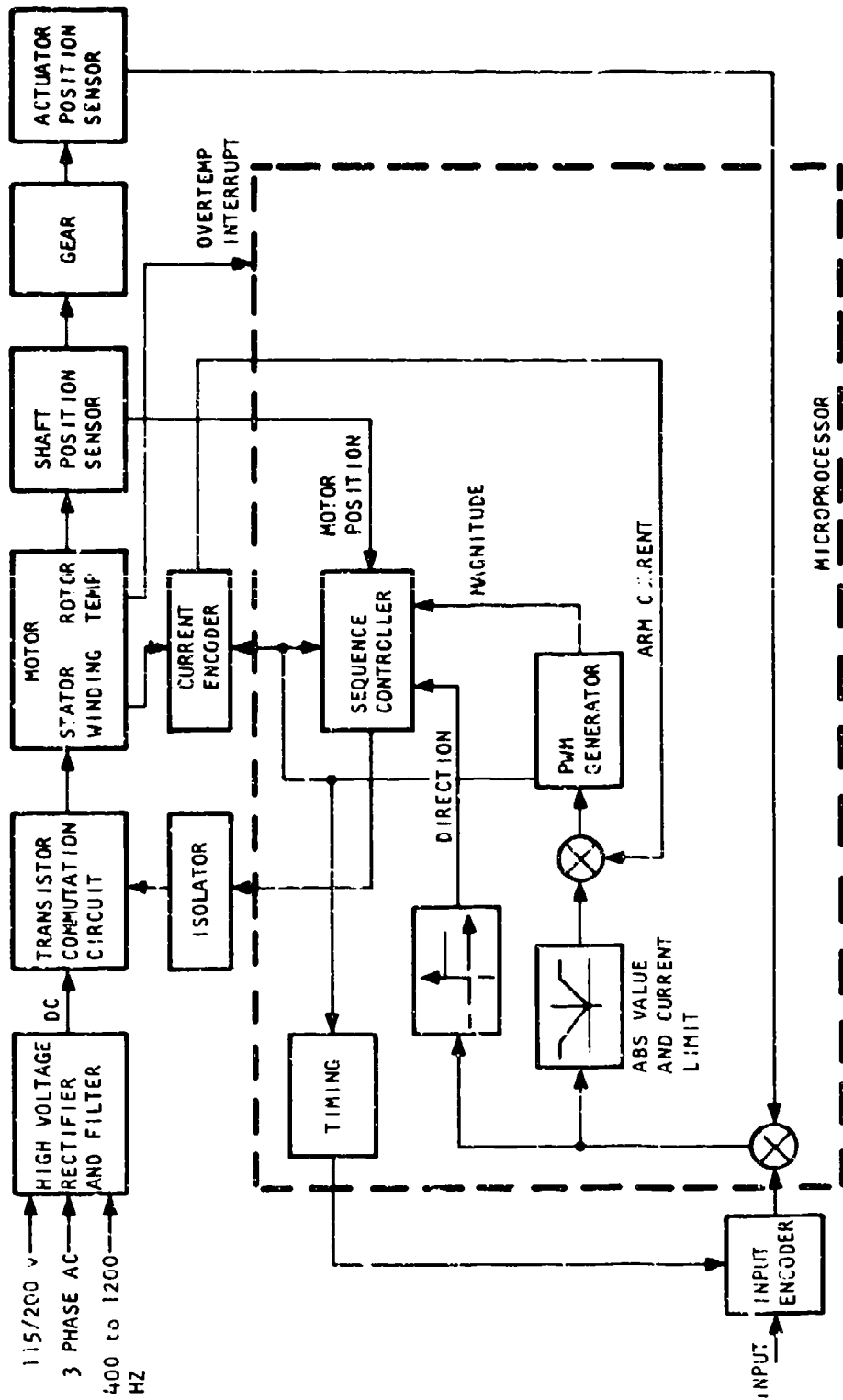


Figure 50. Microprocessor Motor Control

6.1.1.2 Motor Characteristics

For the problem statement given above, the characteristics of the servomotor can be determined as discussed in the following paragraphs.

6.1.1.2.1 Acceleration of the Output

For a given frequency response, an approximate acceleration requirement can be obtained from:

$$\ddot{\theta} = \dot{\theta}_{nl} \times 2 \pi f$$

where $\ddot{\theta}$ = output acceleration (rad/sec²)

$\dot{\theta}_{nl}$ = no load velocity (rad/sec)

f = required frequency response [Hz (90 deg phase shift)]

An example is as follows:

Assume $\dot{\theta}_{nl} = 80 \text{ deg/sec} = 1.397 \text{ rad/sec}$

f = 8 Hz

$$\ddot{\theta} = 1.397 \times (2\pi \times 8)^2$$

$$= 70 \text{ rad/sec}^2$$

Based upon definition of amplitude and frequency response required, the acceleration is as follows.

$$\ddot{\theta} = A (2 \pi f)^2$$

where A = amplitude in radians

Example:

Assume A = $\pm 1.19 \text{ deg} = \pm 0.0208 \text{ rad}$ (from Reference 3)

f = 8 Hz

then

$$\ddot{\theta} = 0.0208 \times (2\pi \times 8)^2$$

$$= 53 \text{ rad/sec}^2$$

The latter value is used as an approximation and will be evaluated by analog computer simulation of the servoloop.

Any or all of several torque requirements may be specified. These include:

- (a) T_s = output stall
- (b) T_r = output torque at some running load
- (c) T_c = output torque required for a load present during the evaluation of the acceleration or frequency response
- (d) A derived torque T_{LL} required to accelerate the load inertia:

$$T_{LL} = \ddot{\theta} \times I_L$$

where I_L = load inertia (lbf-in.-sec²)

An example is as follows:

Assume a load inertia = 46.6 lbf-in.-sec²

$$\begin{aligned} T_{LL} &= 53 \text{ rad/sec}^2 \times 46.6 \text{ lbf-in.-sec}^2 \\ &= 2470 \text{ lbf-in.} \end{aligned}$$

If the maximum power output required is not given, it may be approximated as follows. Use the larger of:

- (a) Assuming a straight line torque speed curve from no load to stall, the peak power output will occur at one-half torque and one-half speed.

$$P_o \text{ (watts)} = \frac{T_s \text{ (lbf-in.)} \times \dot{\theta}_{nl} \text{ (rpm)}}{4K}$$

where $K = 84.5$ (unit conversion)

$$P_o \text{ (watts)} = \frac{T_r \text{ (lbf-in.)} \times \dot{\theta}_{rl} \text{ (rpm)}}{4 \times 84.5}$$

where $\dot{\theta}_{rl}$ = angular velocity under running load in rpm

An example is as follows: since T_r is not specified, use 1.

$$T_s = 37.575 \text{ lbf-in.}$$

$$\dot{\theta}_{nl} = 80 \text{ deg/sec}$$

$$P_o = \frac{37.575 \times \frac{80}{360} \times 2\pi}{550 \times 4} = 2 \text{ hp}$$

6.1.1.2.2 Motor Selection

A tentative motor selection can be made based on peak horsepower requirements.

<u>Power level, hp</u>	<u>Motor diameter, in.</u>	<u>Motor length, in.</u>
0 to 1/8	1.1	2.9
1/8 to 1/2	1.5	3.8
1/2 to 3/4	1.75	4.2
3/4 to 1-1/2	2.25	5.2
1-1/2 to 4	4.0	8.5

Final determination of the motor design will depend on the watt losses generated and the duty cycle. Generated losses are determined by analysis of the motor performance in the servosystem. An example would be to use a 4-in.-dia. motor when 2-hp output is required.

6.1.1.2.3 Performance of the Motor and Geared Actuator

Motor performance is determined based upon considerations of acceleration required at the load, maximum load rate, and actuator gear ratio. These characteristics must be accommodated while minimizing the current supplied to the motor. Section 4 presents the general approach to motor/actuator design. The details of that approach are presented below for the 4-in.-dia, brushless dc motor. The example is as follows:

Assume:

$$T_S = 37,575 \text{ lbf-in. (stall)}$$

$$T_r = \text{none specified (running)}$$

$$T_c = 0 \text{ (concurrent)}$$

$$T_I = 2470 \text{ lbf-in. (inertia load)}$$

$$\ddot{\theta}_O = 53 \text{ rad/sec}^2$$

$$I_M = 1.638 \times 10^{-3} \text{ lbf-in.-sec}^2$$

$$\text{Eff} = 0.9 \text{ (90 percent)}$$

Then T_{T0} is equal to one of the following:

1. $2 (T_{IL} + T_C) = 4940$

2. $T_s = 37,575$

3. $T_r = \text{not specified}$

$$T_{T0} = 37,575 \text{ (the largest of the above values)}$$

$$G = \left(\frac{37,575 - 2470}{1.638 \times 10^{-3} \times 53 \times 0.9} \right)^{1/2}$$

$$G = 670$$

This is the gear ratio that satisfies the particular condition of minimum current required to meet both stall torque and acceleration torque requirements. If a lower gear ratio is used, additional acceleration capability above that required in this example would be obtained; however, additional motor torque (and amplifier current) would be required to provide the required stall torque. If a higher gear ratio is used, a stall torque capability above that required would be provided; however, additional motor torque and amplifier current would be required to achieve the desired acceleration.

The following example shows how to determine the minimum output no-load speed. For the motor considered, the slope of the torque speed curve is:

$$S_{LM} = 6.54 \times 10^{-1} \text{ rad/sec/lbf-in.}$$

at 400 F maximum motor temperature. This is the change in speed resulting from a change in torque loading. The output slope is:

$$S_{LO} = \frac{S_{LM}}{G^2 \times \text{Eff}}$$

Using previously calculated values, an example is:

$$S_{LO} = \frac{6.54 \times 10^{-1}}{(670)^2 \times 0.9} = 1.62 \times 10^{-6} \text{ rad/sec/lbf-in.}$$

The minimum output no-load speed is the largest of:

- (a) The specification value
- (b) $S_{LO} \times T_s$
- (c) $\dot{\theta}_r + (S_{LO} \times T_r)$

where $\dot{\theta}_r$ is the speed required at the running load requirement. For example: assume that the specification requirement of 80 deg/sec is used to determine the acceleration requirement.

1. Spec value = 80 deg/sec = 1.396 rad/sec
2. $S_{LO} \times T_s = 1.62 \times 10^{-6} \times 37,575 = 6.08 \times 10^{-2}$ rad/sec
3. No running load requirement specified

The largest of 1, 2 and 3 is:

$$3) \dot{\theta}_{nl} = 80 \text{ deg/sec} = 1.396 \text{ rad/sec} = \text{minimum output no-load speed.}$$

To determine the minimum motor no-load speed,

$$\dot{\theta}_{MNL} = 1.396 \text{ rad/sec} \times 670 = 935 \text{ rad/sec} = 8932 \text{ rpm}$$

To determine the minimum motor stall torque required,

$$T_{MS} = \frac{T_{TO}}{G \times \text{Eff}}$$

For example, using previously determined values for

T_{TO} , G and Eff

$$\begin{aligned} T_{MS} &= \frac{37,575}{670 \times 0.9} \text{ lbf-in.} \\ &= 62.3 \text{ lbf-in.} \\ &= 997 \text{ ozf-in.} \end{aligned}$$

6.1.1.2.4 Motor Thermal Characteristics

In general, the motors are capable of being operated at average current levels considerably above values thermally acceptable on a continuous basis. Since the motors require several minutes to reach a final operating temperature, the motors can be operated at their maximum current capability for a short period, providing the average current over a period of several minutes does not exceed the motor thermal capability. A thermal analysis of the motor was conducted. The results are shown in Figure 51.

The worst-case condition is for the motor operating at stall in an environment defined for a hot day. For this case, the motor can operate at a maximum duty cycle of 82 percent. Since ground operation of the actuator will likely be limited to duty cycles of 50 percent or less, the resulting maximum motor winding temperature will be 315°F. Table 23 presents a summary of the loss distribution in the motor as a function of operating condition.

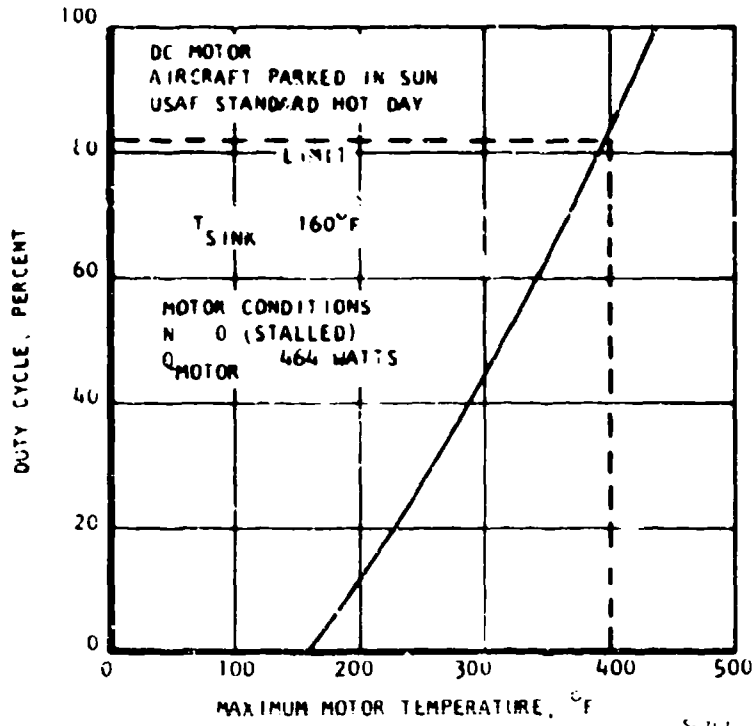


Figure 51. Motor Thermal Analysis Results

TABLE 23

BRUSHLESS DC MOTOR ELECTRICAL LOSSES

Condition	Component	Loss, w
Stalled (29 amp, current limit)	Stator	422
	Other	42
	Total	<u>464</u>
At 2-hp output (6.33 amp, Figure 59)	Stator copper	25
	Stator iron	134
	Bearings	11
	Stray	16
	Total	<u>186</u>
At 3-hp output (9.26 amp, Figure 59)	Stator copper	50
	Stator iron	133
	Bearings	11
	Stray	23
	Total	<u>217</u>
At 4-hp output (12.23 amp, Figure 59)	Stator copper	84
	Stator iron	132
	Bearings	11
	Stray	30
	Total	<u>257</u>

6.1.2 Controller

A functional block diagram of the controller using a microprocessor is shown in Figure 52. The high-voltage rectifiers and filter convert 3-phase, 115/200 vac to 280 vdc. The energy storage element within the filter will be chosen to keep the ripple amplitude low over a three-to-one input frequency range, corresponding to the expected variation from the permanent magnet generator. Monolithic Darlington transistors such as the TRW SVT 60.JJ series will be evaluated for use in the commutation circuit. Optical couplers are used for circuit isolation between the control and power signal lines. The choice of the microprocessor to control the actuation system will be made by considering items such as word length, power requirements, speed, cost, and architecture.

The prospective microprocessor candidates for this application include the M6800 by Motorola; 8080 by Intel, 990 by Texas Instruments, and IM6100 by Intersil. Another means of implementing the microprocessor uses micrologic chips such as the AMU2901 into a 4-bit slice microprogrammed set. Both microprocessor implementations offer extensive software processing power and a family of hardware devices, including prototype development packages. Because of the computer-like structure of the microprocessor, much of the system logic and monitoring function can be transformed into software (a computer program) stored in a storage device. The storage device will be a programmable read-only memory (PROM). Since the PROM is a non-volatile memory, loss of power will not offset the contents.

Figure 53 shows the flow chart of a program that can perform the functions shown in Figure 52. The flow chart shows how the processor reacts to different inputs to implement the following functions:

Servoloop Control--Controls the output to minimize error.

Rotor Excitation Sequencing--Excites the phases of the dc motor according to its characteristics.

Fault Monitoring--Monitor faults or errors in the system and respond accordingly.

Redundancy--Coordination between channels.

Torque Control--A specific torque vs speed relationship is included to obtain better efficiency.

Regeneration--Regeneration mode is incorporated in the system to reduce power consumption and improve system response.

The advantage of using the stored program approach is that little or no hardware change is required if the system requirement is changed or updated; only modification of software is necessary.

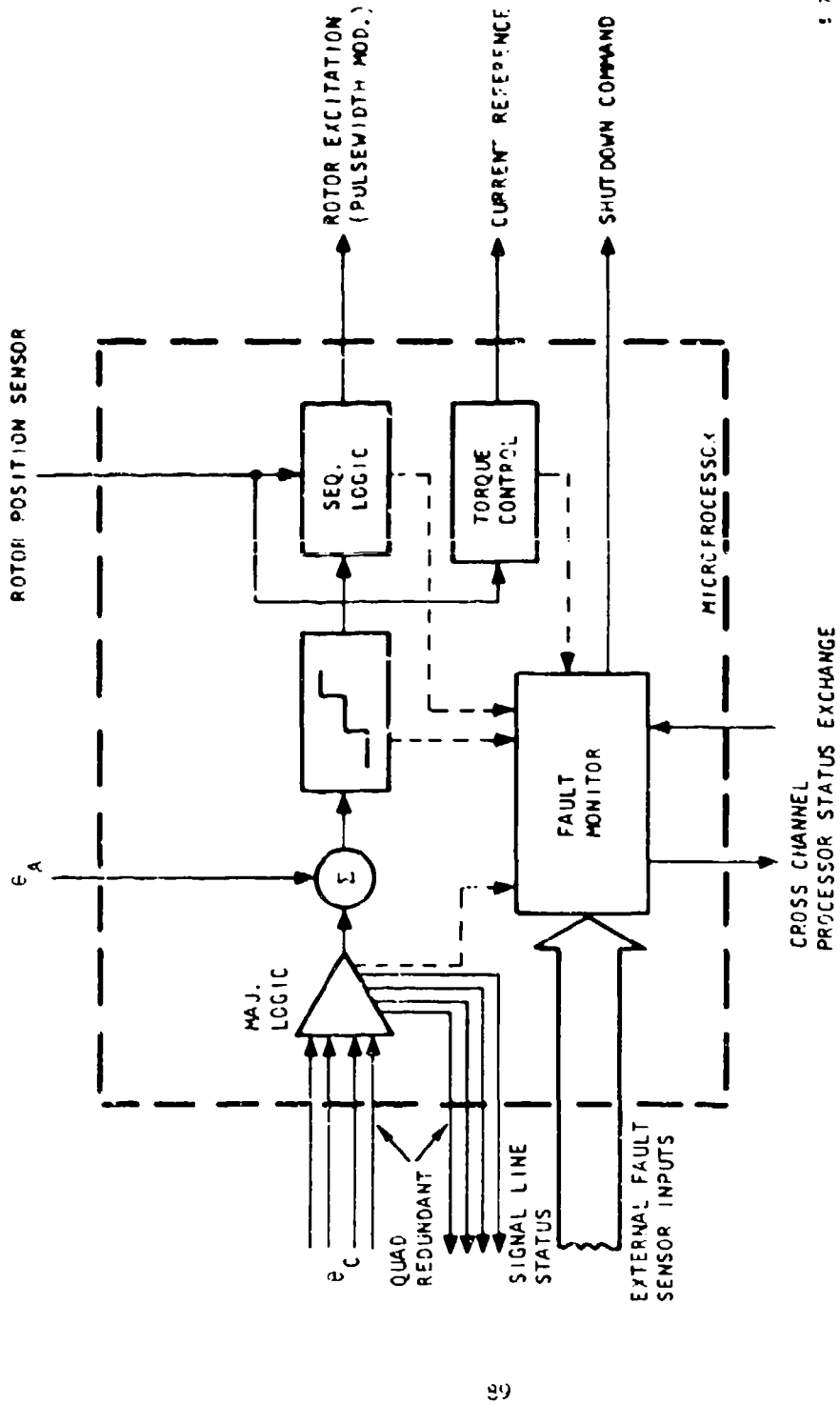


Figure 52. Functions Implemented by a Microprocessor

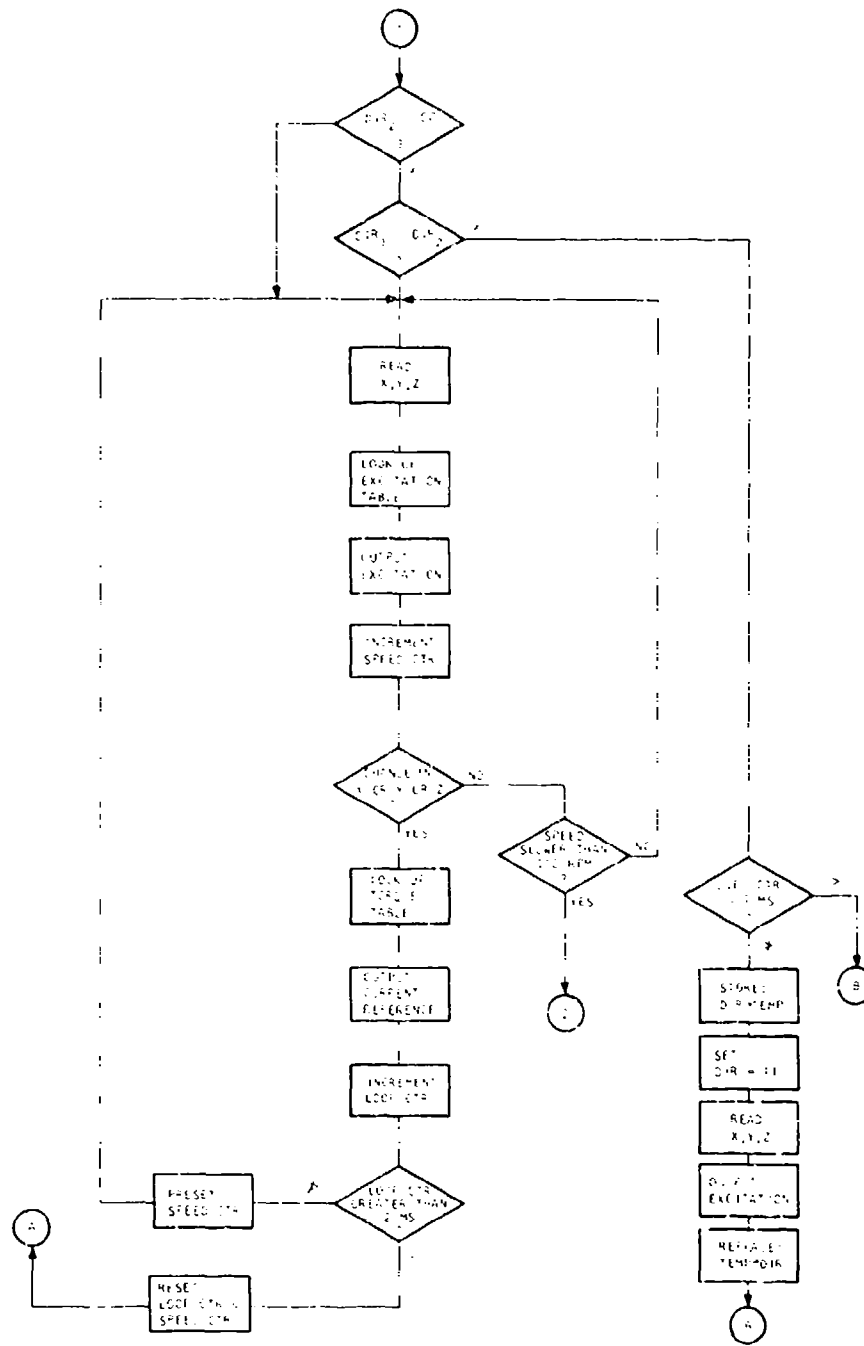


Figure 53. Continued

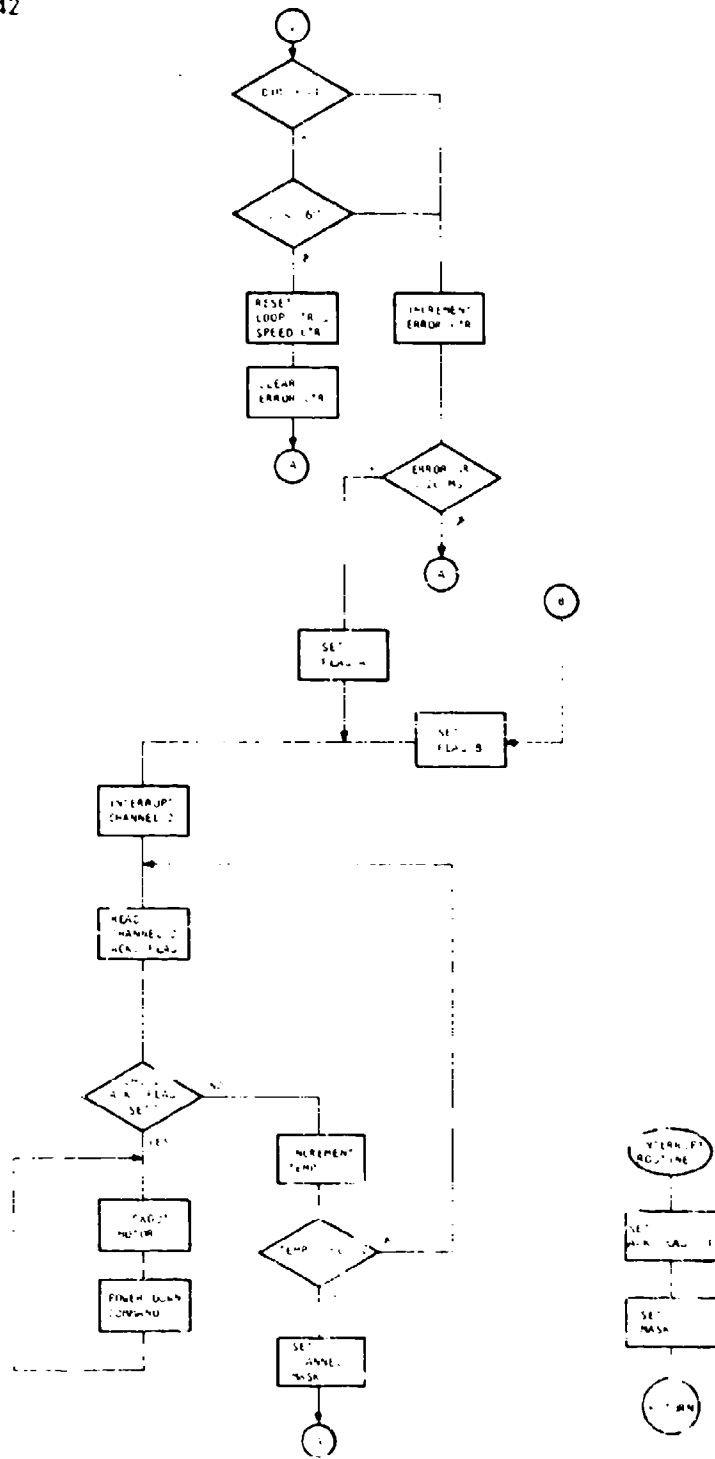


Figure 53. Continued

A nonrecursive digital filter mechanization applicable for a linear control system is shown in Figure 54. The current limit value and the commanded position will be input quantities. The difference between the armature current and commanded current is e_1 . Mechanization of the pulsewidth modulation (PWM) generator is shown in Figure 55. The output of the PWM generator changes to correct for variations in the input dc voltage and the output load demand.

The position sensor coding is illustrated in Figure 56. The sequence controller calculates the logic in accordance with Table 24. Figure 57 contains a description of the analog-to-digital converter. If the controller inputs are digital signals, the data will be direct inputs to the microprocessor. A small transformer-coupled power supply will be used to generate dc voltages required by the controller.

6.2 PRELIMINARY PERFORMANCE SPECIFICATION

6.2.1 Scope

The preliminary performance specification describes the general characteristics of a primary flight control actuation system. The system is a power-by-wire and fly-by-wire design, and the rotary actuator part of the system serves as the control surface hinge.

6.2.2 Description

6.2.2.1 Function

The rotary electromechanical actuation system comprises the following elements, as shown in Figure 58.

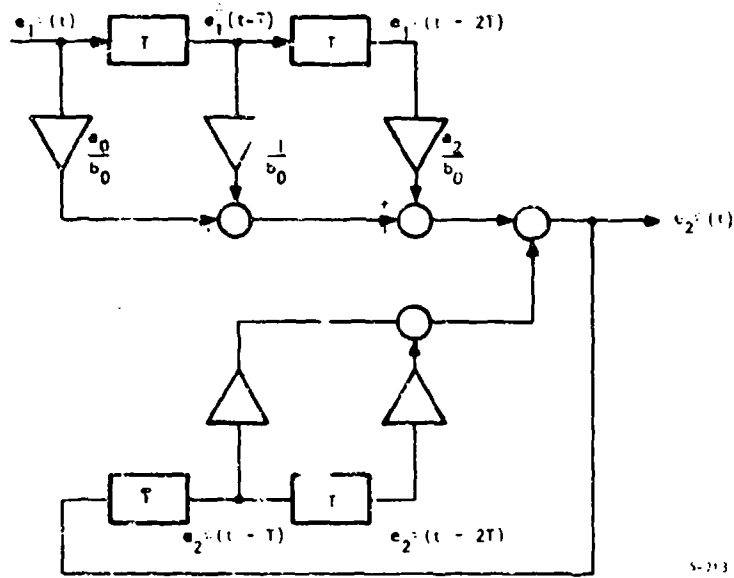
Controller (2 channel, redundant)

Two motors with integral parking brakes

Rotary hinge-line type geared actuator with velocity summing differential

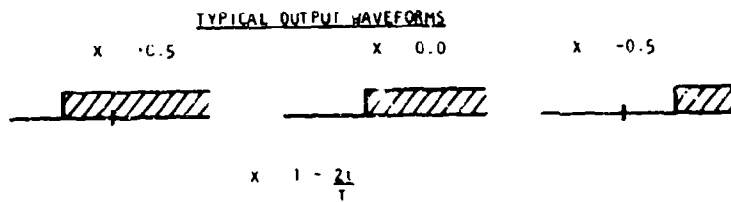
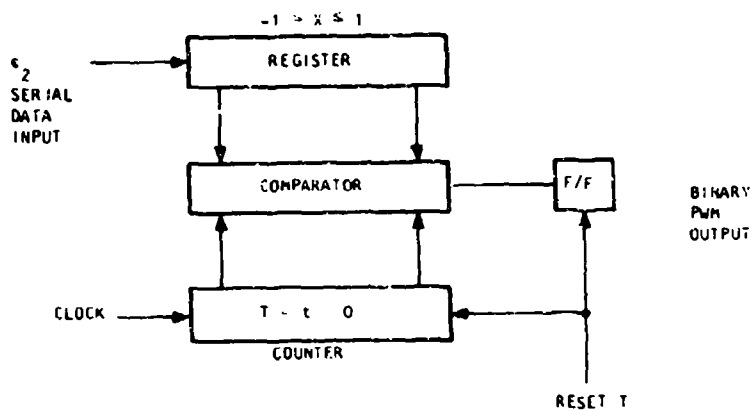
The controller interfaces with control surface position commands from the aircraft automatic flight control system. The digital controller provides power to the servomotor by pulsewidth modulation of power transistor switches. The motor is a brushless dc permanent magnet rotor design directly coupled to the control surface through stages of gearing. Control surface position sensing is used to close the servoloop. The controller includes built-in-test provisions.

Normal operation requires both electric motors to be operating. The actuator gearing includes a velocity summing differential. Either motor can operate the output of the actuator independent of the other electromechanical drive channel. Operation on a single motor results in full torque capability and one-half rate capability at rate limit.



5-213

Figure 54. Nonrecursive Digital Filter Mechanization Diagram



5-216

Figure 55. PWM Generator Functional Block Diagram

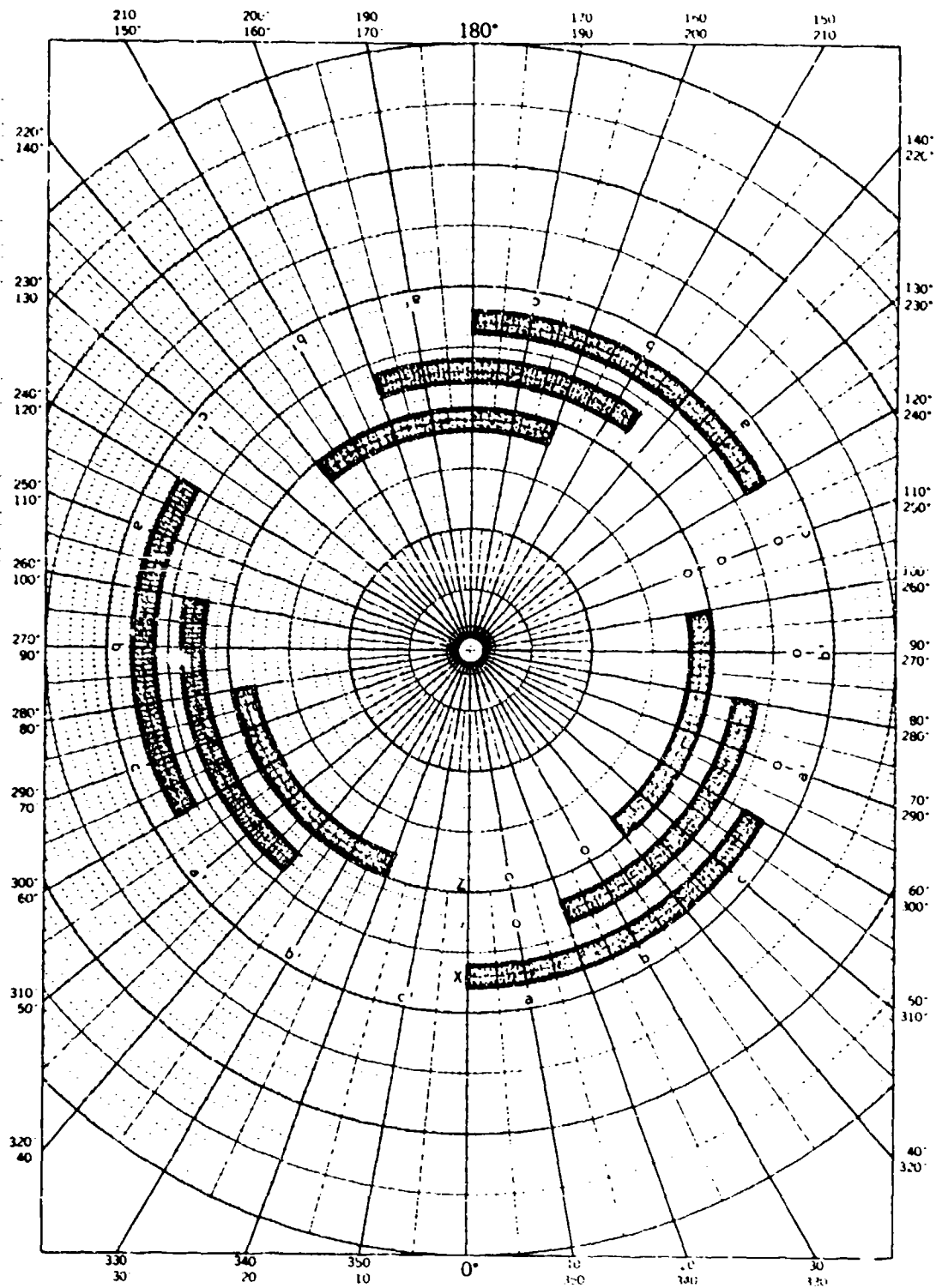
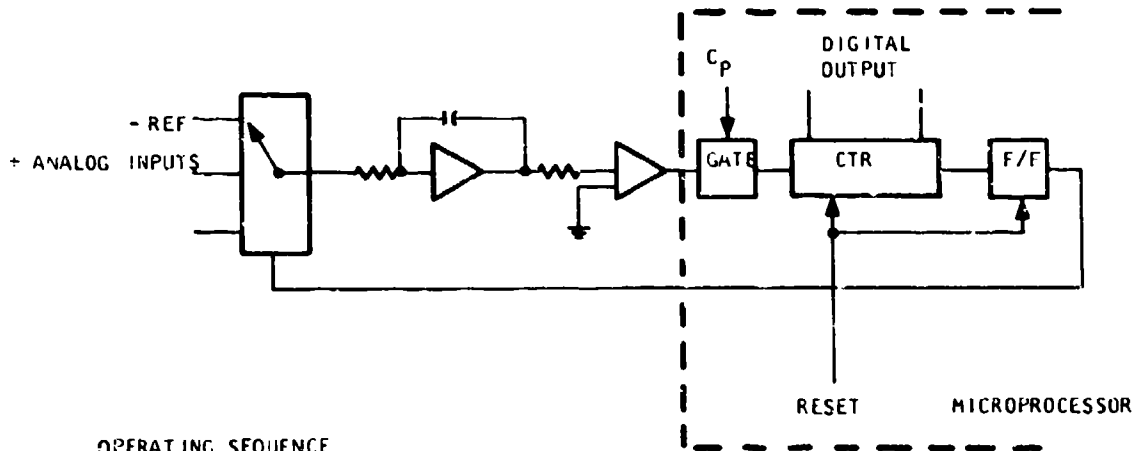


Figure 56. Shaft Position Sensor

TABLE 24
SEQUENCER CONTROLLER TRUTH TABLE

Codes A+, A-, B+, B-, C+, C- are transistor switches
Codes a, b, c, a', b', c' are shaft position states

a	b	c	a'	b'	c'	A+	A-	B+	B-	C+	C-	
												CW TOPQUE
a	b	c	a'	b'	c'	A+	A-	B+	B-	C+	C-	
												CCW TOPQUE



OPERATING SEQUENCE

1. RESET ENABLES INTEGRATION OF ANALOG DATA INPUT.
2. WHEN THE COUNTER OVERFLOWS, INTEGRATION OF THE REF TAKES PLACE.
3. THE NUMBER ACCUMULATED BY THE CTR DURING THE REF INTEGRATION INTERVAL REPRESENTS THE ANALOG INPUT.

3-715

Figure 57. Analog Input Encoder Mechanization Diagram

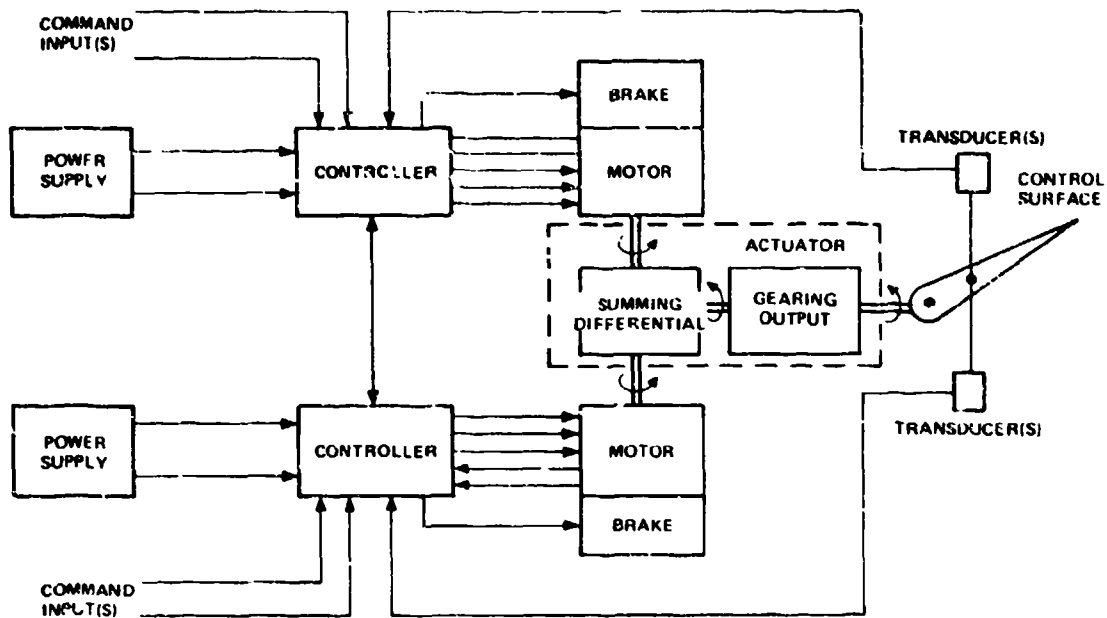


Figure 58. System Model

Electromagnetic brakes are included on each drive motor shaft. The brakes are used to implement the redundancy of the high-efficiency gearing in the dual drive channels. A failed electromechanical drive is held stationary by the brake to allow the operating drive assembly to position the control surface.

6.2.2.2 Controller

A digital microprocessor will be used as the central component of the brushless dc motor controller. As shown in Figure 58, the control is the interface between the motor, the command input, and the electrical power bus. The controller provides a command to the commutation circuit, which provides power to the proper motor stator windings based on sensed rotor shaft position. The dc bus is connected to the windings by the electronic transistor switches. At any instant, two switches are commanded to conduct; every 60 deg, one switch is turned off and a new one is turned on to obtain the required current pattern in the motor armature.

The speed of rotation of the brushless dc motor is controlled by varying the average dc voltage supplied to the motor by the electronic commutator. Pulsewidth modulation techniques are used to generate the required average voltage. The major characteristics of the microprocessor controller are summarized in Table 25.

The controller is programmed to provide a fixed current limit corresponding to maximum stall requirements. The current limit also may be programmed as a function of time, motor speed, or other independent properties useful in defining the performance characteristics for aircraft.

TABLE 25
CONTROLLER CHARACTERISTICS

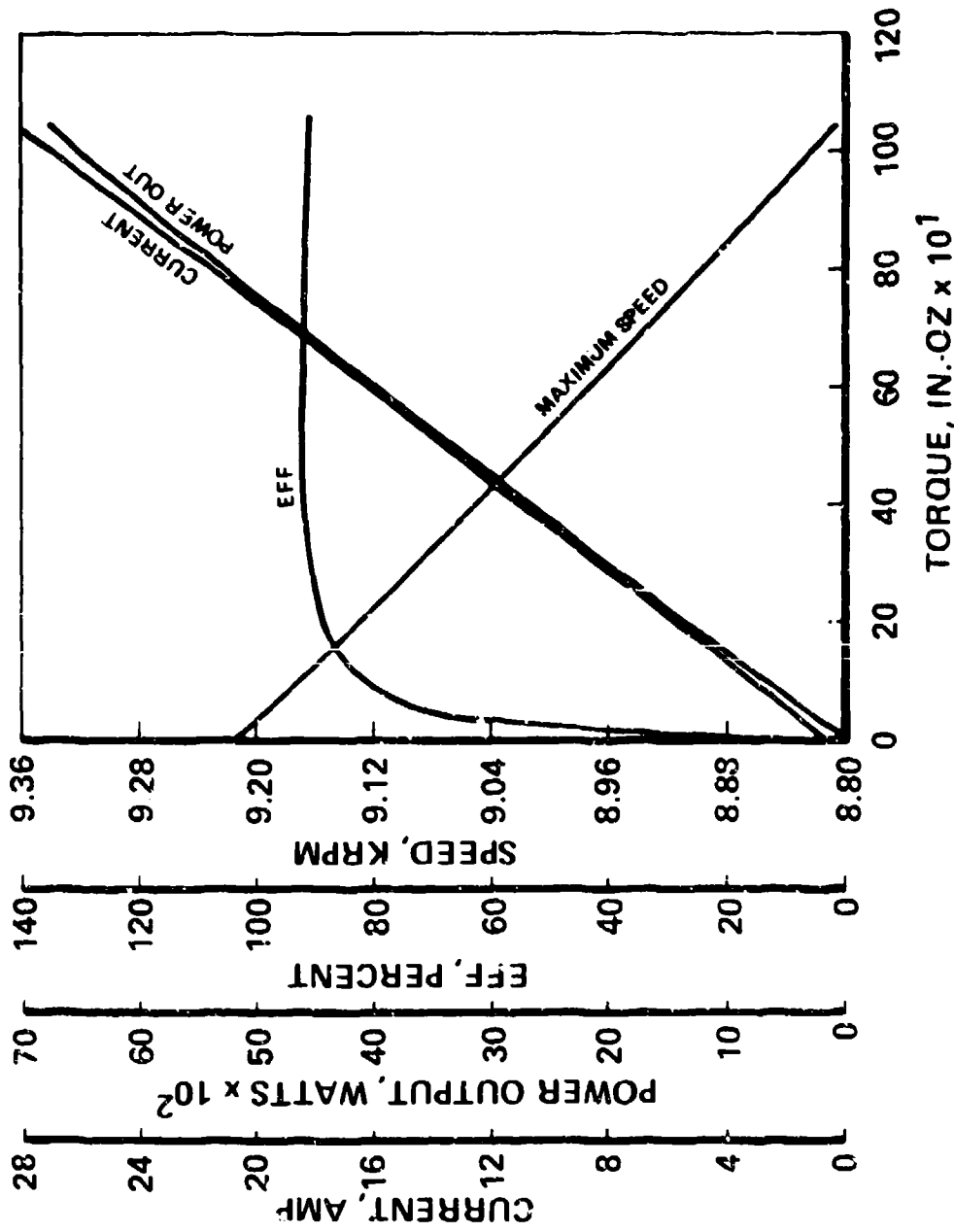
Command Input	2-channel, voltage position analog
Adaptive Inputs	4 (maximum), 0 to 5 vdc
Power Input	270 vdc
Output	265 vdc
	29 amp current limit at stall
Weight	5.25 lb (flight configuration)

6.2.2.3 Motor

The motor is a permanent magnet, dc, brushless type comprising a wound stator and rare-earth-cobalt permanent magnet rotor. The motor assembly also will include separately excited dc brake and shaft position sensor. The position sensor detects the rotor position and activates the electronic commutator. Performance of the motor is presented in Figure 59. Table 26 summarizes the significant design characteristics of the motor assembly.

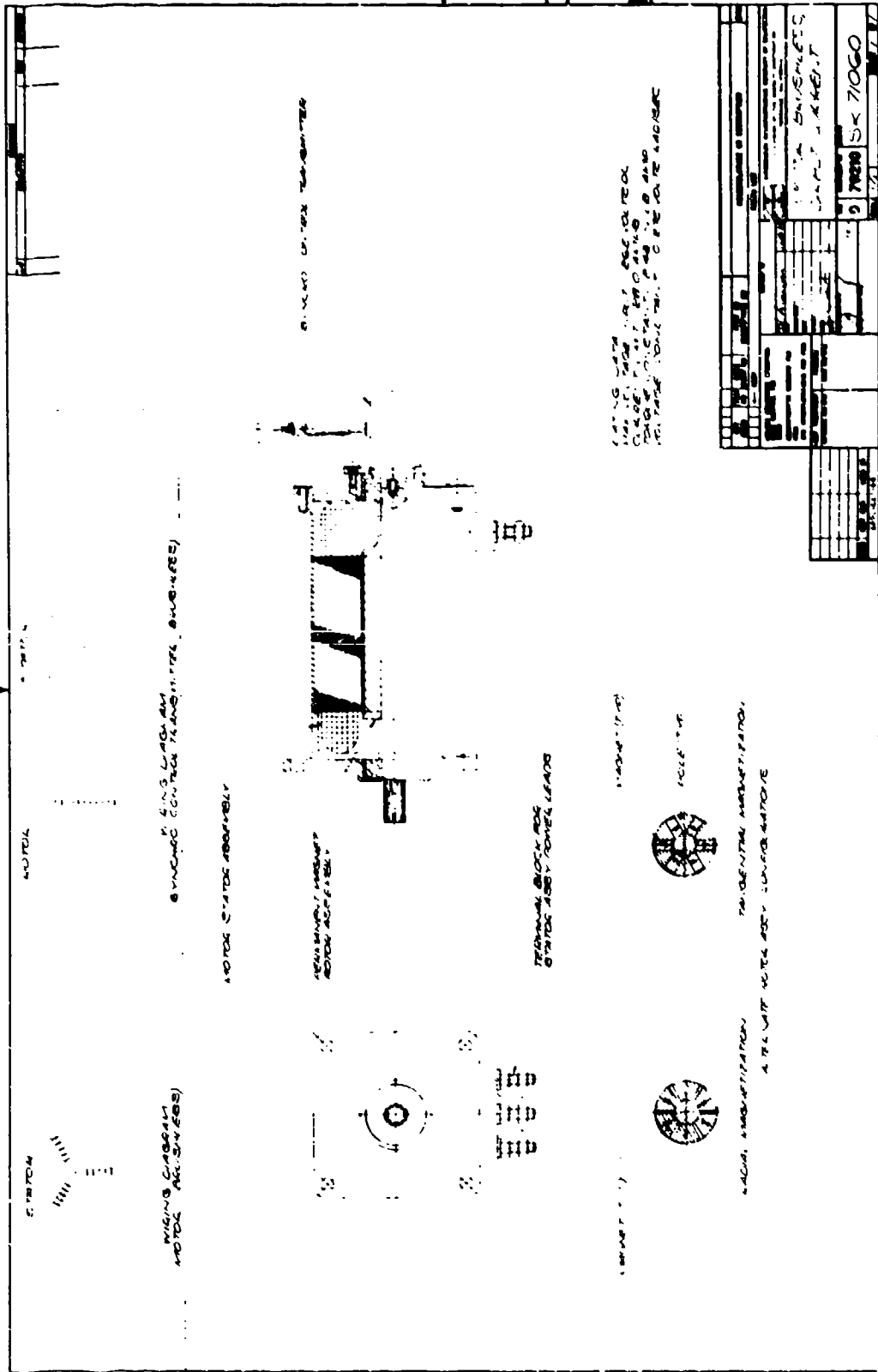
TABLE 26
MOTOR CHARACTERISTICS

Rated voltage	265 vdc
No-load speed	9200 rpm
Torque per amp	34 ozf-in./amp
Stator resistance (68°F)	0.33258 ohm
Rotor inertia	1.638×10^{-3} lbf-in.-sec ²
Time constants	0.006 sec, electrical
	0.016 sec, mechanical
Back EMF	28.7 v/1000 rpm
Brake voltage	270 vdc
Brake torque	75 lbf-in. (minimum)
Envelope	See SK71060
Weight, excluding brake	18 lb



-885-A

Figure 59. Motor Performance



6.2.2.4 Actuator

The actuator is a rotary hinge-line device that serves as the structural attachment between the control surface and the wing structure. The dual-redundant electric motors are mounted on the actuator. The two input shafts operate into a velocity summing differential. The output of the differential drives into the compound planetary, rotary output stage. Spur gearing is used throughout the assembly. The major characteristics of the assembly are presented in Table 27.

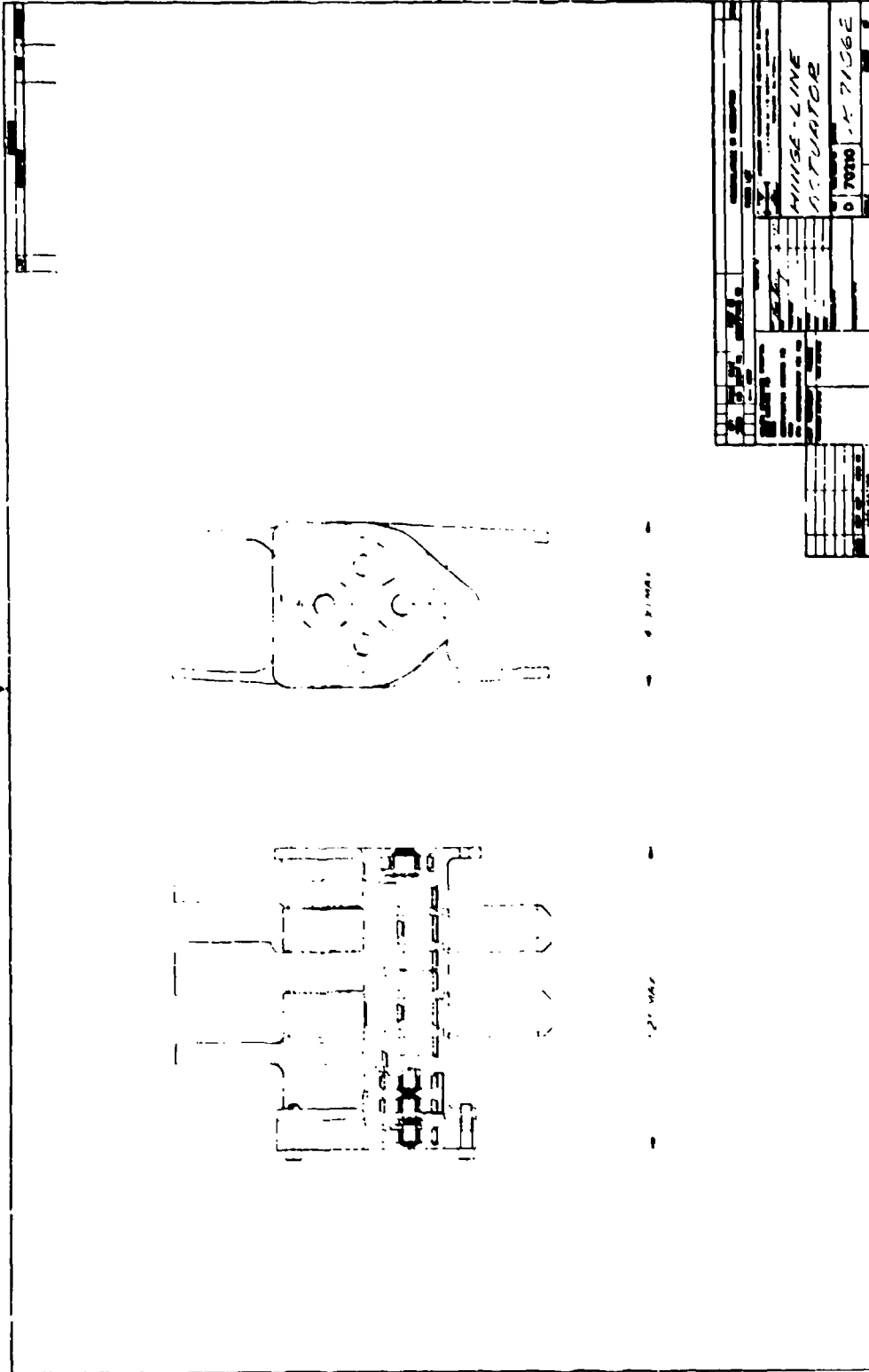
TABLE 27
ACTUATOR CHARACTERISTICS

Stall torque	37,500 lbf-in.
Rate	80 deg/sec
Life	100,000 cycles
Gear ratio	670:1
Gear configuration	(1) Input: single-stage planetary (2) Differential: planetary (3) Output: compound planetary
Spring rate	3.75×10^6 lbf-in./rad
Envelope	See SK71062
Weight	12.5 lb (14.5 lb including differential)

6.2.2.5 Electrical Considerations

The system will operate on 115/200-vac, 3-phase power and will have built-in spike and short-circuit protection. The system will have BIT/self-test capability. In the event of a failure, the channel will automatically shut down and an alternate mode of operation will be established. System sensitivity and repeatability will not be affected by voltage variations as allowed by MIL-STD-704.

Electrical and lightning protection bonding will be in accordance with MIL-B-5087. System warmup time will not exceed 5 sec. The controller will utilize solid-state and printed-circuit board construction wherever possible.



All removable units and subassemblies will be interchangeable between systems and keyed to prevent improper installation.

6.2.2.6 Mechanical Considerations

The mechanical overload safety factor for the attach fitting and gear housing will be at least 200 percent and up to a maximum of 600 percent. The unit shall be designed with weight, reliability and maintainability as primary design considerations. The unit will have a minimum operational life expectancy of 1000 hr without overhaul. Preventative and corrective maintenance is allowed. The actuator backlash will be limited to 1/4 deg rotation at the output, with the motor input shaft held rigid.

6.2.2.7 System Considerations

The system will have a static tracking error between the control surface command and the control surface of 1/2 deg maximum. Provision will be made for torque limiting. This may be implemented by computation of surface position as a function of Q (airspeed and altitude). The motor actuator assembly may be cooled passively by heat rejection to the aircraft structure. The local heat rise at the mounting surface will not exceed 200°. The actuation system will have a frequency response bandwidth of 8 Hz.

6.2.2.8 Environmental

The design of the actuation system and components will be based upon the environmental testing requirements listed below:

<u>Environment</u>	<u>Specification</u>	<u>Method</u>	<u>Procedures</u>
Altitude	MIL-STD-810	500.1	-
Temperature	MIL-STD-810	501.1 502.1	II I
Humidity	MIL-STD-810	507.1	I
Saltspray	MIL-STD-810	509.1	-
Sand and Dust	MIL-STD-810	510.1	-
Vibration	MIL-STD-810	514.2	(category b.2)
Shock	MIL-STD-810	516.2	I Fig. 516.2-1 (a) and (c)
EMIC	MIL-STD-461	-	-
Explosive Atmosphere	MIL-STD-461	511.1	I
Rain	MIL-STD-461	506.1	(modified)
	-	-	-

6.3 ANALOG ANALYSIS

The dynamic characteristics of the actuator closed loop were generated using an analog computer simulation of the baseline system. A functional block diagram of the simulation is presented in Figure 60. The block diagram includes the control surface and its associated hinge moment loading curve; however, the response characteristics presented below are for the actuator closed loop only under no-load conditions.

For the closed-loop performance data, a position feedback servoloop with a pulse-width-modulated (PWM) controller is assumed. The PWM controller converts the actuator-position to command-input-error signal into an appropriate motor voltage that is limited by a preset maximum allowable motor current. This type of controller provides a linear relationship between the position error voltage and the effective voltage applied at the motor terminals. The gain of the controller was set to provide an actuator rate output equivalent to a control surface rate of 45 deg/sec for a 1-deg error input. Values of the motor parameters used were as specified for the baseline motor configuration.

Because of the large electrical time constant relative to the nonsaturated mechanical time constant, the loop damping is very light. Some form of phase compensation is required to provide the proper damping; for this simulation, compensation in the feedback path was utilized. The frequency response data obtained are presented in Figures 61 and 62. The time response of the loop is equivalent to an effective first order time constant of approximately 0.02 sec.

6.4 MOCKUP

A wood and metal mockup was constructed showing the general arrangement of the electromechanical rotary actuator installed in a simulated wing spar structure and control surface. Figure 63 is a photograph of the unit. The control surface is capable of being moved manually.

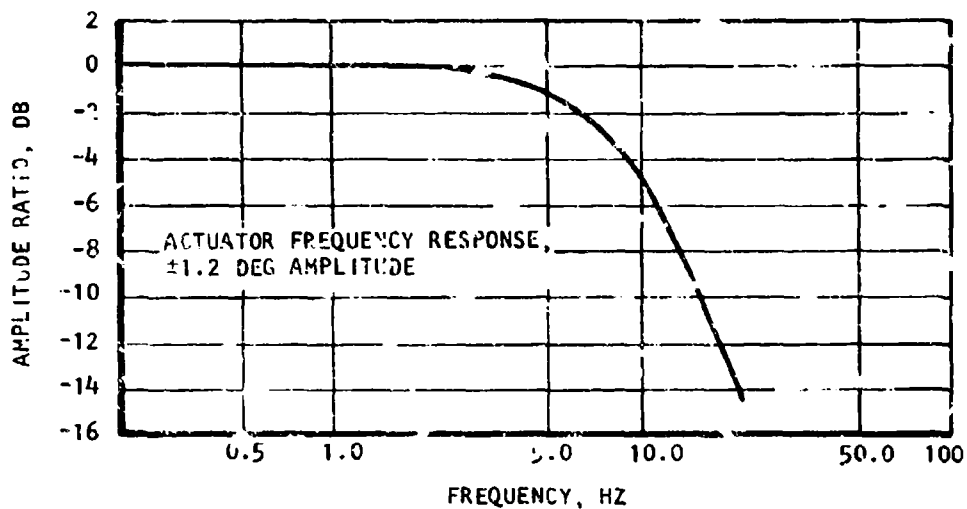


Figure 61. Amplitude Ratio vs. Frequency

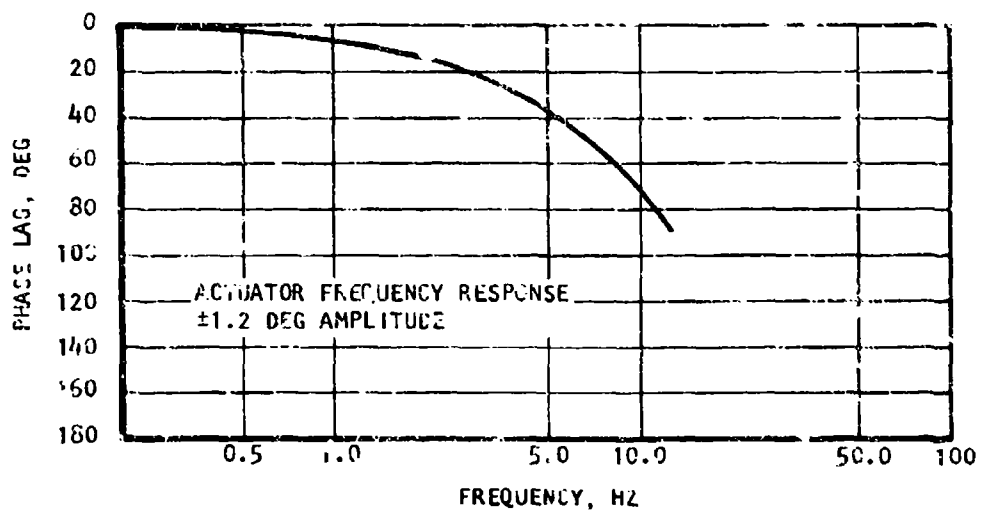


Figure 62. Phase Lag vs. Frequency

S-4359

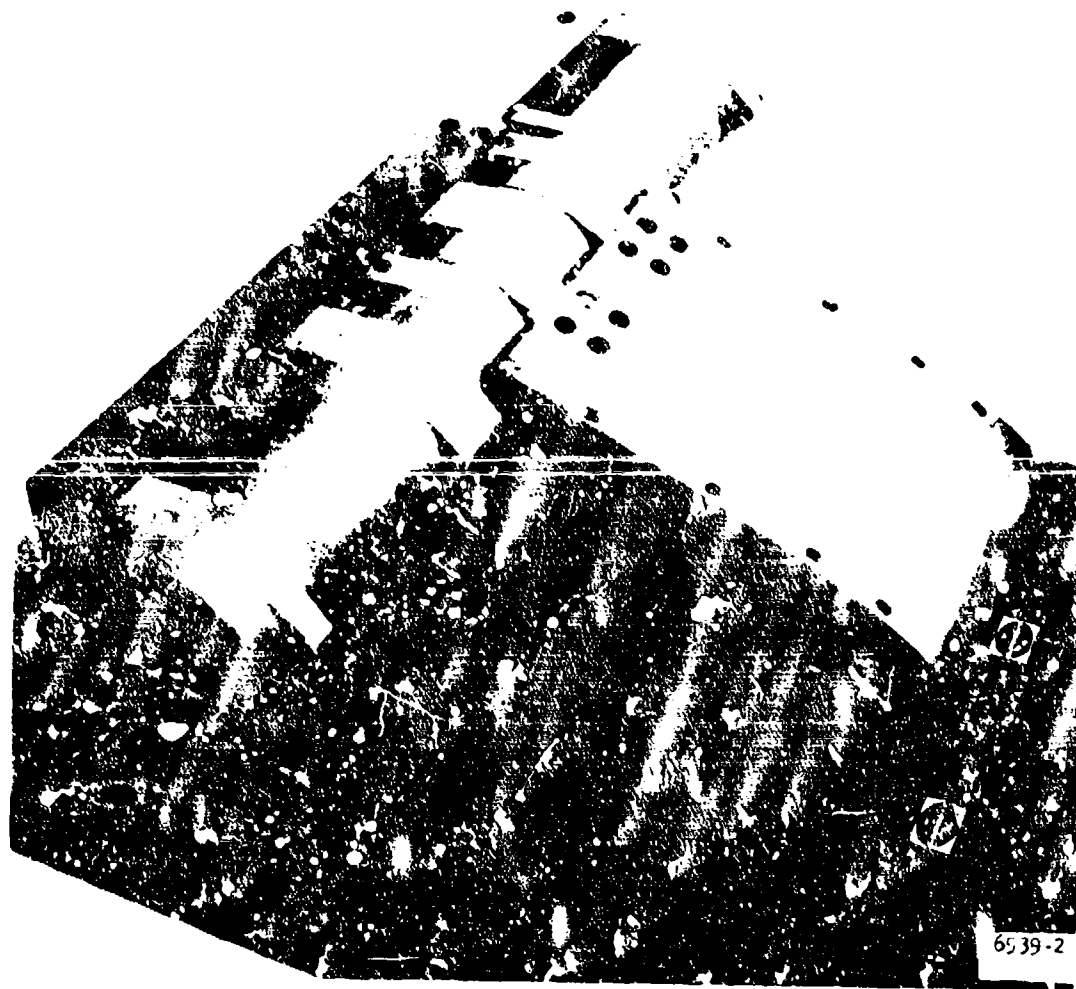


Figure 3. EM Actuator Mockup

7. PROGRAM PLANS

This section presents the plan for design, fabrication, and evaluation testing of an electromechanical rotary hinge-line actuator. The program plan includes a schedule and summary description of the tasks required for development of the actuation system. The preliminary test plan includes brief descriptions of the tests to be conducted, the required facilities and supporting test equipment, and the expected results of the test.

7.1 PROGRAM PLAN

The objective of this program is to design, fabricate, and test an electromechanical flight control actuator. The program is organized into five tasks covering a 25-month period. The program schedule is presented in Figure 64. The following paragraphs present detailed task descriptions.

7.1.1 Task 1: Design

The objective of this task is to conduct system studies to provide the component designer with the necessary technical inputs for detailed component design required to attain component and system performance goals. This includes the modeling of system components for use in system performance prediction and sizing studies and the preparation of detailed problem statements for components. Component characteristics determined from the preliminary design will be used. Detailed component specifications, design sketches, and configuration layouts will be prepared and purchased components and potential vendors identified. Component characteristics will be used to define system configuration and establish interfaces; these will include command input redundancy, thermal control, mounting details, and test monitoring. Initial coordination and resolution of interfaces and program goals will be accomplished at the program kickoff meeting.

System dynamic performance will be defined for design and off-design operation; also, detailed component performance requirements will be defined. Design documentation will be prepared to support manufacture and test of the system, define technical and procurement problem areas, and develop cost-effective solutions. Detail sketches, installation and assembly drawings, and procurement and source selection documentation will result from this effort. Design documentation and drawings will be prepared in sufficient detail for development manufacturing purposes and to provide an accurate history of the component/system design.

A system performance specification will be prepared to complement the design drawings. The specification will describe requirements for materials, finishes, and construction that are compatible with current airframe standards

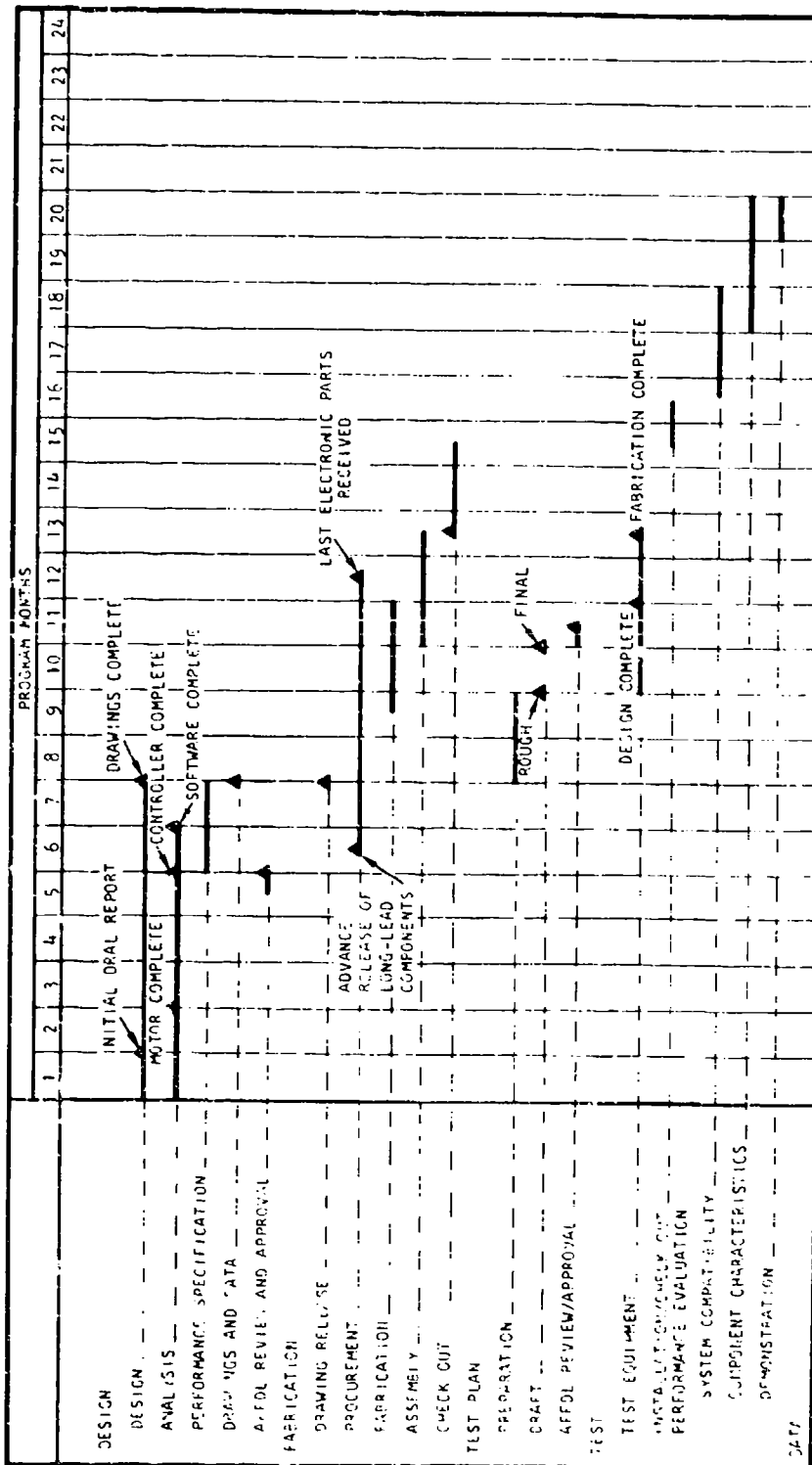


Figure 64. Program Schedule for Design, Fabrication, and Evaluation Testing of Electromechanical Rotary Hinge-Line Actuator

and environmental criteria. System effectiveness objectives, including reliability, maintainability, system safety, and human factors, also will be established.

During the sixth program month, a design review will be held. The purpose of the review will be to assess the evolving actuation system design and to establish a design record of the actuation system to be fabricated. During this review, data will be presented to show that the design satisfies all aspects of performance and realistic test installation features. Approval of the design will allow release of long-lead items for procurement; specifically, electronic components and the rare earth magnet material used in the servomotor.

7.1.2 Task 2: Fabrication

The objective of this task is to fabricate, test, and assemble the components of the electromechanical actuation system. Initiation of Task 2 will occur in the eighth program month after release of the design drawings from Task 1. (Advanced release of long-lead items will occur in the sixth program month.) Procurement of materials and components will begin with long-lead items in a timely and cost-effective manner for the fabrication phase. The advance release of parts will result in delivery of the component parts in accordance with the assembly and manufacturing schedule of the related components. Outside production will include procurement of the samarium-cobalt magnets and installation in the rotor assembly.

Fabrication will include component parts of the motors, gearboxes, and controllers. As fabrication progresses, the assemblies will be subjected to manufacturing tests as required. Availability of assembled components and scheduling of component tests are planned to minimize total test time and maximize utilization of test fixtures.

As each major system element is completed, the unit will be checked out. This component checkout will demonstrate and verify component capability and compliance with the stated program goals. Test plans and procedures developed in Task 3 and the components and test equipment fabricated in Task 1 will be required to support these tests. The results of component tests will be documented.

7.1.3 Task 3: Test Plan

The objective of this task is to formulate plans for development test of the actuation concept. Each plan will list the tests required, test conditions, parameters to be measured, test equipment and facility requirements, instrumentation (including calibration), and data and report requirements. Sufficient procedural definition will be included in each plan to permit approximation of program schedule status and expenditures. The plan will be available for review and approval in the eleventh program month.

7.1.4 Task 4: Test

The objective of this task is to test and evaluate component performance in terms of the specified goals. Completed components and assemblies will be installed in the demonstration test fixtures. The actuation system assembly will be evaluated to (1) assure compatibility with related components and test equipment, (2) show that the system functions as designed, and (3) show that the actuation system is ready for performance evaluation testing. The design and construction of certain special test equipment will be necessary to support these tests. This will include test fixtures, load fixtures, and test panels.

System tests will be conducted in accordance with the approved test plan to prove component compatibility and verify system-level performance parameters. These tests will be designed to verify analytical predictions for comparison with test results and program goals. All tests may be witnessed; appropriate prior notification will be given. The test results of the individual components and the results of the system-level tests will be analyzed. Acceptance criteria for the components will be defined based upon the work statement.

Possible design modification or rework of some components may be required to satisfy acceptance criteria. Recommendations of the modifications and design improvements will be documented. Analysis of the test results will be a significant part of the final report.

7.1.5 Task 5: Data

The objective of this task is to document technical and program results from each of the program tasks in accordance with the schedule.

7.2 PRELIMINARY TEST PLAN FOR ACTUATION SYSTEM DEMONSTRATION

Demonstration testing will be conducted upon a representative configuration of the electromechanical actuation system. The system will be installed in a laboratory test facility, with appropriate structural and electrical interfaces simulated. Specifically, the structural interface, thermal management provisions, and control interfaces with a typical aircraft will be simulated to the highest practical degree. Controller electronics will be deleted from this simulation. Electronics will be breadboard configuration. Testing will be conducted to verify the compatibility of the installed actuation system with the simulated structure, actuator assembly, controller, and multiple control signal interfaces. Tests to be performed will prove redundancy management; capability to provide adaptive modification of selected parameters in the controller such as variable current limit, temperature limits, servo gain, power regeneration, filter bandwidth and sensitivity, and variation of no-load rate. Tests also will be conducted at both the component and system levels to evaluate the detail performance characteristics of the actuator/controller components. These tests will include:

- (a) Duty cycle capability performed at room temperature and elevated temperature

- (b) Frequency response including small signal, large signal, no-load, and loaded
- (c) Hysteresis and resolution
- (d) Efficiency and power factor
- (e) Actuator spring rate/stiffness
- (f) Weight

Figure 65 presents the task logic for the demonstration test phase. Figures 66 through 67 present individual test briefs for the proposed demonstration testing. These identify equipment requirements, facility interfaces, and criteria for test acceptance, and show the depth of data to be collected.

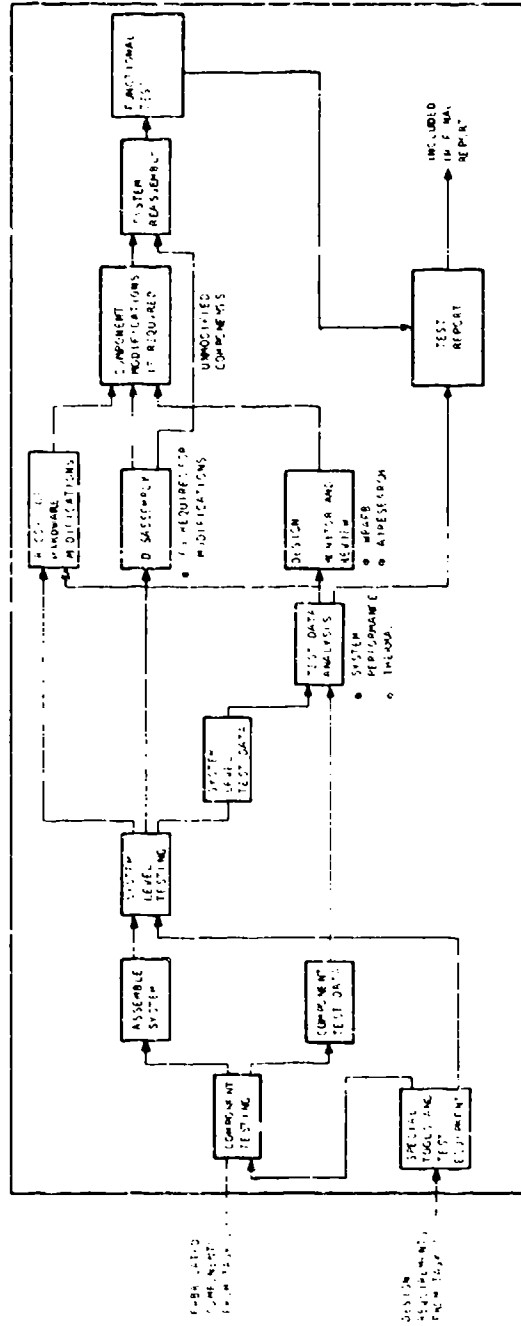


Figure 65. Test Logic Diagram

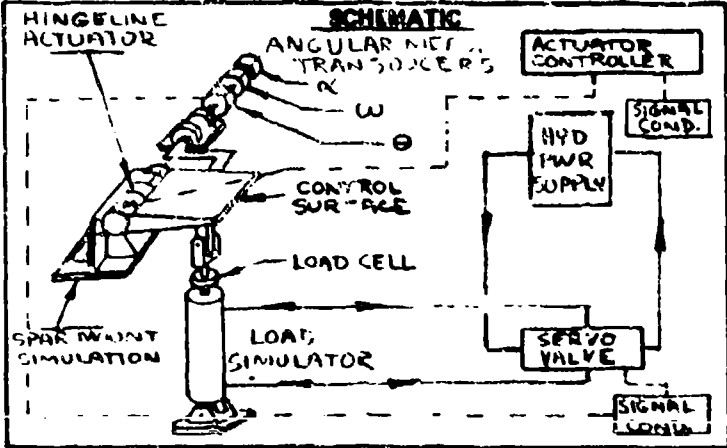


TEST PERFORMANCE

Prepared by: K.N. DULLACK
 Part No. _____
 Date 11-13-75

OBJECTIVE
 TO DEMONSTRATE THE OPERATIONAL CHARACTERISTICS OF THE CONTROLLER AND HINGELINE ACTUATOR ASSEMBLY.

FACILITY
 HYDRAULIC TEST LABORATORY



- EQUIPMENT AND INSTRUMENTATION**
1. HOLDING FIXTURE
 2. LOADING SYSTEM
 3. HYDRAULIC SUPPLY
 4. SERVO VALVE & CONTROLS
 5. ANGULAR TRANSDUCERS POS, VEL, ACCEL.
 6. LOAD CELL
 7. SIGNAL CONDITIONING
 8. OSCILLOGRAPH
 9. DC POWER SUPPLY

PROCEDURE

SEE SPECIFIC TEST SHEETS

REQUIRED DATA

ANGULAR POSITION, ANGULAR VELOCITY, ANGULAR ACCELERATION
 HINGE LOAD, VOLTAGE, CURRENT, TEMPERATURE, STRAIN

ACCEPT/REJECT CRITERIA

CONFORM TO SPECIFIC PERFORM. REQUIREMENTS

NOTES

PERFORMANCE TESTING INCLUDES FREQUENCY RESPONSE, STIFFNESS, POWER EFFICIENCY, ACCELERATION, POSITION RESOLUTION AND VELOCITY

Figure 66 . Performance Test and Test Setup



TEST
FREQUENCY RESPONSE

Prepared by: K. N. DULLACK
Part No. _____
Date 11-13-75

OBJECTIVE

TO DETERMINE THE FREQUENCY RESPONSE CONTROL LIMITS.

FACILITY

HYDRAULIC TEST LABORATORY

SCHEMATIC

EQUIPMENT AND INSTRUMENTATION

1. OSCILLOGRAPH
2. SINE WAVE GENERATOR
3. POSITION INDICATOR
4. PERF. TEST EQUIP.

PROCEDURE

1. APPLY BIAS COMMAND SIGNAL TO CONTROLLER.
2. SUPERIMPOSE A 5 TO 10 HZ, ± 5 DEGREE SIGNAL OVER THE BIAS COMMAND.
3. RECORD DATA.

REQUIRED DATA

INPUT COMMAND (mv) VS. ANGULAR POSITION (θ)

ACCEPT/REJECT CRITERIA

TEST DEMONSTRATION

NOTES

Figure 67. Frequency Response

115



**TEST
STIFFNESS**

Prepared by: K. N. DUNLACK

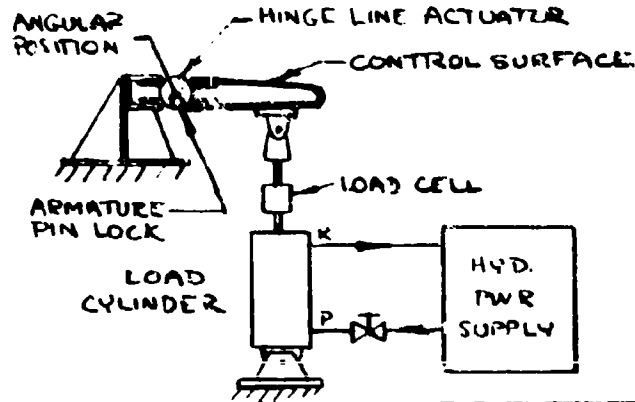
Part No. _____

Date 11-13-75**OBJECTIVE**

TO DEMONSTRATE THE SPRING
RATE OF THE ACTUATOR

FACILITY

HYDRAULIC
TEST LABORATORY

SCHEMATIC**EQUIPMENT AND
INSTRUMENTATION**

1. HOLDING FIXTURE
2. HYD LOAD SYSTEM
3. ARMATURE LOCKING
DEVICE,
4. ANGULAR POSITION
5. LOAD CELL
6. OSCILLOGRAPH

PROCEDURE

1. INSTALL ARMATURE LOCK UP PINS.
2. INSTALL ACTUATOR IN SET-UP.
3. APPLY LOAD TO CONTROL SURFACE
4. RECORD DATA

REQUIRED DATA

CONTROL SURFACE POSITION(θ) VS. LOAD (IN. LBS)

ACCEPT/REJECT CRITERIA

TEST
DEMONSTRATION

NOTES

Figure 6d. Stiffness Test



TEST
POWER EFFICIENCY

Prepared by: K. N. DILLACK
Part No. _____
Date 11-13-75

OBJECTIVE

TO DETERMINE ENERGY INPUT, OUTPUT
RELATIONSHIP.

FACILITY

HYDRAULIC
TEST LABORATORY

SCHEMATIC

**EQUIPMENT AND
INSTRUMENTATION**

1. PERF. TEST EQUIP.
2. VOLTAGE ANALOG
3. CURRENT ANALOG
4. LOAD CELL
5. OSCILLOGRAPH

PROCEDURE

1. INSTALL ASSEMBLY IN SET-UP.
2. FULLY DEPLOY CONTROL SURFACE AGAINST
VARIOUS LOAD RATES.
3. RECORD DATA
4. REDUCE DATA (POWER CONSUMPTION)

REQUIRED DATA

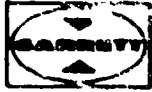
INPUT POWER (VOLTS & AMPS) VS LOAD (IN LBS)

ACCEPT/REJECT CRITERIA

TEST
DEMONSTRATION

NOTES

Figure 59. Power Efficiency Test



TEST
ACCELERATION

Prepared by: K. N. DULLACK

Part No. _____

Date 11-13-75

OBJECTIVE

TO DEMONSTRATE THE NO LOAD
ACCELERATION RATE

FACILITY

HYDRAULIC
TEST LABORATORY

SCHEMATIC

**EQUIPMENT AND
INSTRUMENTATION**

1. PERF. TEST EQUIP.
2. ACCELERATION TRANS.
3. LOAD INERTIA (CALC)
4. OSCILLOGRAPH

PROCEDURE

1. INSTALL ASSEMBLY IN SET-UP,
LOAD CYLINDER DISCONNECTED.
2. APPLY FULL DEPLOYMENT SIGNAL TO CONTROL
3. RECORD DATA
4. REDUCE DATA (DETERMINE ACCELERATION)

REQUIRED DATA

MOTOR POWER (WATTS), ACCELERATION

ACCEPT/REJECT CRITERIA

DETERMINE THE
 T/I RELATIONSHIP

T: MOTOR TORQUE
I: TOTAL INERTIA

NOTES

Figure 70 . Acceleration Test



TEST
POSITION RESOLUTION

Prepared by: K. N. DULLICK
Part No. _____
Date 11-13-75

OBJECTIVE

TO DETERMINE THE HISTORESIS BAND BETWEEN THE INPUT COMMAND AND THE CONTROL SURFACE POSITION

FACILITY

HYDRAULIC TEST LABORATORY

SCHEMATIC

EQUIPMENT AND INSTRUMENTATION

1. PERC. TEST EQUIP.
2. DIGITAL VOLTMETER
3. POSITION INDICATOR

PROCEDURE

1. INSTALL ASSEMBLY IN SET-UP.
2. APPLY VARIOUS INPUT COMMAND VOLTAGES.
3. RECORD DATA
4. PLOT HYSTORESIS CURVE

REQUIRED DATA

COMMAND VOLTAGE , ANGULAR POSITION (DEG)

ACCEPT/REJECT CRITERIA

TEST DEMONSTRATION

NOTES

Figure 71. Position Resolution Test



TEST
VELOCITY

Prepared by: K.N. DULLACK

Part No. _____

Date 11-13-75

OBJECTIVE
TO DETERMINE THE ANGULAR
VELOCITY VS. TORQUE PARAMETERS.

FACILITY
HYDRAULIC
TEST LABORATORY

SCHEMATIC

**EQUIPMENT AND
INSTRUMENTATION**

1. PERF. TEST EQUIP.
2. VELOCITY TRANS.
3. LOAD CELL
4. OSCILLOGRAPH

PROCEDURE

1. INSTALL ASSEMBLY IN TEST SET UP
2. APPLY STEP INPUT COMMANDS FOR VARIOUS LOADS
3. RECORD DATA
4. REDUCE DATA

REQUIRED DATA

VELOCITY, TORQUE

ACCEPT/REJECT CRITERIA

TEST
DEMONSTRATION

NOTES

Figure 72 . Velocity Test

8. REFERENCES

1. Statement of work, Contract No. F33615-75-D-3055
2. AiResearch proposal, Electromechanical Actuation Feasibility Study, Report No. 74-10866.
3. Hydraulic Power Control Actuator. Specification No. 10-30433, the Boeing Company Airplane Division, Wichita Branch, Wichita, Kansas.
4. Technical guidelines provided during program orientation meeting, as reported in AiResearch Report No. 75-55.
5. Laithwaite, E.R., "Linear Electric Machines - A Personal View", Proceedings of IEEE, Volume 63, No. 2, Feb 1975.
6. Electromagnetic Harmonic Drive Low Inertia Servo Actuator, ADS-TDR-63-166, Dec 1963.
7. Brown, J.M., "Rare Earth Magnets - A New Trend in Dc Motors", Control Engineering, Oct 1975.
8. Newton, G.C. and R. W. Ratche, "Can Electric Actuators Meet Missile Requirements", AIEE Paper, 61-711, 1961. AIEE Transactions, Volume 80, Part 2, No. 57, Nov 1961, pp 306-312.
9. Parker, Rollin J. and Robert J. Struders, Permanent Magnets and Their Application, 1962.
10. Inagaki, J., M. Kuniyoshi, and S. Tadakuma, "Commutators Get The Brushoff," IEEE Spectrum, June 1973, pp 52-58.

APPENDIX A

F-100 AIRCRAFT CHARACTERISTICS

This appendix describes the F-100 aircraft characteristics of significance to the control surface actuation system. These data were supplied by North American Rockwell, Los Angeles Aircraft Division, as part of the technical support performed under subcontract to AIRsearch.

ACTUATION SYSTEM DESCRIPTION

The F-100 aileron and horizontal stabilizer aerodynamic control surfaces are normally operated by two independent hydraulic systems, designated the number 1 and number 2 hydraulic power systems. The rudder is actuated by the number 2 hydraulic power system, and/or a utility (third) hydraulic power system. Wing flaps, speed brake, landing gear, wheel brakes, and nose-wheel steering all operate off the utility system. In addition, these aircraft are equipped with a ram-air turbine system (RAT) consisting of an air-driven turbine and a constant-displacement hydraulic pump. The RAT provides an alternative source of power for the flight control system in the event that engine speed drops below 40 percent. A block diagram of the system is shown in Figure A-1.

The electromechanical actuation system approach to providing the required dual-redundant drive system for each major control surface is shown in Figure A-2. This redundancy is provided by the following system elements.

- (a) Two electric alternators on the main propulsion engine, each sized to provide full electrical demand for control surface actuation as well as auxiliary power demands
- (b) A RAT to provide get-home capability for the flight control surfaces and utility equipment actuation in the event of an engine failure

CONTROL SURFACE CHARACTERISTICS

The hinge moments and aerodynamic loads used in the initial design phase of the F-100 D and F aircraft are summarized in the following paragraphs. These data have been extracted from Rockwell Report NA55-402-1, F-100D Hydraulic Flight Control Design Report. The F-100 aileron system shown in Figure A-3 comprises a split (two-segment) aileron on each wing. The two segments are tied together by a connecting rod and are operated as a single unit by a single actuator in each wing.

The design requirement for the F-100 was that the aircraft have a roll rate of 160 deg/sec at Mach 1 at 10,000 ft. This occurs with an aileron deflection angle of 11.2 deg. To meet this requirement, a hinge moment of 132,000 in.-lb per aileron is required. To establish the hinge moment for the inboard and outboard segments, the total load is considered proportional to the area moment for each aileron segment as compared to the area

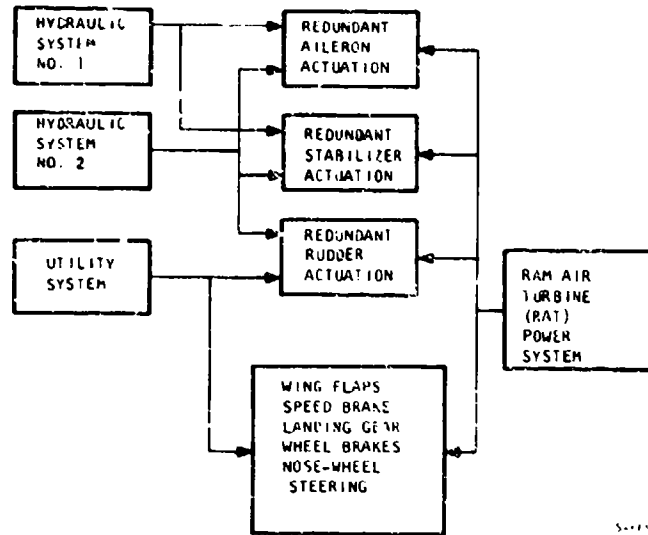


Figure A-1. F-10G Hydraulic Power Distribution System

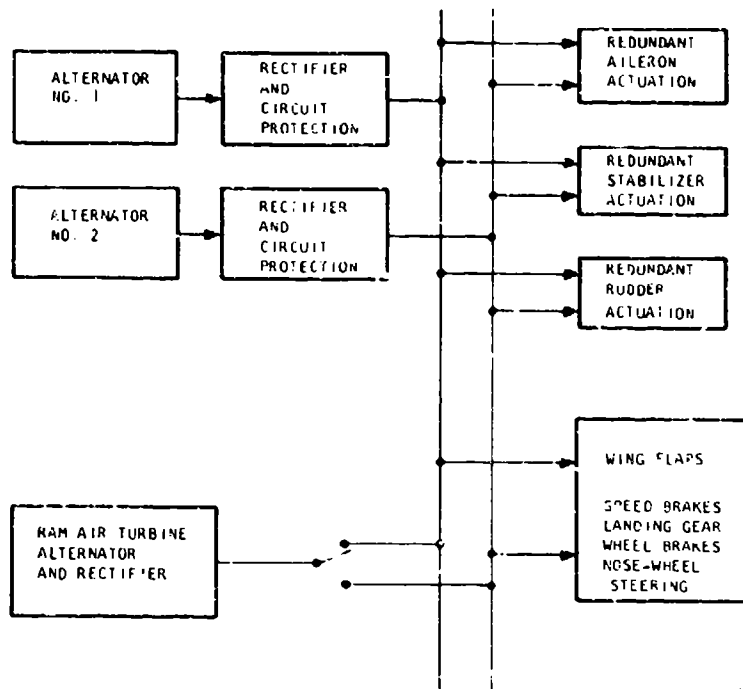


Figure A-2. Candidate Electrical Power Distribution System

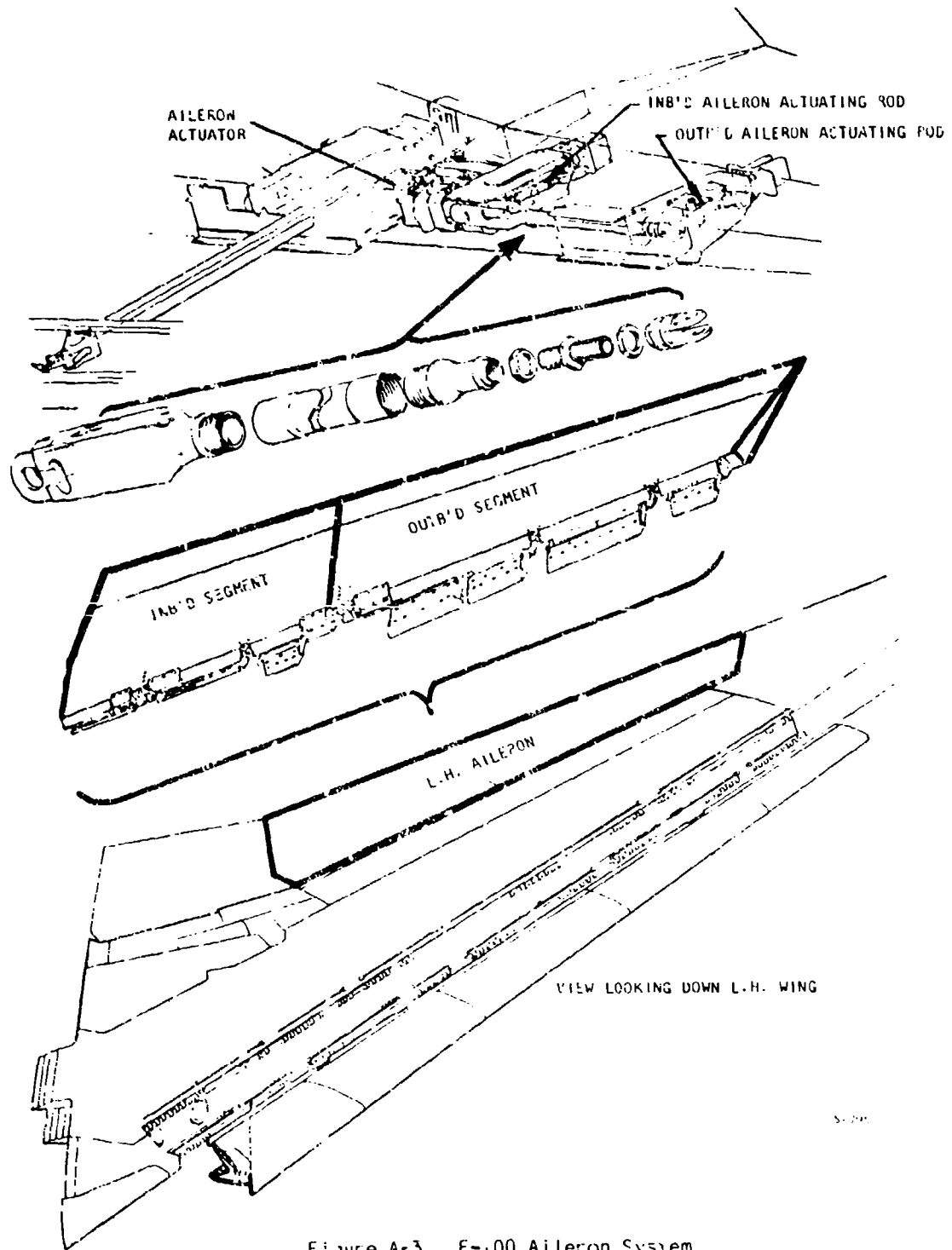


Figure A-3. F-100 Aileron System

moment for the complete aileron. Thus, at the design limit given above, the hinge moment for the inboard aileron is 80,600 in.-lb and the outboard is 51,400 in.-lb. Figures A-4 and A-5 are plots of hinge moment versus aileron deflection rates and aileron deflection for a complete aileron. To obtain a value for the inboard or outboard aileron segment, the value obtained from Figures A-4 and A-5 must be altered by ratios of 61 percent for the inboard segment and 39 percent for the outboard segment.

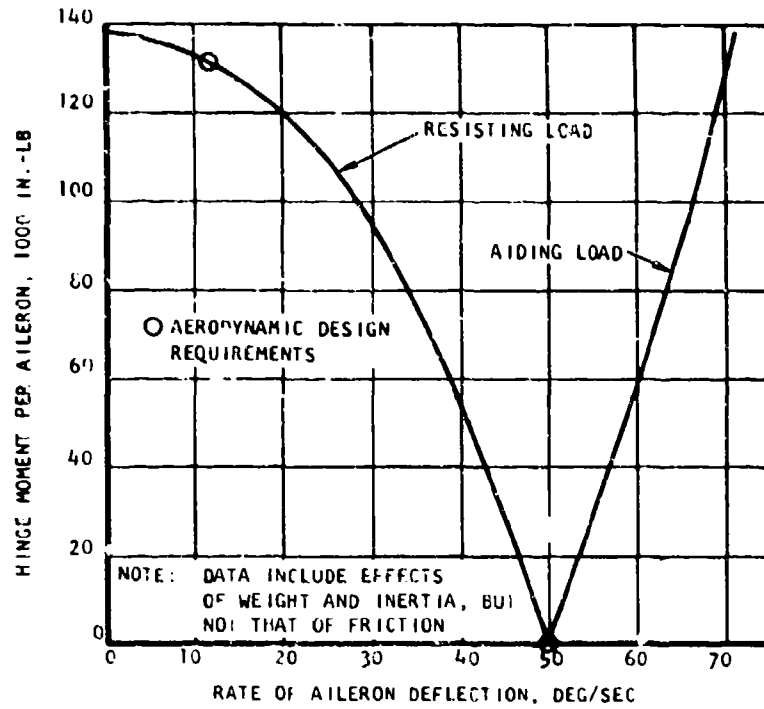
To prevent excessive structural loads on the aileron system, hinge moments were limited to a maximum of 91,500 in.-lb on the inboard aileron segment and 58,500 in.-lb on the outboard segment. This is accomplished by bypassing hydraulic pressure through pressure relief valving in the existing hydraulic system. The total aileron deflection is ± 15 deg.

The rudder was designed to produce 1 deg of yaw at all altitudes and speeds up to $0.95 V_D$; to maintain a maximum of 3 deg of yaw in 1-g maximum rolls at all speeds up to $0.95 V_D$; and to obtain full rudder deflection at $1.75 V_D$ with zero yaw. To support these design requirements, a maximum hinge moment of 4300 in.-lb will be developed. Figures A-6 and A-7 are plots of rudder hinge moment versus rudder deflection and rudder deflection rates. Table A-1 summarizes the rates and hinge moment data for the control surfaces as a function of aircraft operating mode.

TABLE A-1

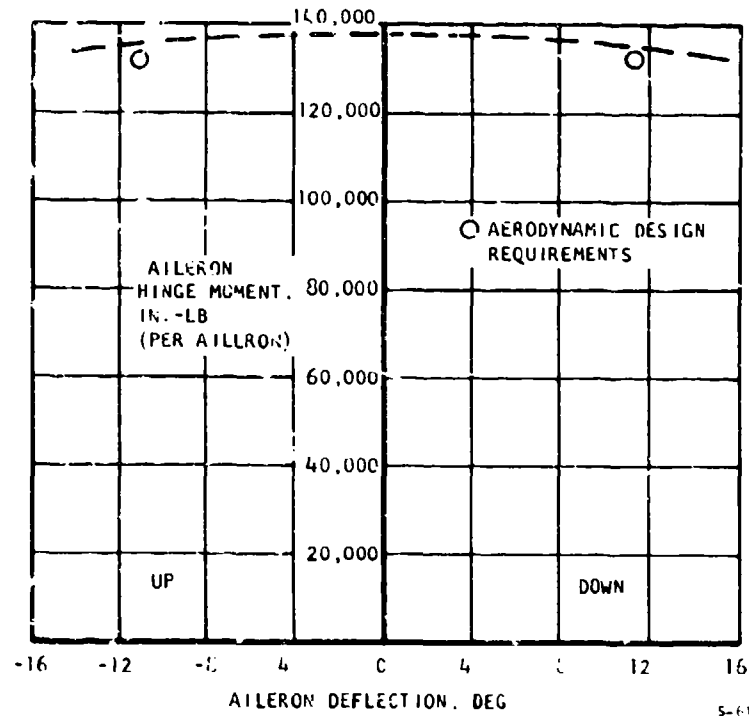
SUMMARY OF SURFACE DEFLECTION RATES AND HINGE MOMENTS
AS A FUNCTION OF FLIGHT CONDITIONS

Operating Mode	Surface	Rate, deg/sec	Hinge Moment, in.-lb
Maximum	Aileron	50	0
	Stabilizer	20	0
	Rudder	50	0
Combat	Aileron	10	132,000
	Stabilizer	4	500,000
	Rudder	1	4300
Cruise	Aileron	0.2	60,000
	Stabilizer	0.25	100,000
	Rudder	0	0
Landing	Aileron	3.33	10,000
	Stabilizer	5.0	20,000
	Rudder	1.0	800



S-615

Figure A-4. Aileron Operating Requirements, Hinge Moment vs. Deflection Rate



S-616

Figure A-5. Aileron Operating Requirements, Hinge Moment vs. Aileron Deflection

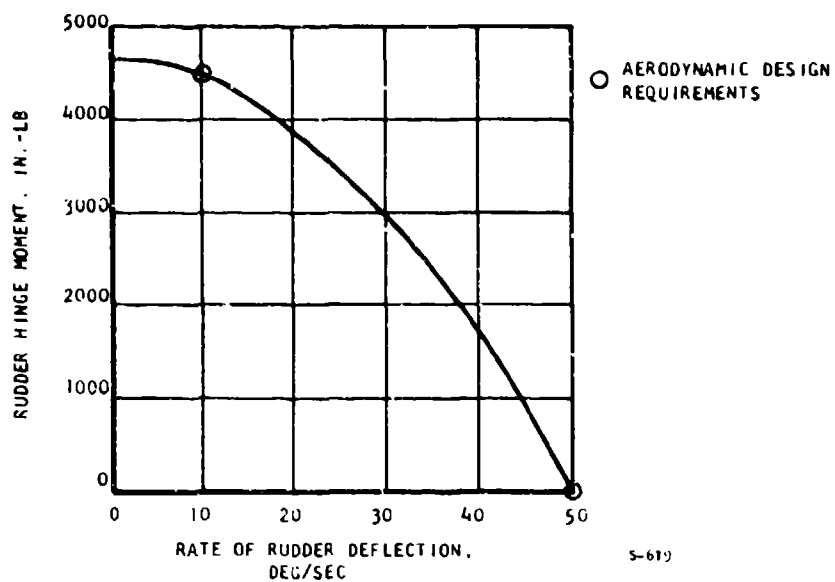


Figure A-6. Rudder Operating Requirements

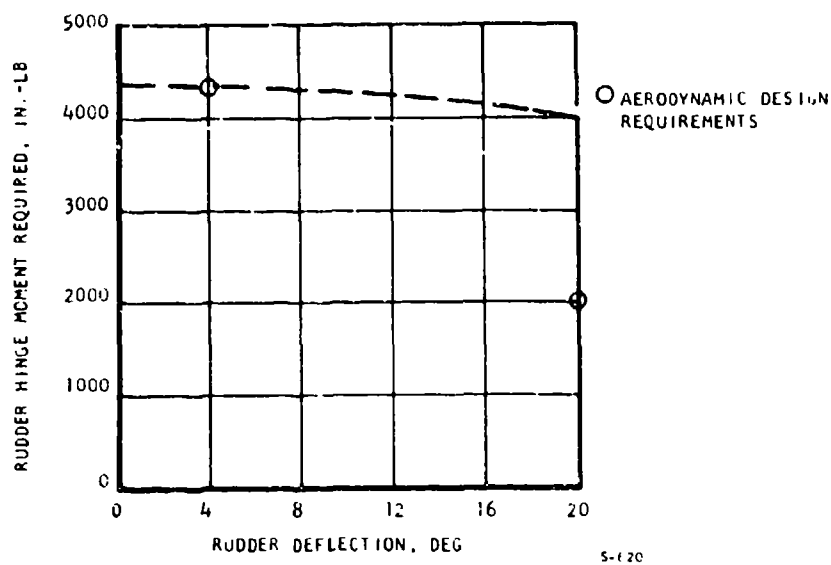


Figure A-7. Rudder Operating Requirements

CONTROL SURFACE DUTY CYCLE

Figures A-8 through A-11 present the duty cycle for the rudder and aileron control surfaces of the F-100. These data include (1) a presentation of total deflection as function of time for various flight conditions and (2) an example of the duty cycle experienced during an emergency descent of the aircraft.

CONTROL INTERFACE

The electromechanical actuator system input signals can be categorized into the following areas: (1) failure sensing, (2) system feedback control, (3) basic flight controls, and (4) aircraft flight envelope control. For failure sensing, the system shall be capable of monitoring the essential safe operating parameter, provide automatic changeover from the primary mode of operation to the secondary, and alert the pilot of any failures. The essential safe operating conditions are defined by the following

- (a) Maximum operating temperatures (motor, bearings, etc.)
- (b) Input/output signal anomalies as a function of angular displacement and time
- (c) Control system electronics built-in-test (BIT)

For the system feedback control category, the system must continually monitor the pilot's input command and the control surface position signal and generate the command signal to the control surface to maintain it within the limits established in (b) above. Basic flight control signals comprise the following:

- (a) Trim--The system presently installed in the F-100 is a mechanical system. The electrical signal from the trim switch repositions the fixed end of the feel bungee through a jack screw; thus, the control stick zero-force position and the surface trim position are changed. The electrical signal generated by the trim switch is fed directly into the normal input signal.
- (b) Damper--The system presently in the F-100 aircraft basically senses angular accelerations and stick position, and generates an opposing signal into the appropriate axis. The signal operates a hydraulic valve to admit fluid into the surface damper actuator.
- (c) Mach Number Sensitivity (Gradient Changer)--The F-100 aircraft is equipped with a system to automatically retrim the horizontal stabilizer as the mach number increases above 0.85. The signal generated by the mach number transducer is fed into a jack-screw-operated variable link in the stabilizer trim system.
- (d) Pitch Correction--The F-100 aircraft is equipped with a system to automatically retrim the horizontal stabilizer as the flaps are lowered.

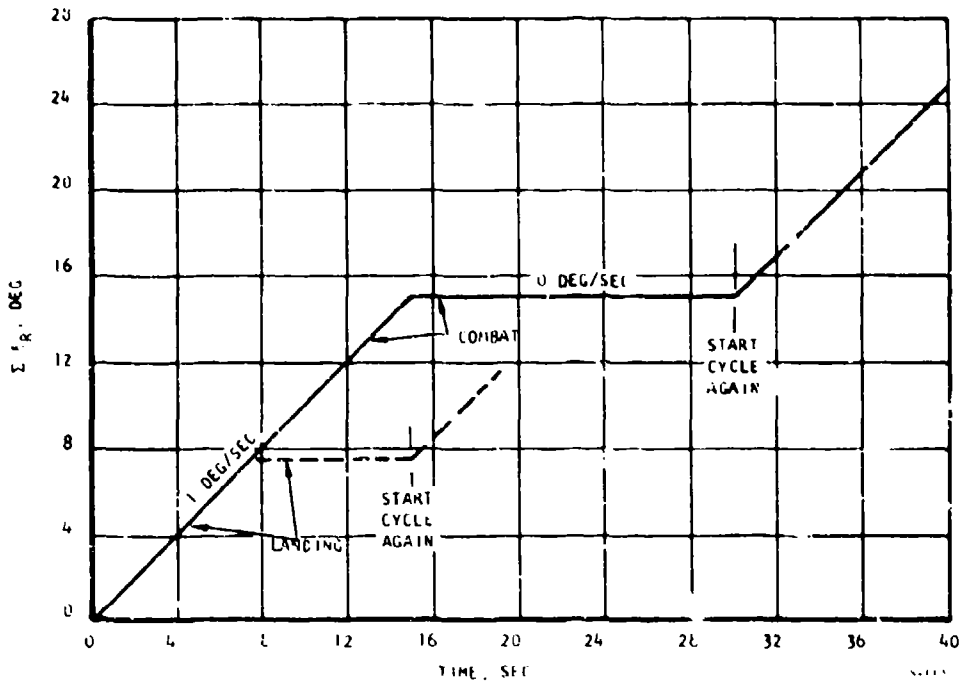


Figure A-8. Rudder Duty Cycle

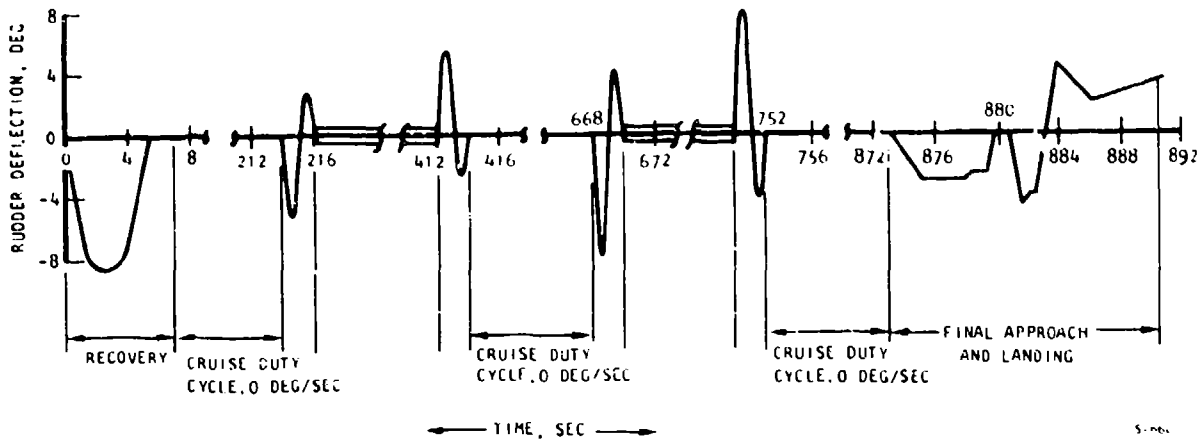


Figure A-9. Rudder Deflection During Emergency Descent

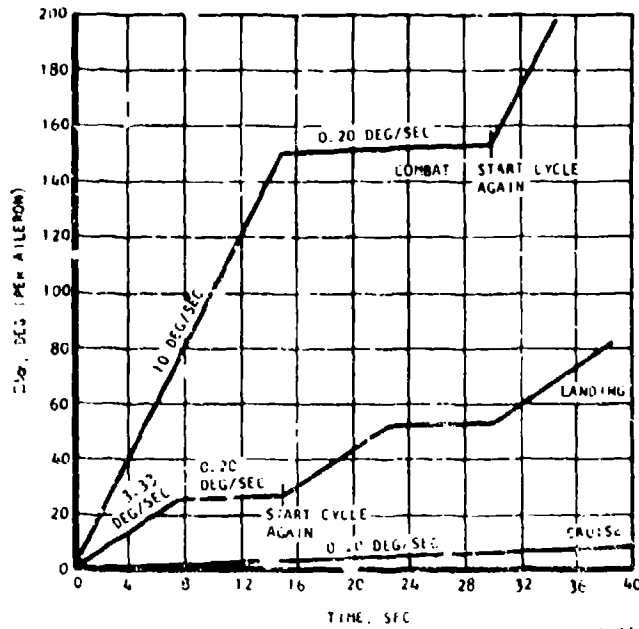


Figure A-10. Aileron Duty Cycle

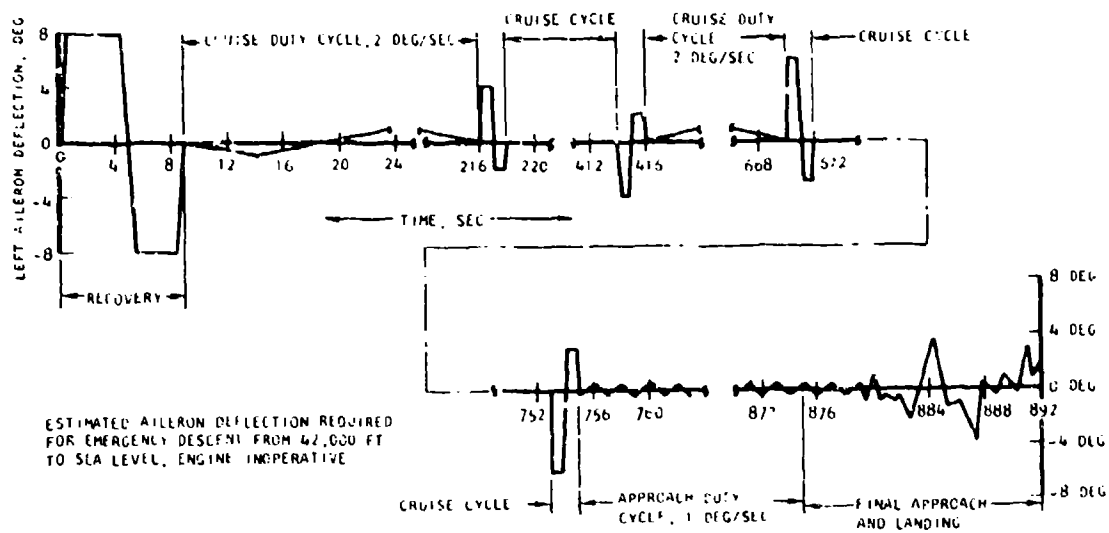


Figure A-11. Estimated Aileron Deflection Required for Emergency Descent from 42,000 Ft to Sea Level, Engine Inoperative

For the aircraft flight envelope control category, although the F-100 is not equipped with autopilot or autoland systems, their inputs are also mechanically summed into the flight controls. When fly-by-wire is incorporated into an aircraft, all basic flight control input, together with autopilot and autoland, can be summed electrically. By an electrical summation of systems, the total aircraft weight is decreased while the versatility is increased. The next step in the natural progression of events is to develop an onboard flight control computer. The F-16 is the first production aircraft to incorporate a fly-by-wire system. The F-16 also incorporates an onboard computer. The F-16 deviates from standard aerodynamic practices in that it is designed to be an unstable aircraft, thus increasing its maneuverability. The flight computer provides the electrical summing of all of the required parameters, and also monitors the critical flight and structural parameters and prevents the pilot from exceeding the aircraft flight envelope. It senses angle-of-attack, normal acceleration, etc., and biases the pilot's input signal such that the command signal to the control surface will not allow the aircraft to enter an over-g or stall condition.

In addition, two areas that are not actual inputs to the flight control system but are design considerations for the actuation subsystem are hinge moment limiting and fail-safe provisions. For hinge moment limiting, provisions should be made in the actuating system to prevent the aileron hinge moment from exceeding certain limits. This requirement also must be met with the electromechanical system. Fail-safe provisions are required for the following:

- (a) In the event of total power failure, the control surface must return to a trail, or neutral, position.
- (b) The electromechanical system shall provide adequate control surface damping during operating or failure modes.

ENVIRONMENT

The thermal environment definition provides a major parameter for electric servomotors and electronic controllers. Temperatures that can exist within the aileron and rudder actuator compartments are given below. These temperatures result from aerodynamic heating, and in the case of the rudder, convection heating from the aircraft engine is included. These values do not account for heat that may be generated from equipment operating in these compartments. At present, these compartments do not have any heat generating units.

Aileron

Since all heat in the aileron actuator compartments is generated by aerodynamic heating, temperatures at typical flight conditions are as follows:

<u>Condition</u>	<u>Temperature, °F</u>
Cruise	50
Combat	110

Sea level, MIL power dash	175
Sea level, afterburner dash	152
Parked in sun on Air Force standard hot day	160

Rudder

Temperatures zones in the rudder area will vary considerably, depending upon their proximity to the engine compartment. The maximum expected temperatures are given below for the three representative zones shown in Figure A-12.

Zone 1--The maximum structure temperature along the rudder hinge-line is approximately 192°F.

Zone 2--The ambient air in this zone (the vicinity of the existing rudder actuator) will have a maximum temperature of 230°F.

Zone 3--The maximum temperature in zone 3 is 300°F. This is the location of the existing hydraulic actuator.

CONTROL SURFACE MASS PROPERTIES

The mass properties of the aileron and rudder on the F-100 aircraft are summarized below. This summary includes the weight, center of gravity, and moment of inertia for the inboard and outboard aileron segments and the rudder. The values given in Table A-2 are for the movable surfaces only, and do not include the control or actuating systems. The coordinate system for the aileron and rudder center of gravities is given in Figures A-13 and A-14.

TABLE A-2

CONTROL SURFACE MASS PROPERTIES

Surface	Weight, lb	Moment of Inertia, lb-in. ²
Inboard aileron	36.01	$\Sigma WX^2 = 3255$ $\Sigma WXY = 16,996$
Outboard aileron	73.04	$\Sigma WX^2 = 3135$ $WXY = 1328$
Rudder	48.12	$\Sigma WX^2 = 1175$

POWER DISTRIBUTION

These data apply to the existing F-100 electrical power system, and are included only to show that the power system could handle a single electro-mechanical actuator for one outboard aileron for flight test evaluation during

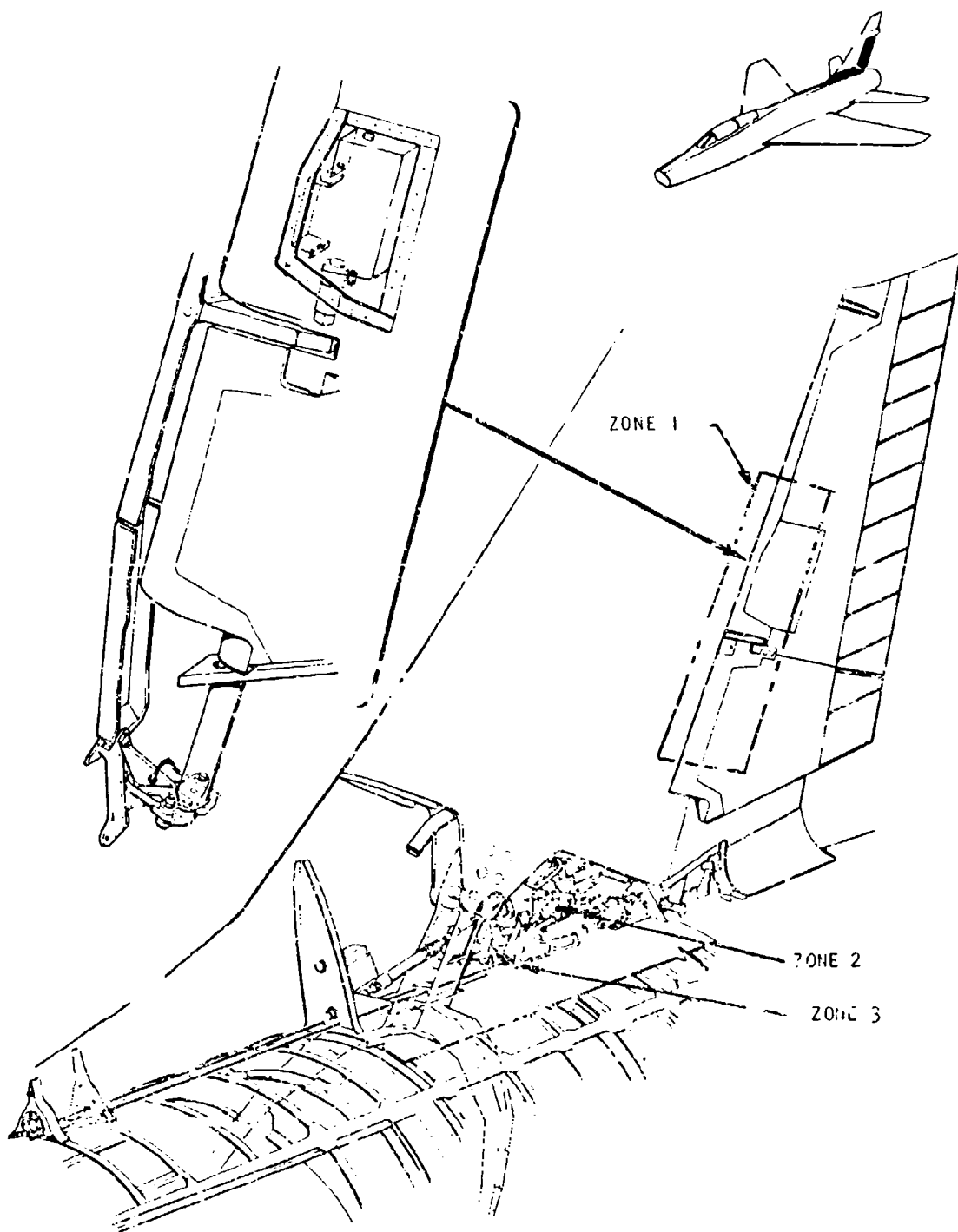


Figure A-12. Rudder Temperature Zones

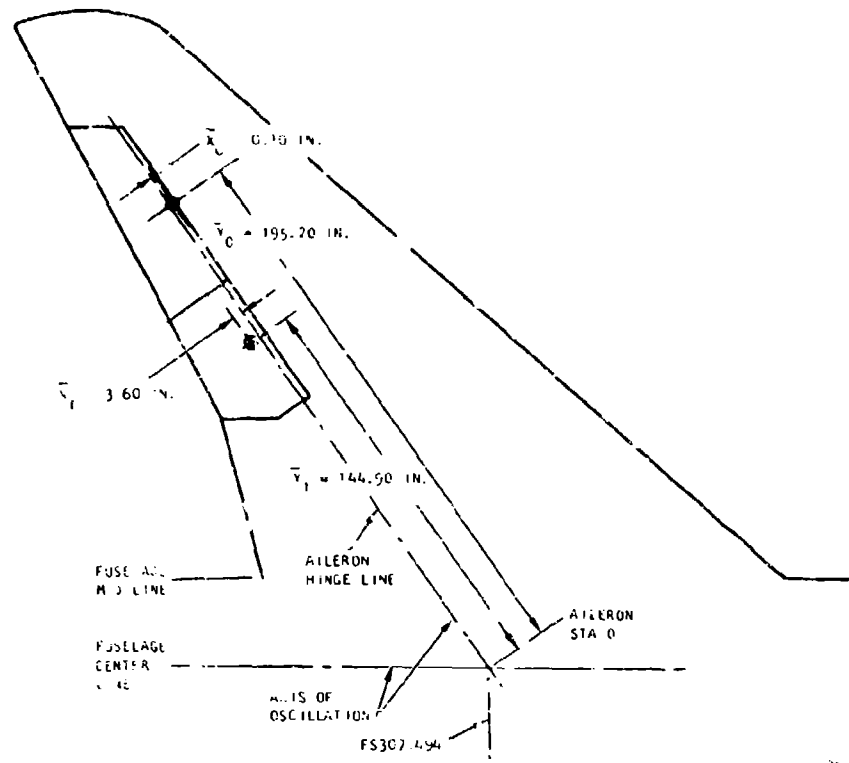


Figure A-13. Aileron Coordinates; View Looking Down LH Wing

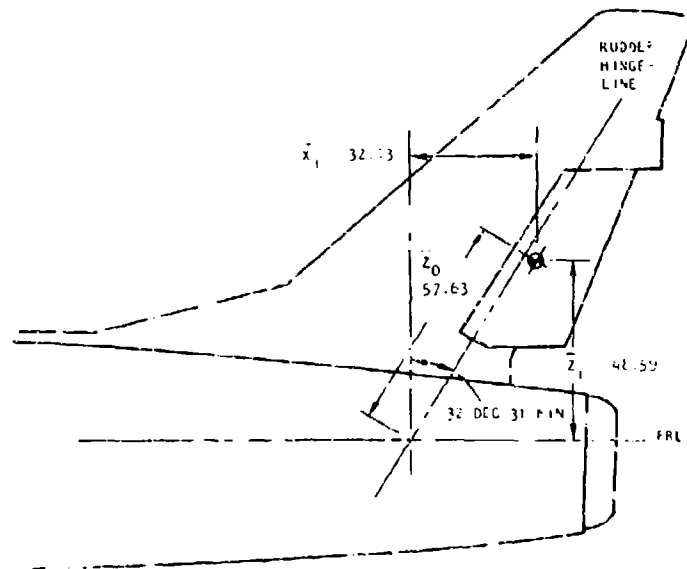


Figure A-14. Rudder Coordinate System

a subsequent program phase. It is clear that an aircraft designed for electromechanical actuation systems would also include a completely different power source sized for the intended use and duty cycle.

Primary electrical power for the F-100 is provided by a 200-amp, 28-vdc generator and a 20-kva, 115/200-v, 400 Hz alternator. In lieu of MIL-STD-704, the generating systems in the F-100 were designed to meet MIL-E-7894, which allows a frequency variation of 380 to 420 Hz and a nominal steady-state voltage in the range of 102 to 124, with an 18-v variation. However, the systems in the F-100F will operate at 396 to 404 hz and 114 to 116 v steady-state with variations and transients as allowed by MIL-E-7894. In the last several years, systems have been added to the F-100 that were designed to MIL-STD-704. As each installation was made, tests have been conducted to ensure that the quality of the power provided at the system input was within the envelope of MIL-STD-704. In all cases, the power was acceptable and no additional filtering or conditioning required. The electrical load analysis for the F-100 indicates that the 200 amp dc generator is running at a load of 8.8 to 12.5 kva for various flight conditions. These loads are representative of an operational aircraft and can be decreased by deactivating certain systems that will not be required for this test program.

PERFORMANCE CRITERIA AND TRADEOFFS

No-Load Response

The position closed-loop response of the F-100 surface servoactuator is equivalent to an effective first-order time constant of 0.05 sec (loop gain of 20 rad/sec) or better. (Corresponds to 3.2 Hz at 3 db point.) For input frequency and amplitude combinations resulting in an actuator rate of 1/100 or the design no-load maximum rate, the effective time constant is no greater than 0.10 sec (loop gain of 10 rad/sec). These apply to the linear operating regimes (i.e., non-rate saturation). The servo/actuator output is controllable (repeatable) within 0.2 percent of full stroke. The output resolution will be no greater than 0.05 percent of full stroke.

Response Under Load

The F-100 aileron actuator time constant for the design load condition (reference Figure A-4) is no greater than 0.21 sec. For rate demands equivalent to 1/100 of the maximum no-load rate, the time constant is no greater than 0.40 sec. These rates apply to non-rate saturated commands.

Aircraft Performance

A preliminary analysis of data developed from the performance curves and equations for the Pratt & Whitney J-57 engine (installed in the F-100 aircraft) indicates that a sizable savings in horsepower must be obtained by the electromechanical system before a noticeable change in aircraft performance or range will be realized. For each 10-hp change at the engine accessory pad, the engine thrust will change 0.00176 percent and the specific

fuel consumption will change 0.0066 percent. The engine thrust is directly related to aircraft performance such as velocity and rate of climb, while the aircraft range and loiter time are a function of the engine specific fuel consumption.

HYDRAULIC CONTROL SYSTEM WEIGHT

A preliminary weight survey was conducted for the F-100 aircraft. Table A-3 shows the weight of the complete hydraulic primary flight control system with an electromechanical system for the roll, pitch and yaw axis. The flaps, wheel brakes, nose gear steering, and speed brake system are not included.

TABLE A-3
F-100F REVISED FLIGHT CONTROL SYSTEM DELETIONS

Controls	Weight, lb
Automatic flight controls	(43)
Servos	34
Plumbing and fluid	9
Aileron controls	(243)
Mechanical	28
Hydraulic	206
Artificial feel	9
Horizontal tail controller	(224)
Mechanical	49
Electrical	21
Hydraulic	90
Artificial feel	64
Rudder controls	(80)
Mechanical	27
Hydraulic	31
Artificial feel	14
Vibration damper	8
Power control system	(242)
Pumps	31
Accumulators	41
Reservoirs	24
Valves, filters, etc.	23
Plumbing	68
Fluid	24
Emergency system	31
Structure	(139)
Aileron hinges	88
Rudder hinges	4
Rat door and mech.	47
Total Deletions	971

APPENDIX B

B-52 RUDDER AND ELEVATOR CONTROL SYSTEM

The rudder and elevator actuation system comprises three major assemblies: (1) a rudder actuator, (2) an elevator actuator, and (3) a hydraulic power supply. The characteristics of these assemblies are described below.

ACTUATORS

The actuator consists of a dual tandem hydraulic cylinder, including integral input servomechanisms, position feedback, and summing linkages. The actuators are capable of operation based upon either mechanical command inputs or electrical command inputs. The performance characteristics of the two actuators are presented in Table B-1.

TABLE B-1
ACTUATOR PERFORMANCE CHARACTERISTICS

	Actuator	
	Rudder	Elevator
Stroke (including cross arm)	<u>+19</u> deg	<u>+19</u> deg.
Torque (4.5 in. arm) (4.0 in. arm)	12,000 in.-lb	36,000 in.-lb
Rate	80 deg/sec	80 deg/sec
Weight	52 lb	57 lb
Load Inertia	17,008 lb-in.	17,894 lb-in.
Stiffness	40,000 lb-in.	50,000 lb/in.
Bandwidth	4 Hz	4 Hz
MTBF, goal	2500 hr	2500 hr
input command (mechanical)	2.7 in. input gives 2.6 in. output	3 in. input gives 2.93 in. output

An approximate duty cycle is obtained from the cycling endurance tests for the actuators. These are summarized in Table B-2.

TABLE B-2
ACTUATOR ENDURANCE REQUIREMENTS

<u>Elevator Actuator (at 1 Hz)</u>		
<u>Input command,</u> <u>in.</u>	<u>Spring rate,</u> <u>lb/in.</u>	<u>No. of</u> <u>Cycles</u>
<u>+ 0.157</u>	9000	400,000
<u>+ 0.392</u>	5000	65,000
<u>+ 0.626</u>	5800	24,000
<u>+ 1.165</u>	5800	5000
1.465	5800	1000
<u>Rudder Actuator (at 1 Hz)</u>		
<u>Input Command,</u> <u>in.</u>	<u>Spring Rate,</u> <u>lb/in.</u>	<u>No. of</u> <u>Cycles</u>
<u>+ 0.138</u>	3700	400,000
<u>+ 0.346</u>	2400	65,000
<u>+ 0.554</u>	2400	29,000
<u>+ 1.04</u>	2400	5000
<u>+ 1.3</u>	2400	1000

HYDRAULIC POWER SUPPLY

The hydraulic power supply (HPS) from hydraulic power to the rudder and elevator actuators. The HPS provides a total of 4-gpm flow and a cutoff pressure of 3000 psi. The hydraulic pump is driven by a 118/200-v, 3-phase 400-Hz direct-coupled motor. The unit also includes a backstop reservoir to provide peak power demand to the actuators. The component characteristics are presented in Table B-3.

TABLE B-3
HPS COMPONENT CHARACTERISTICS

Component	Characteristics	Value
Motor pump	Weight	35 lb
	Efficiency	60 percent minimum
	Duty cycle	4 gpm for 2 min, 2 gpm rms
	Maximum current, operating	30 amp/phase
Reservoir	Weight	23 lb
	Capacity	490 cu in.

APPENDIX C

F-15 RUDDER CONTROL SURFACE ACTUATOR PERFORMANCE

The F-15 rudder is controlled by a rotary hydraulic actuator. The actuator is located on the hinge-line of the control surface. The major characteristics of the actuator are presented below.

Output torque	15,500 \pm 250 in.-lb
Maximum torque	15,500 in.-lb (unit will smoothly back-drive to neutral at a minimum rate of 15 deg/sec)
Rate	137 \pm 14 deg/sec, no-load
Bandwidth	3 Hz minimum
Weight	23.4 lb (dry)
Dimensions	6.4 by 3.5 by 16.7 in.

APPENDIX D

F-3 RUDDER CONTROL SURFACE ACTUATOR PERFORMANCE

The F-8 rudder control subsystem is located in the aft section of the vertical tail. The hydraulic cylinder has two tandem pistons on a single piston rod. Each piston is powered from a separate hydraulic power supply for redundancy. The valves are mounted in a separate assembly and connected by a linkage arrangement that provides synchronization. Feedback is accomplished using a scissor type mixing linkage. The major performance characteristics are presented below.

Stroke	<u>+17</u> deg
Rate	80 deg/sec
Hinge moment	36,000 in.-lb
Stiffness	0.66×10^6 in.-lb/rad

APPENDIX E
TOROIDAL DRIVE ANALYSIS

INTRODUCTION

The feasibility of using a mechanical servo (variable roller drive) in a electromechanical actuator system has been analysed. The complete details of the analysis are presented in AIRsearch Report No. 76-12633. This appendix summarizes the analyses. The servo system investigated (see Figure E-1) converts high-speed, low-torque input to a low-speed, high-torque output through control and output rollers of a toroidal servo. Variable gear ratios are achieved by varying the angle (ψ_c) of the control roller from -30 to $+30$ deg. Other geometric parameters affecting servo performance such as radius of the rollers, distance of the rollers from the rotational axis and tilt of output roller were fixed for a configuration, but were varied during the analysis, so that key parameters were included without complicating in-depth analysis of problem areas.

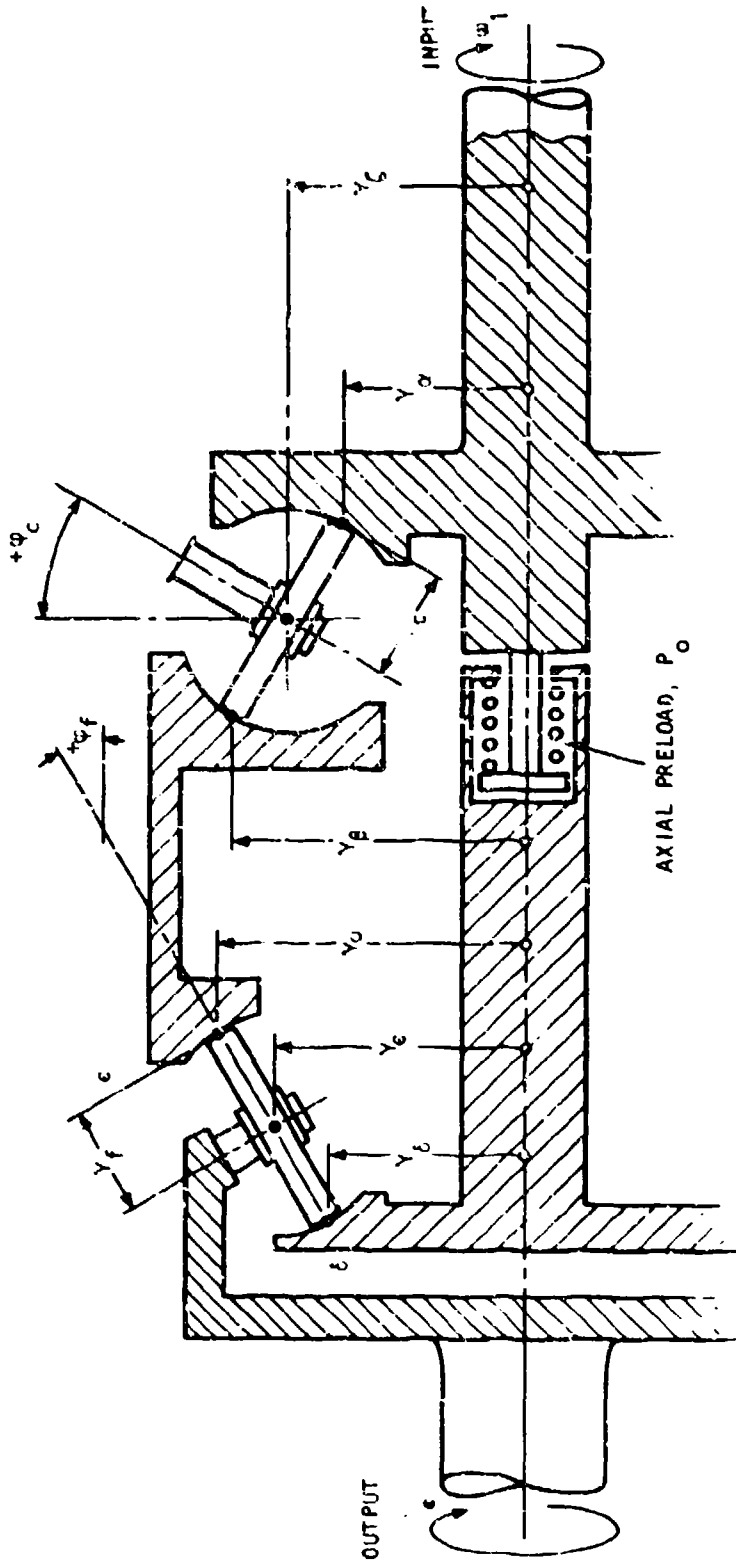
The investigation covered the following areas, which are summarized in this appendix.

- Kinematics
 - Gear ratio
 - Symmetry
 - Linearity
- Radii of curvature at roller contacts
- Hertz stress at roller contacts
- Performance
 - Force and torque balance
 - Preload and frictional force
 - Life
 - Frequency response
- Synthesis

For illustration, the analysis was centered on an example with the following requirements:

Envelope, 4.0 in. dia.

Output torque, $T_\phi = 37,500$ lb-in. at stall

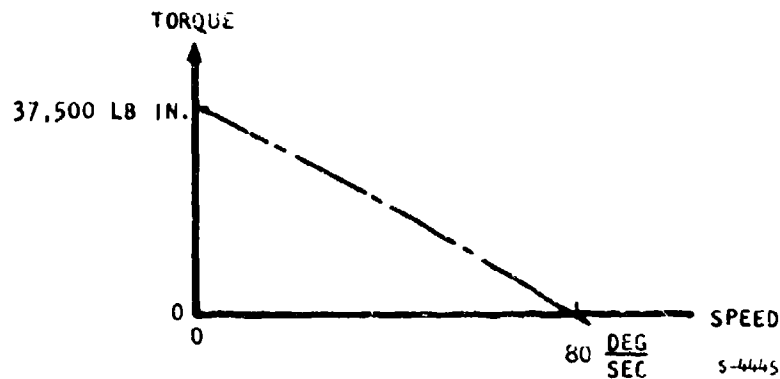


S-4448

Figure E-1. Generalized VRD Arrangement

Output speed, $N_c = 80$ deg/sec at no load

Torque characteristics are given below:



Life, 8000 hr

Frequency response

$f = 8$ Hz at no load

KINEMATICS

The basic parameters are the roller radius, the distance the rollers are located from the rotational axis, and the tilting angle of the rollers. For convenience, these can be reduced to the roller parameter X .

$$X = \frac{\text{Distance of roller center from actuator centerline}}{\text{Roller radius}}$$

and the roller tilting angle φ .

These two parameters are applicable to the fixed roller and the variable-angle control rollers.

If the gear ratio is defined as j ,

$$j = \frac{\text{output speed}}{\text{Input speed}}$$

then (See Figure E-1)

$$j = 1/2 \left[1 + \frac{\sin \phi_f}{\frac{Y_e}{Y_f}} \right] \left[\frac{\frac{Y_e}{Y_f} - \sin \phi_f}{\frac{Y_e}{Y_f} + \sin \phi_f} - \frac{\frac{Y_e}{Y_c} - \sin \phi_c}{\frac{Y_e}{Y_c} + \sin \phi_c} \right]$$

Introducing

$$A = 1/2 \left[1 + \frac{\sin \phi_f}{\frac{Y_e}{Y_f}} \right] \quad 1/2 \left[1 + \frac{\sin \phi_f}{\frac{Y_e}{Y_f}} \right]$$

$$B_f = \frac{\left(\frac{Y_e}{Y_f} \right) - \sin \phi_f}{\left(\frac{Y_e}{Y_f} \right) + \sin \phi_f} = \frac{x_f - \sin \phi_f}{x_f + \sin \phi_f}$$

$$B_c = \frac{\left(\frac{Y_e}{Y_c} \right) - \sin \phi_c}{\left(\frac{Y_e}{Y_c} \right) + \sin \phi_c} = \frac{x_c - \sin \phi_c}{x_c + \sin \phi_c}$$

The functions B_f and B_c are structurally identical. The gear ratio j is then:

$$j = A (B_f - B_c)$$

Variations of function A with changes in control roller tilting angle are shown in Figure E-2. Variations of B_c (B_f is fixed for this analysis) are shown in Figures E-3 through E-5.

As a check of the equations, values were assigned to key parameters in the system shown in Figure E-5.

From Figure E-6,

$$Y_e = 2.5$$

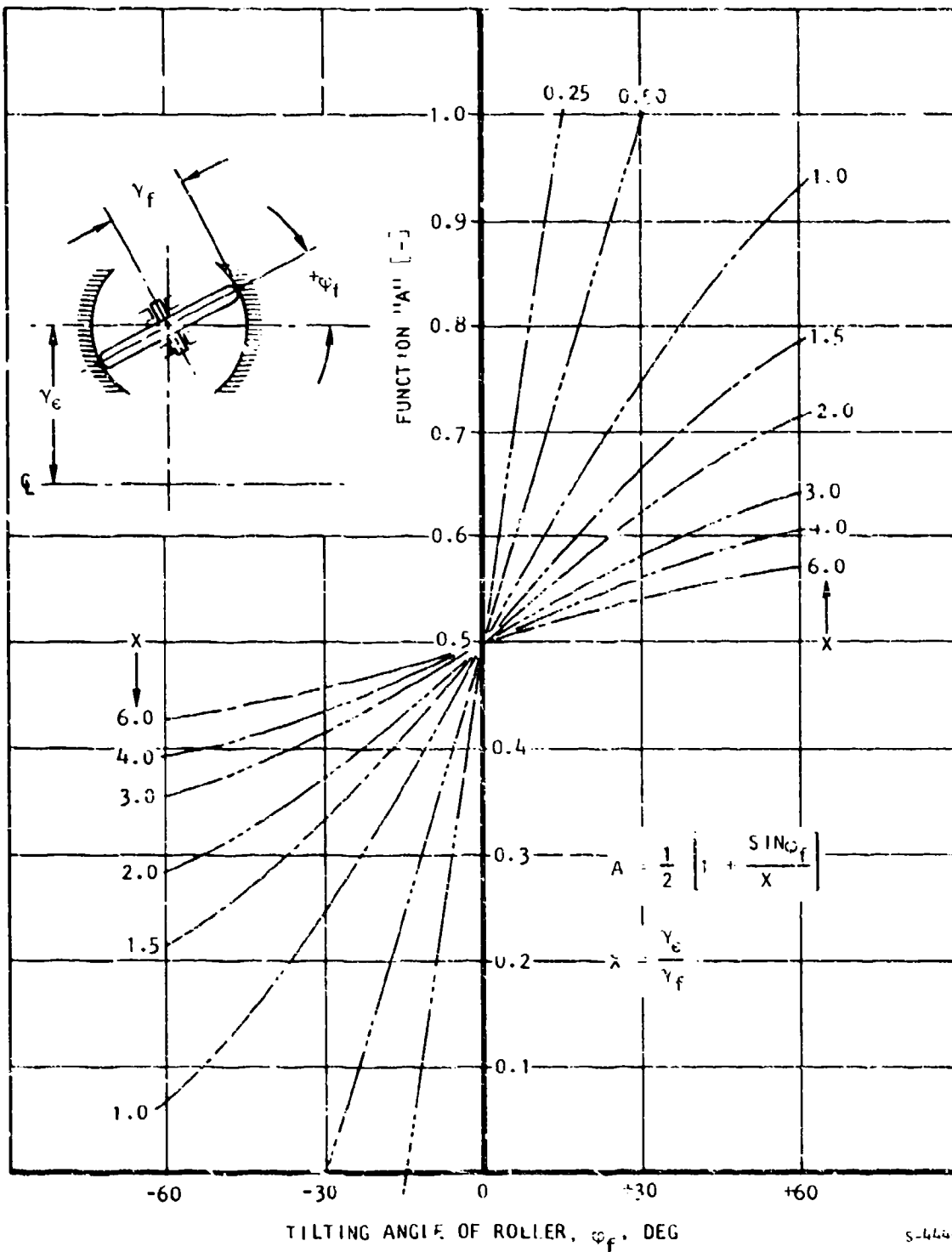
$$Y_f = 1.2$$

$$x_c = \frac{Y_e}{Y_f} = \frac{2.5}{1.2} = 2.0833$$

$$\phi_f = 30 \text{ deg}$$

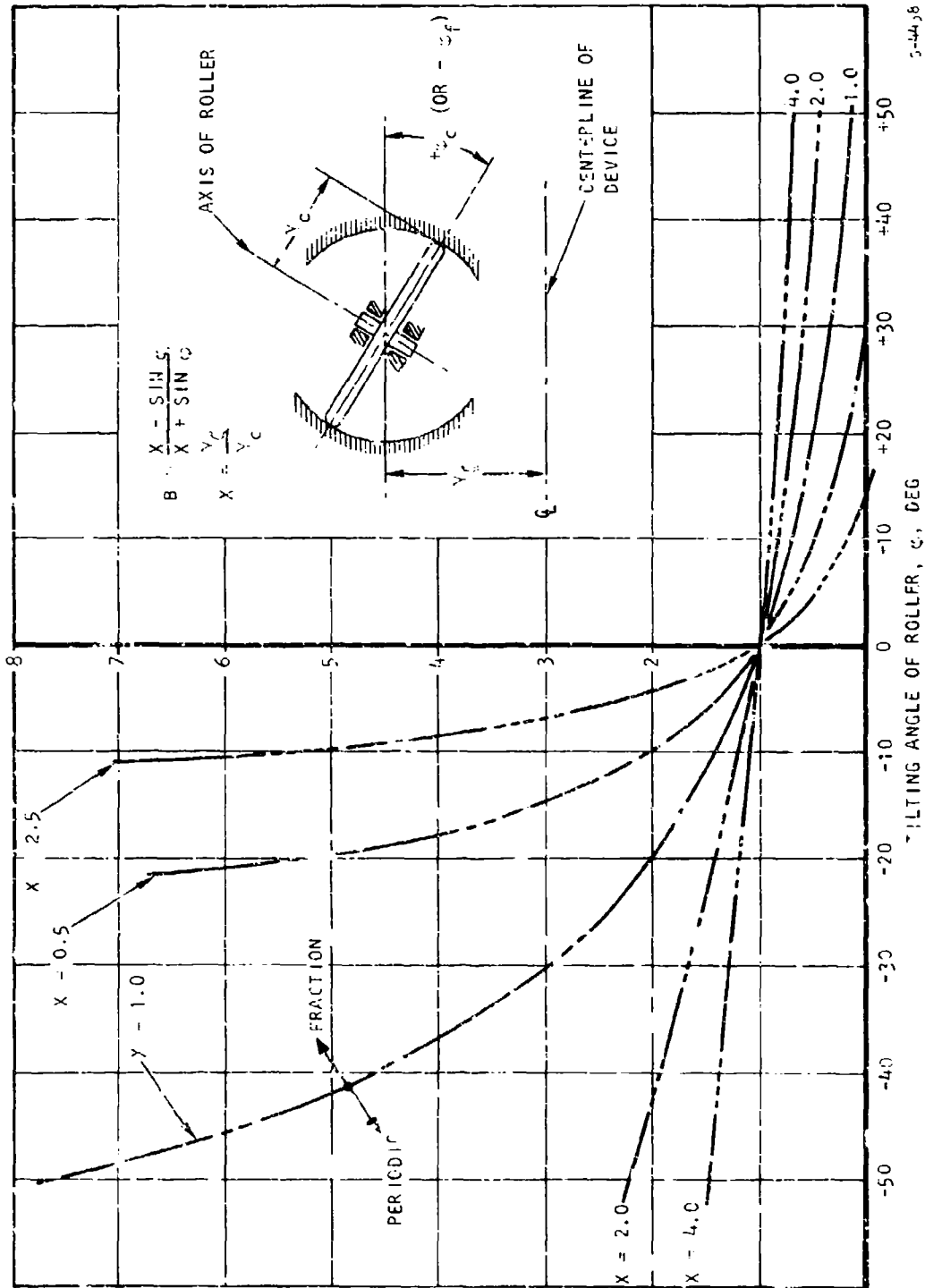
$$\sin \phi_f = \sin 30 \text{ deg} = 0.5$$

$$A = 1/2 \left[1 + \frac{\sin 30}{\frac{2.5}{1.2}} \right] = 1/2 \left(1 + \frac{0.5}{2.0833} \right) = \frac{1.2400}{2} = \frac{0.6200}{(1)}$$



5-4440

Figure L-2. Variations of function A with Roller Tilt



5-4438

Figure E-3. Variations of Function B with Roller Tilt

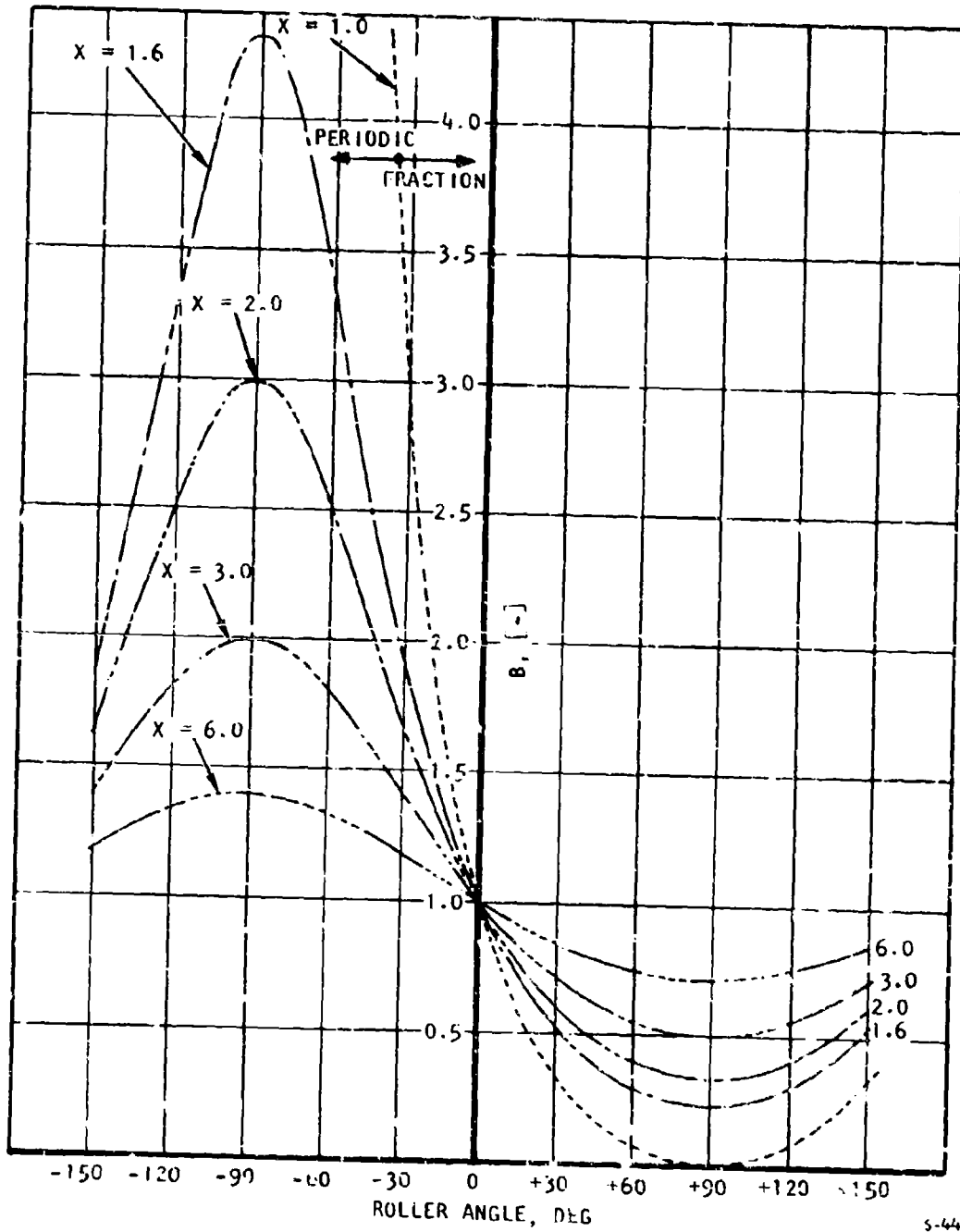


Figure E-4. Variations of Function B with Roller Tilt

S-4439

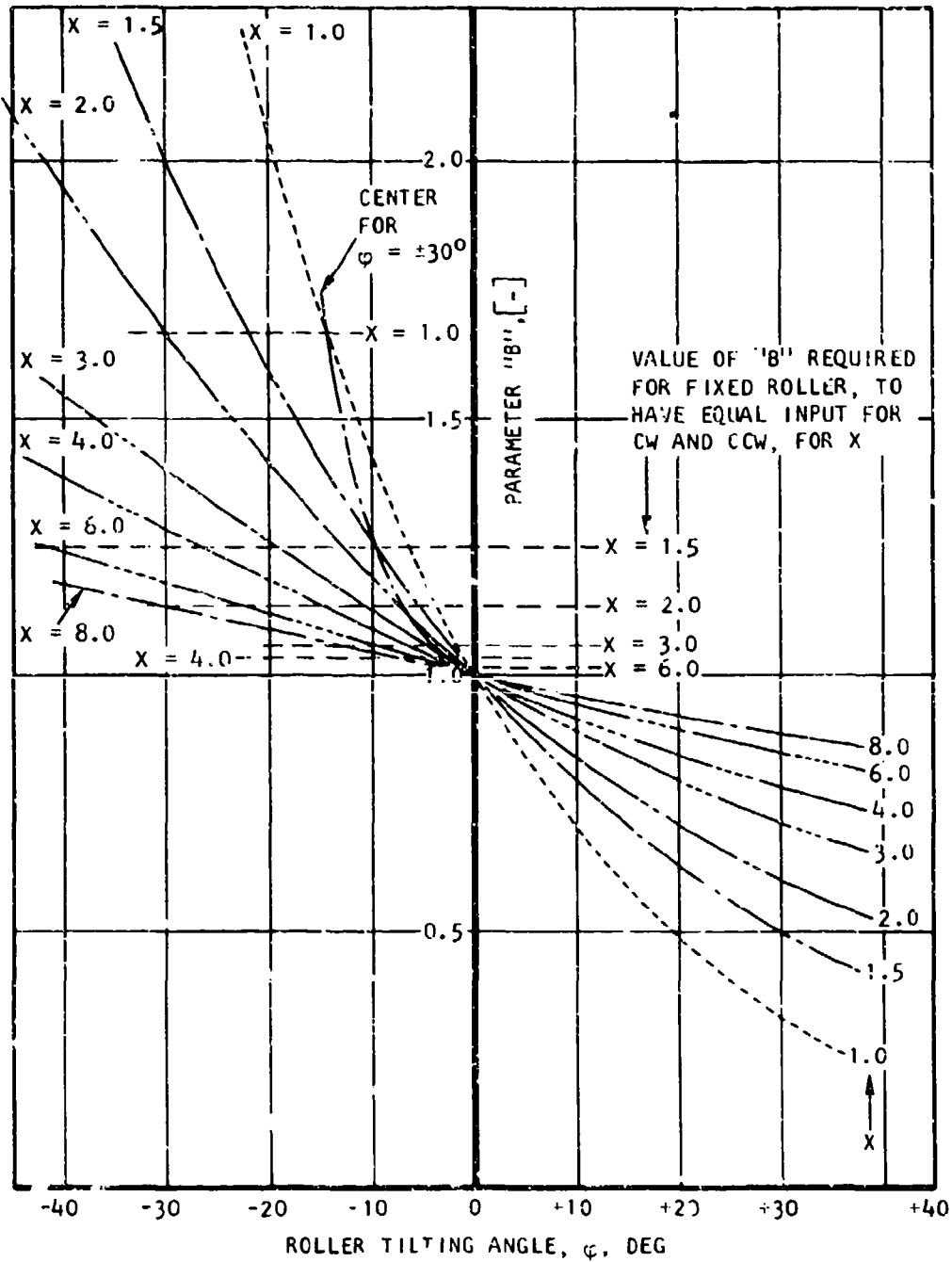


Figure E-5. Variations of Function B with Roller Tilt

S-4436

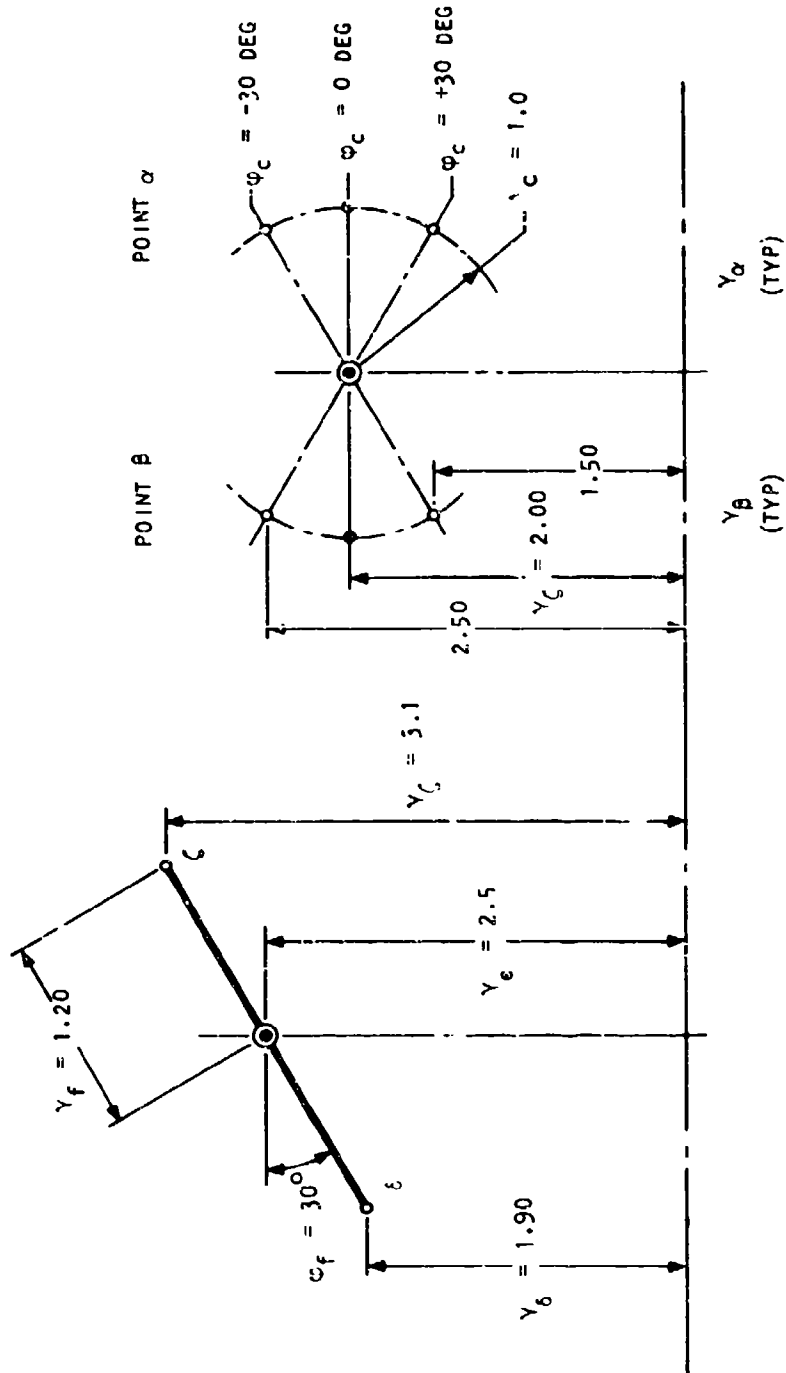


Figure E-6. Example to Check Equations

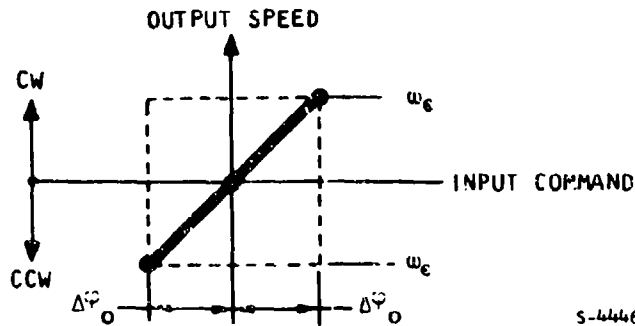
$$B = \frac{x_2 - \sin\phi_f}{x_2 + \sin\phi_f} = \frac{2.08333 - 0.50}{2.08333 + 0.50} = 0.61290$$

Results are shown in Table E-1

TABLE E-1
EXAMPLE RESULTS

ϕ_c [DEG]	$\sin\phi_c$ [-]	y_c [in.]	y_b [in.]	$\frac{y_c - \sin\phi_c}{y_c + \sin\phi_c}$ [-]	$\frac{\omega_e}{\omega_i}$
+30	+0.50	1.50	2.50	+0.60000	+0.00800
0	0	2.00	2.00	+1.00000	-0.24000
-30	-0.50	2.50	1.50	+1.66667	-0.65334

For any control servo, it is desirable to have a linear and skew-symmetric curve, as shown in the figure below which shows the speed versus input command relationship.



Gear Ratio

A study of gear ratio was made

where

$$j = \frac{\omega_e}{\omega_i}$$

ω_e = output angular velocity

ω_i = input angular velocity

The study shows that linearity and skew-symmetry can be achieved at specific parametric values only. Figure E-7, plotted for gear ratio changes of $\pm 30^\circ$ deg and the same absolute value of speed extremes, shows that linearity improves with increasing X value. Figure E-8 is a plot of the variation in gear ratio j with a full 360 deg change in both roller angles and with X kept constant.

Linearity and Skew Symmetry

Linearity and skew symmetry analyses were made for the servo. The problem reduces to determining the inflexion points on the curves shown on Figure E-8. At these points, the second derivative of

$$j = \frac{\omega_e}{\omega_i}$$

given by $\frac{d^2 j}{d\varphi^2} =$

$$\text{where } j = \frac{\omega_e}{\omega_i} = 1/2 \left[\frac{1 + \sin\varphi_b}{x_f} \right] \left[\frac{x_f - \sin\varphi_f}{x_f + \sin\varphi_f} - \frac{x_c - \sin\varphi_c}{x_c + \sin\varphi_c} \right]$$

In the derivative x_c , x_f and φ_j are assumed to be constants.

Differentiating gives inflexion points at the values of φ_c shown below

x_c	φ_c
1.0	-88.0
1.5	-59.3
1.5	-121.7
3.0	-34.163
6.0	-18.459

RADIUS OF CURVATURE

Radius of curvature of the roller and the toroid must be known to determine the contact stress. Determining the two principal radii of curvature for the roller is simple because it is assumed that the roller has a 55 percent conformity to the toroid (established practice in ball and screw applications). Conformity geometry is shown in Figure E-9.

One of the principal radii of the toroid is similarly straightforward; it is identical with the roller radius. The second principal radius is determined as follows.

55 PERCENT CONFORMITY (CUSTOMARY WITH BALL SCREWS)

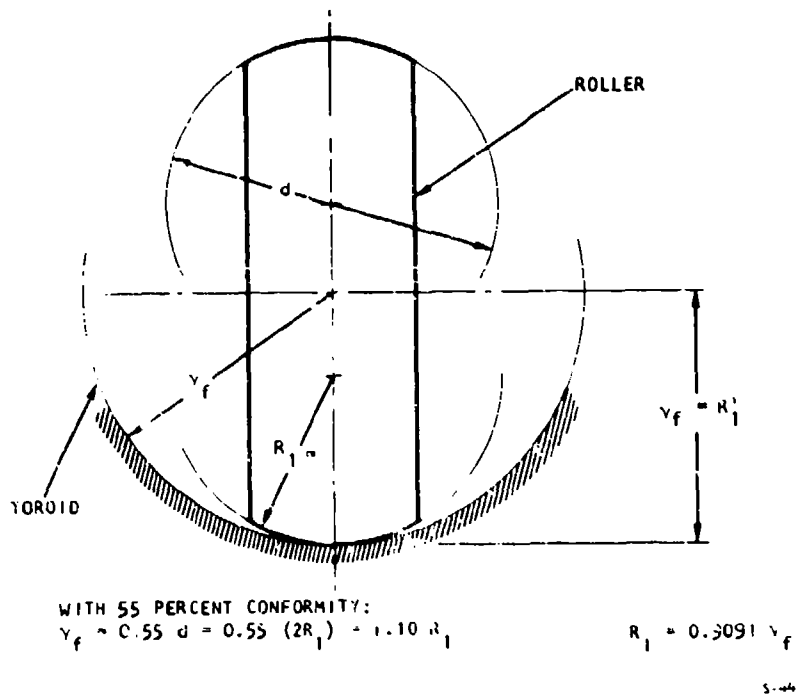
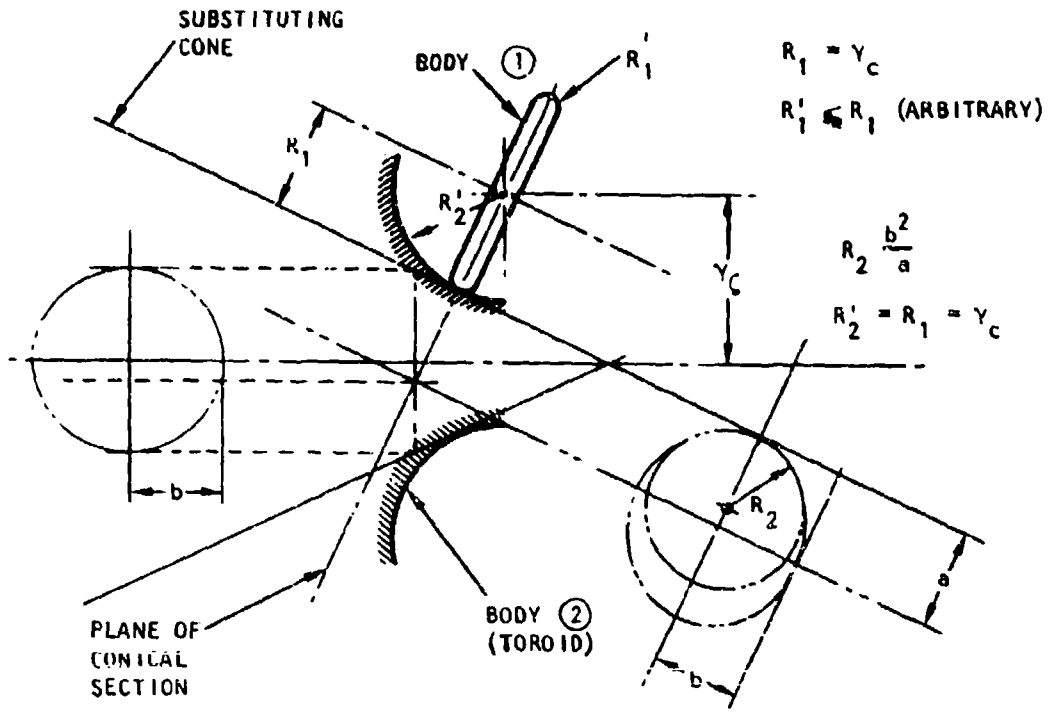


Figure E-9. Conformity Between Toroid and Roller

A cone is fitted into the toroid so that the cone touches the toroid at the point where it is in contact with the roller. The radius of curvature in question is taken as the radius of curvature of the conical section, which is in the plane of the roller (as shown in Figure E-10).

For the example, approximately six roller parameters were selected, assuming a +20 deg roller tilting angle. The selection of the six roller parameters is shown on Figure E-11. The variation of toroid radius of curvature with roller tilting angle is shown on Figure E-12.



S-4433

Figure E-10. Radius of Curvatures

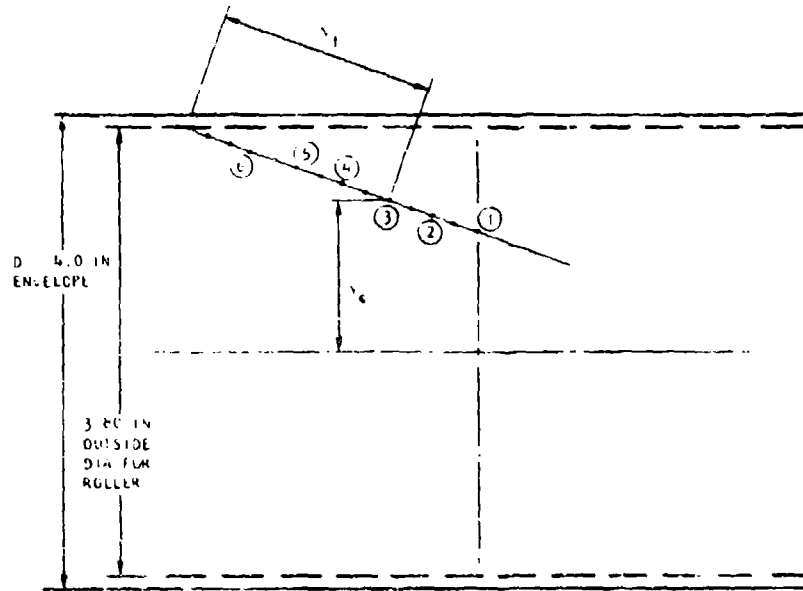


Figure E-11. Envelope Restrictions

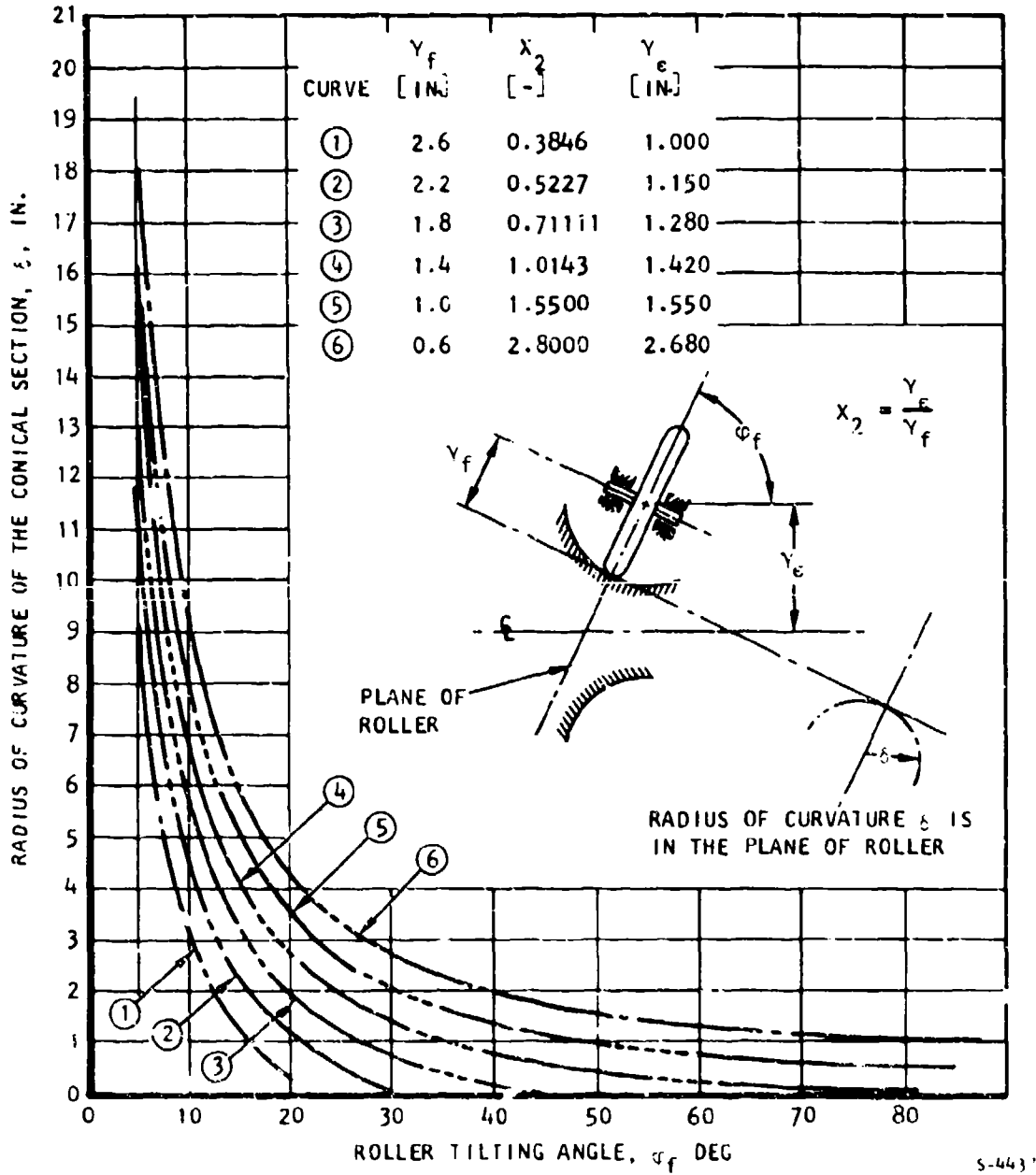


Figure E-12. Variation of Toroid Radius of Curvature with Tilting Angle

HERTZ STRESS AT ROLLER CONTACTS

Hertz stress was calculated for the roller-toroid contact areas. The problem is the most general case of Hertz stress (Roark, Page 231, Case 8) where two bodies are in contact, the two principal radius of curvature are known for each body, and the respective orientation ϕ of the minimum radius of curvature also is given. It is applied to the roller contact as shown in Figure E-13. The calculated unit Hertz stresses are plotted in Figure E-14.

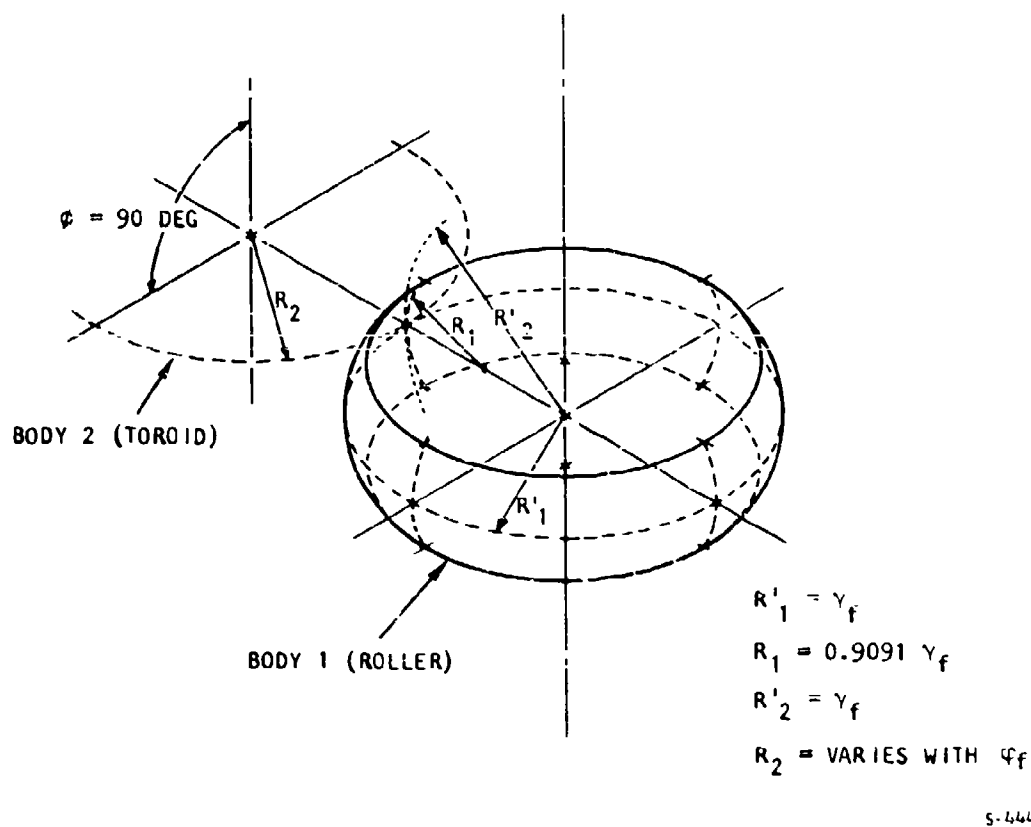


Figure E-13. Methodology in Calculating Roller Contact Areas

Roark, Raymond J., Formulas for Stress and Strain, Fourth Edition, McGraw Hill, New York, 1965, p. 231.

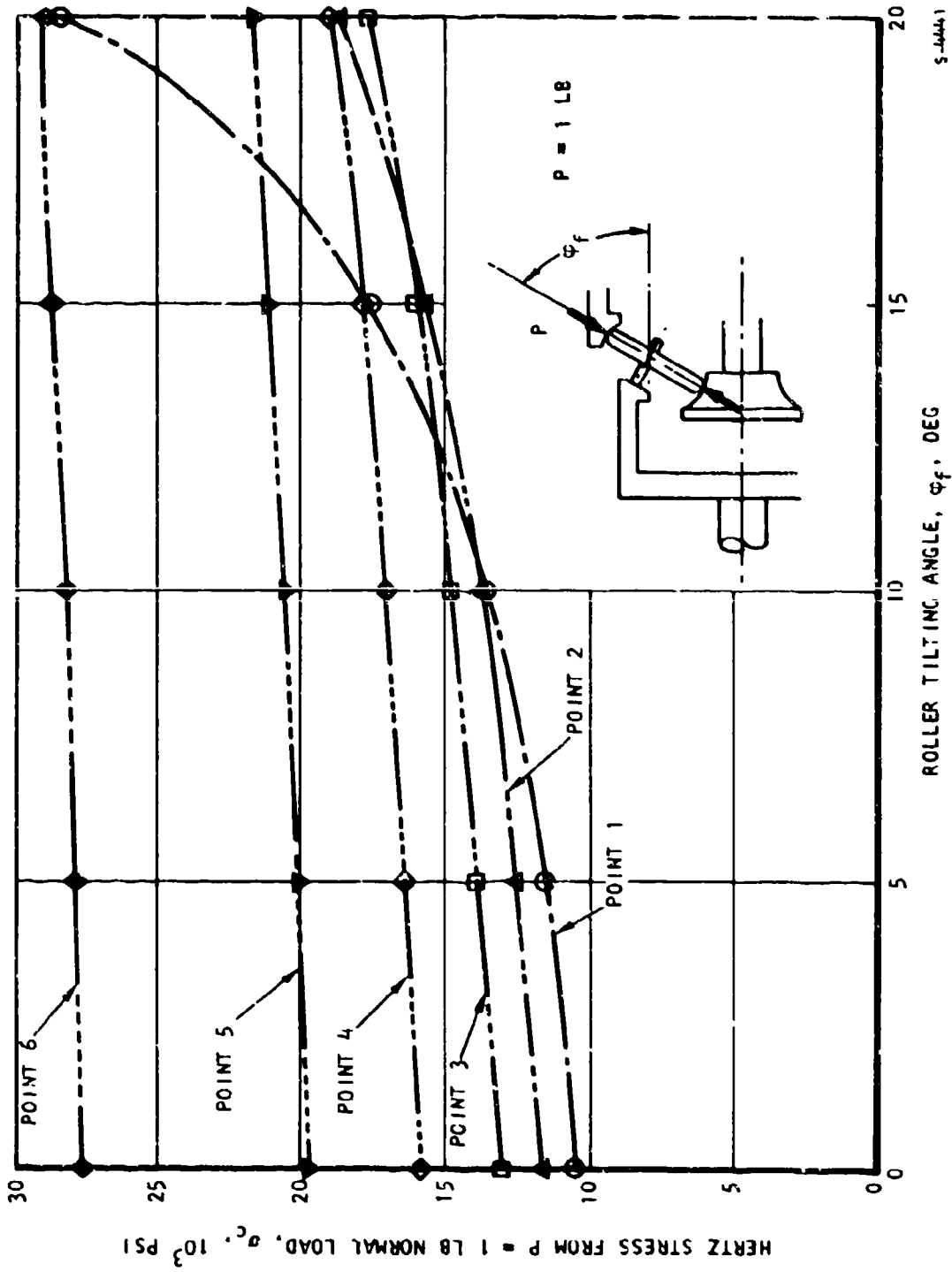


Figure E-14. Hertz Stress for Unit Normal Load

PERFORMANCE

To calculate performance, a force balance was traced through the drive train and the results were checked against the kinematic calculations. For the calculations, the performance volume presented earlier were used.

Figure E-15 shows the force balance on the system from output to input, from which basic force balance equations may be written:

Output torque	$T_0 = AY_e$
Fixed roller	$BY = A/2$
Cylindrical toroid	$BY - CY_B = 0$
Reaction at the control roller	$D = 2C$
input shaft	$BY_B - CY_a + T_i = 0$

Combining these equations gives the ratio:

$$\frac{T_i}{T_0} = \frac{1}{2Y_e Y_B} (Y_Y Y_a - Y_D Y_c)$$

which $T_i = 0$ if $Y_Y Y_a = Y_B Y_c$

and $Y_Y/Y_c = Y_B/Y_a$ is gear ratio ω

The derived equations were used to calculate $\frac{\omega_0}{\omega_1}$ (Figure E-6) for comparison

with those calculated at the same conditions using the derived kinematic equations. From Figure E-6,

$$Y_e = 2.5 \text{ in.}$$

$$Y_B = 1.9 \text{ in.}$$

$$Y_Y = 3.1 \text{ in.}$$

$$Y_c = 2.0 \text{ in.}$$

Results are tabulated in Table E-2.

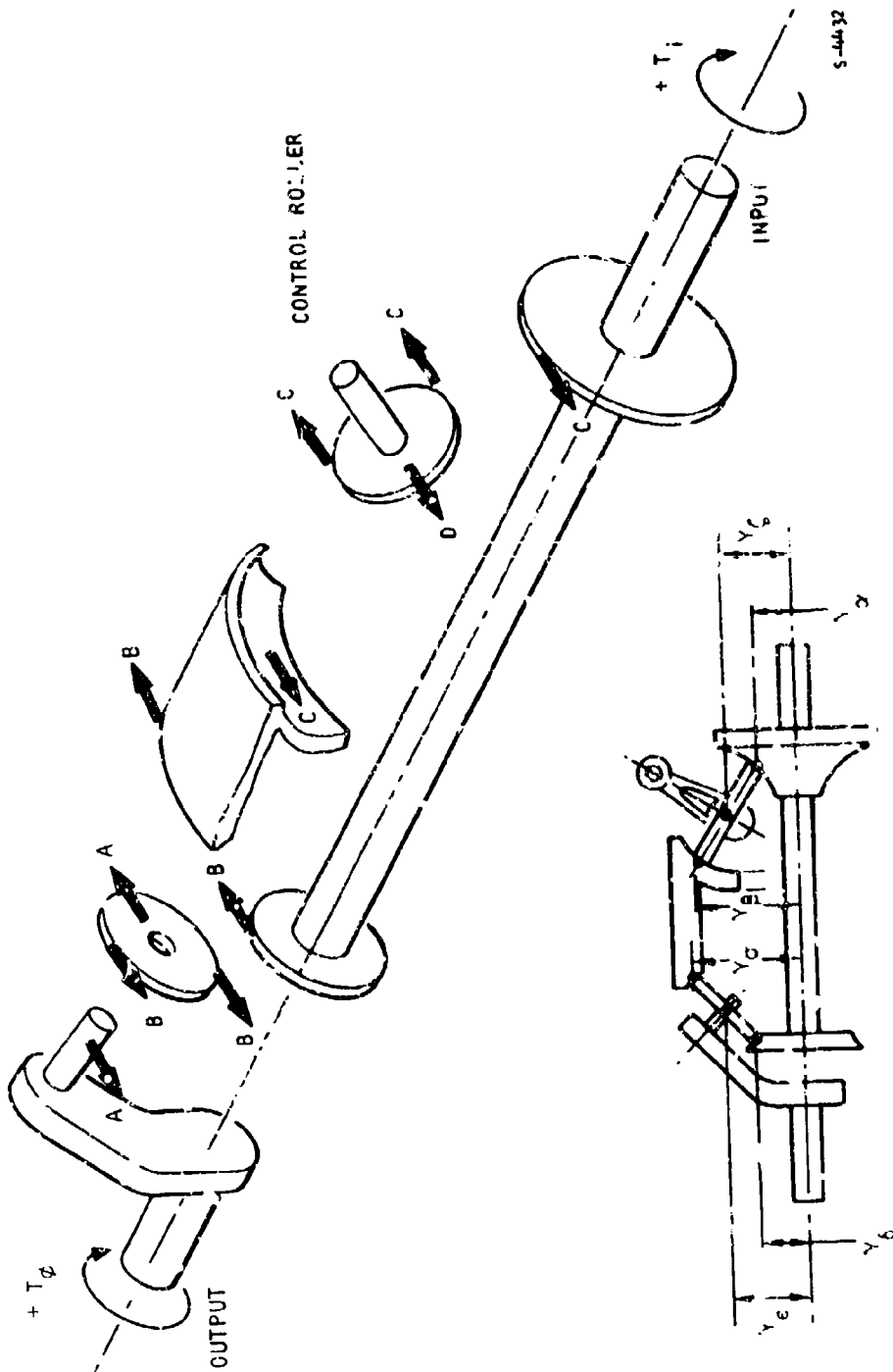


Figure E-15. Force and Torque Balance

TABLE E-2
EVALUATION OF FORCE BALANCE EQUATIONS

Point	$\psi_c = -30 \text{ deg}$		$\psi_c = 0 \text{ deg}$		$\psi_c = +30 \text{ deg}$	
	v	w	v	w	v	w
α	2.50	+1.0	2.00	+1.0	1.50	+1.00
β	-2.50	-1.66667	-2.00	-1.00	-1.50	-0.60000
Γ	-5.16667	-1.66667	-3.100	-1.00	-1.86000	-0.60000
δ	+1.900	+1.0	+1.900	+1.0	+1.900	+1.00
ϵ	-0.63333	-0.653333	-0.4000	-0.24000	+0.02000	+0.00800
$\frac{w_{out}}{w_{in}}$		-0.653334		-0.24000		+0.00800
$\frac{v_{out}}{v_{in}}$		-0.65334		-0.24000		+0.00800

*From Table E-1

Preload and Frictional Force

Sufficient frictional force is necessary to prevent sliding at the point of roller-to-rail contact. Calculations were made to determine the preload required to develop the necessary frictional force and to establish the relation between this force and the required output torque, as shown in the force diagram of the fixed roller.

The tangential force at S, B is

$$B = A/2 = \frac{T_{ST}}{2nY_e}$$

A = tangential force at e

T_{ST} = stall force, 37,500 lb

n = Number of rollers

Y_e = Distance of e from rotating axis

The force required to prevent slipping is

$$Q = B\mu$$

where μ = coefficient of friction

= 0.08 approximate mean value of coefficients with a Hertz stress of 400,000 psi and a modest (<1 in./sec) sliding

and the required preload

$$P_f = nQ \cos \phi_f$$

where $\phi_f = 20$ deg

Combining, substituting, and applying a 20 percent margin to the selected configuration,

$$Y_e = 1.28 \text{ in.}$$

$$P = \frac{764288}{Y_e} = 206,475 \text{ lb}$$

Life Determination

For the life determination, the configuration selected was defined more fully as shown in Figure E-16, which defines the kinematics, and Figure E-17, which shows the physical dimensions. Verification of the design parameters with this example is shown in Table E-3.

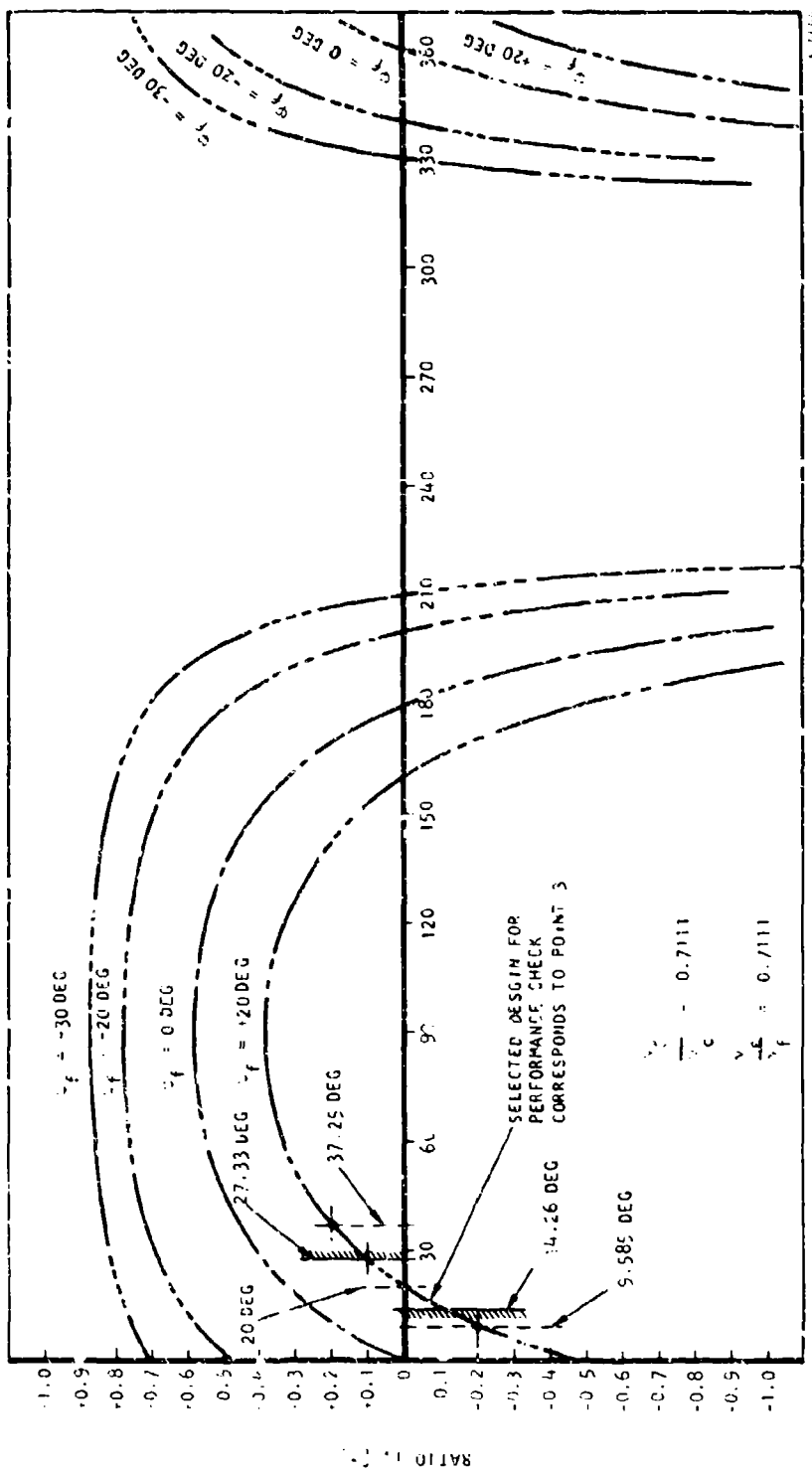
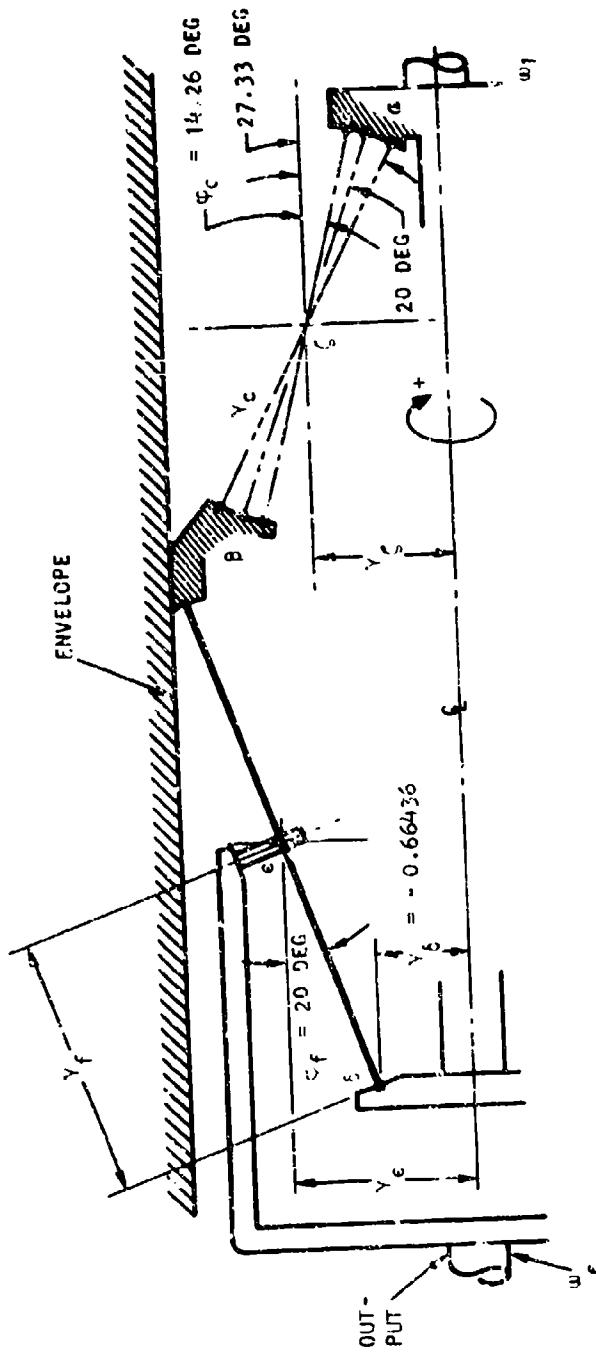


Figure E-16. Kinematics of variable Roller Drive



$$\left. \begin{array}{l} Y_c = 1.28 \\ Y_f = 1.8 \end{array} \right\} \frac{Y_c}{Y_f} = 0.71111$$

$$\phi_f = +20 \text{ DEG}$$

$$\left. \begin{array}{l} Y_c = 1.000 \\ Y_c = 1.40627 \end{array} \right\} \frac{Y_c}{Y_c} = 0.7111$$

S-4435

Figure E-17. Schematic of Selected Design

TABLE E-2
 VERIFICATION OF DESIGN REQUIREMENTS

Control Roller Position deg	Point a		Point b		Point c		Point d		
	V_x in. sec	$\dot{\theta}$ rad sec	V_x in. sec	$\dot{\theta}$ rad sec	V_x in. sec	$\dot{\theta}$ rad sec	V_x in. sec	$\dot{\theta}$ rad sec	
+14.26	0.65369	1	0.65360	1.34640	-0.48545	-0.65360	1.89564	-0.48545	-0.97024
+20.00	0.51903	1	0.51903	1.48097	-0.35047	-0.51903	1.89564	-0.35047	-0.66436
+27.33	0.35436	1	0.35436	1.64564	-0.21533	-0.35436	1.89564	-0.21533	-0.40819
	Point a		Point b		Point c		Point d		
	V_x in.	$\dot{\theta}$ rad sec	V_x in. sec	V_x in.	$\dot{\theta}$ rad sec	V_x in. sec	V_x in.	$\dot{\theta}$ rad sec	V_x in. sec
+14.26	0.66436	1	-0.53325	1.28	-0.09995	-0.17794			
+20.00	0.66436	1	-0.56436	1.28	0	0			
+27.33	0.66436	1	-0.66436	1.28	+0.10001	+0.17809			
	$V_c = \frac{V_x + V_y}{2}$								

Since the number of Hertz stress cycles is related to the operating time, calculations were made to determine the number of cycles incident to the 8000-hr life. Hertz cycles were determined using the selected system geometry as a basis and the design verification parameters in Table E-3; the time for one roller revolution (1.21931 sec and 800 deg/sec input) was used to calculate the number of contacts (2 per revolution) for the 8000-hr life, or 47.24×10^6 contacts. Similarly, the number of contacts for the disk in contact with the output roller was computed to be 127.996×10^6 contacts for 8000 hr. A plot of allowable contact stress against bearing life for angular contact bearings is shown in Figure E-18.

Frequency Response

Frequency response for the system was determined as a function of the inserted gear ratio. Requirements for frequency response at no load was ± 1 deg sinusoidal motion at $f = 8$ Hz. For purposes of calculating the mass moment of inertia, the roller drive was considered to be equivalent to a cylindrical steel cylinder of 3.5 in. dia and 3.5 in. length, from which

$$\theta = \rho_s \frac{Vr^2}{2}$$

from which $\theta = 0.0495$ lb-in. sec

$$i = 0.0745 \text{ rad}$$

$$f = 8 \text{ Hz}$$

$$= 50.265 \text{ rad/sec}$$

$$T_d(i) = 37,500 \text{ lb}$$

from equations for sinusoidal

$$\text{displacement } \varphi = \varphi_0 \sin \omega t$$

$$\text{speed } \dot{\varphi} = \omega \varphi_0 \cos \omega t$$

$$\text{acceleration } \ddot{\varphi} = \omega^2 \varphi_0 \sin \omega t$$

The maximum value of acceleration required is given by

$$e = \omega^2 \varphi_0$$

but the available acceleration is given by

$$e(i) = \frac{T_d(i)}{\theta}$$

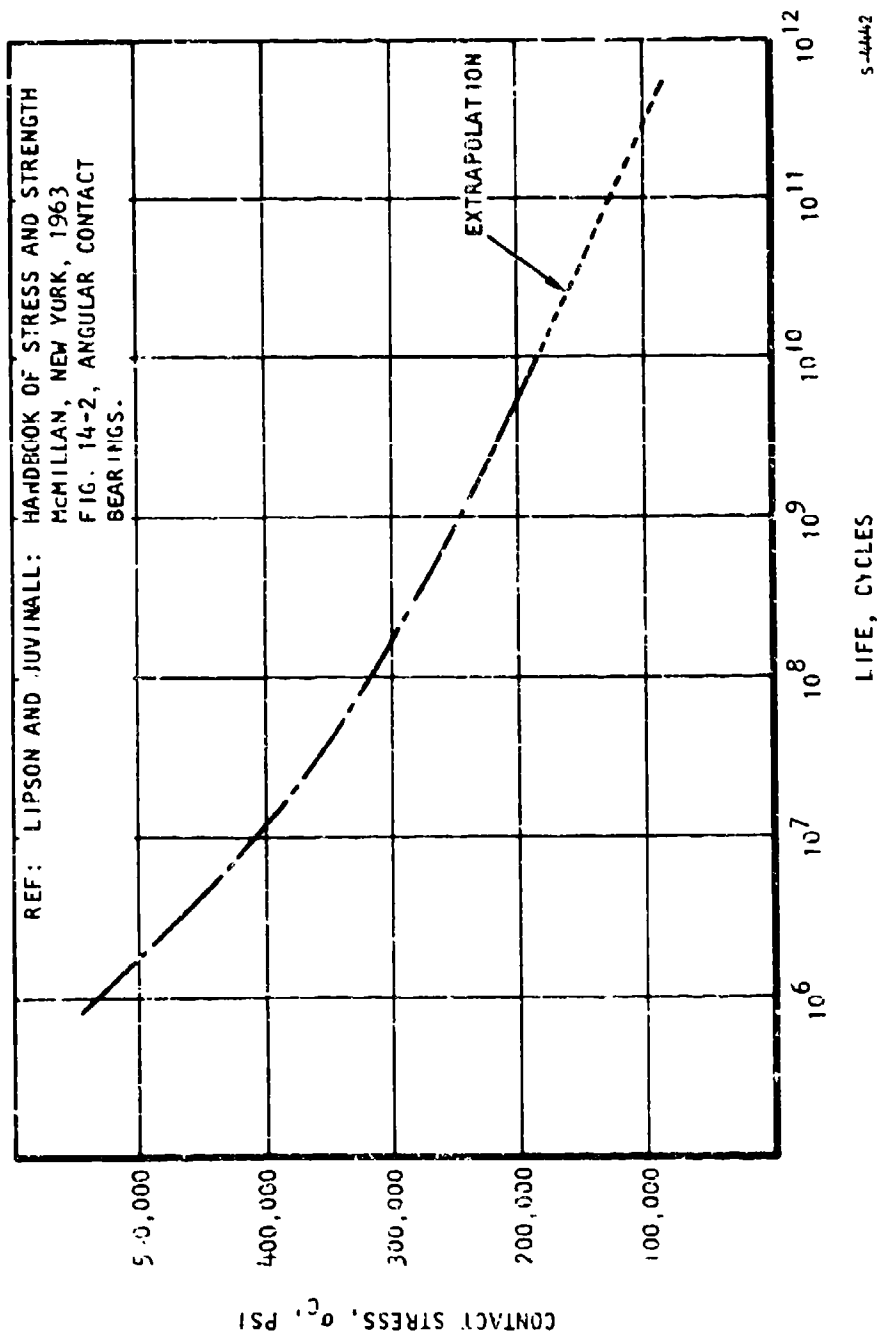


Figure E-18. Allowable Contact (Hertz) Stress

Values of torque, maximum acceleration, sinusoidal amplitude, and frequencies for various gear ratios are given in Table E-4.

TABLE E-4
FREQUENCY RESPONSE FOR SELECTED SYSTEM

Gear Ratio i , [-]	Maximum Output Torque T_0 , [lb-in.]	Maximum Available Acceleration ϵ , $\frac{\text{rad}}{\text{sec}^2}$	Amplitude of Sinusoidal Motion for 1 deg at panel, φ_0 [rad]	Frequency, f Hz
1	37,500	757,570	0.01745	1048.6
2	18,750	378,780	0.03491	524.3
4	9375	189,390	0.06981	262.1
8	4687	94,690	0.13963	131.1
16	2344	47,350	0.27925	65.5
32	1172	23,670	0.55851	32.8
64	586	11,837	1.11701	16.4
128	293	5918	2.23402	8.19
256	146.5	2959	4.46804	4.10
512	73.24	1479	8.93609	2.05
1024	36.62	739	17.87219	1.02
1048	18.31	370	35.74434	0.512

SYNTHESIS

Results of the analysis show that a variable roller drive in the given envelope will meet the specified preload, life, frequency response, and input speed requirements within a limited range of gear ratios, $118 \leq i \leq 132$, only. However, the concept warrants further verification by actual hardware design and test. The results are tabulated as a function of gear ratio in Table E-5 and Figure E-19. Limitations in gear ratio are defined below and in Figure E-19.

TABLE E-6
SUMMARY OF DESIGN PARAMETERS

Gear Ratio, 1	Output Torque Required T_{OUT} LB-IN.	Axial Preload Required P with 1.2 safety	Roller Pressure Required Q, LB	Hertz Stress σ_c psi	Total Number of Hits For 6000 hr.		Life At stress T_c cycles	Life L, hr	Required Input Speed N, rpm
					on the output roller n_1	on the disc in contact with output roller n_2			
1	37500	206475	105663	850700	47.240×10^6	128.00×10^5		133.33	
2	18750	103200	54530	675207	96.48×10^6	256.0×10^6	130.10^3	4.06	
4	9375	51620	27465	535500	188.96×10^6	512.0×10^6	95×10^3	533.3	
6	4687	25810	13730	425330	377.9×10^6	1.024×10^5	7.06×10^6	1066.6	
16	2344	12904	6866	337500	755.8×10^6	2.048×10^2	55×10^6	2133	
32	1172	6452	3433	267950	1.511×10^5	4.096×10^6	460×10^6	4267	
64	586	3226	1515	212650	3.073×10^5	6.192×10^5	3.3×10^5	8533	
128	293	1613	658.3	166800	6.046×10^5	16.38×10^5	19.0×10^5	17066	
256	146.5	806.5	429.2	13980	12.09×10^5	32.77×10^5	75×10^5	3432	
512	73.22	403.3	214.6	108345	24.19×10^5	65.54×10^5	240×10^5	68265	
1024	36.62	201.6	107.3	84407	48.37×10^5	131.1×10^5	550×10^5	135500	
2048	18.31	100.8	53.64	66349	96.75×10^5	262.1×10^5		273100	

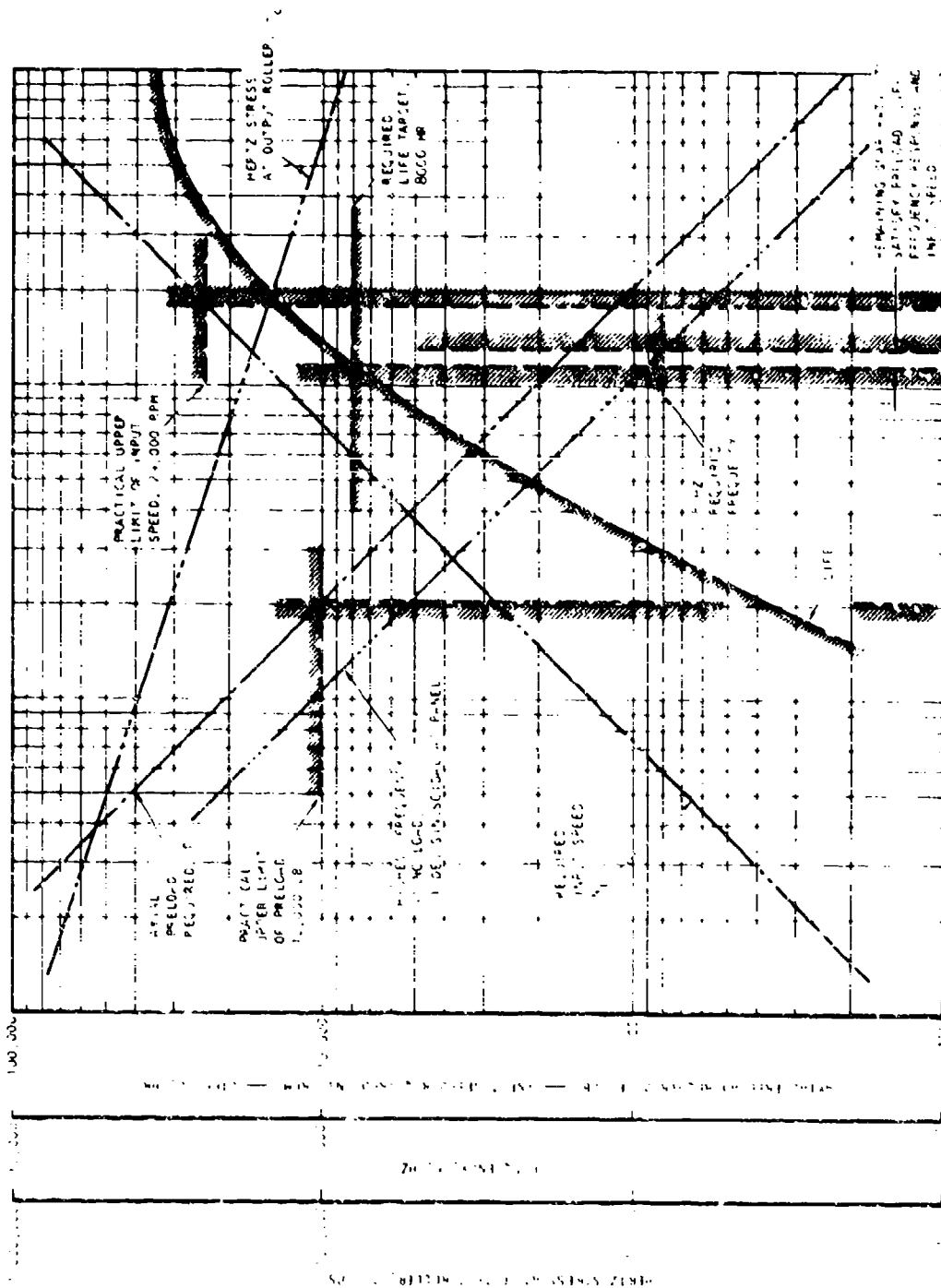


Figure E-19. Motor Drive Performance Summary

- $i = 20$ because the practical limit of axial preload is about 10,000 lb in the given envelope, and $i < 20.8$ would require preload in excess of 10,000 lb.
- $i = 180$ Because the highest practical input speed is 24,000 rpm (2-pole, 400-Hz system) and higher gear ratio i would require higher input speed than 24,000 rpm.
- $i = 118$ Because the obtainable life is less than 8000 hr if $i < 118$
- $i = 132$ Because at higher i , the $f = 8$ Hz frequency response cannot be satisfied.